Fabrication of High Strength Titanium Matrix-Nano Carbons Composites Using Solution-Coating Technique in Powder Metallurgy Route

By

Thotsaphon Threrujirapapong

Department of Mechanical Engineering

Graduate School of Engineering

Osaka University

2011

Fabrication of High Strength Titanium Matrix-Nano Carbons Composites Using Solution-Coating Technique in Powder Metallurgy Route

By

Thotsaphon Threrujirapapong

Department of Mechanical Engineering

Graduate School of Engineering

Osaka University

2011

Table of Contents

Chapter 1

General Introduction

1.1 Titanium and titanium alloys

Titanium is the ninth most abundant metal on the earth and the fourth most abundant structural metal. It was discovered by William Gregor, the British mineralogist and chemist in 1791 and it took 141 years before Wilhelm Justin Kroll from Luxembourg demonstrated that titanium could be extracted commercially in 1932. 16 years later, the DuPont Company was the first to produce titanium commercially in 1948. [1-3]. And today, titanium and it alloys are mostly used in the aerospace structures because they are high specific strength materials, but other sectors such as automotive, motorcycle, chemical, medical applications and even sports and luxury goods are also gaining their usage of titanium and it alloys [1-4].

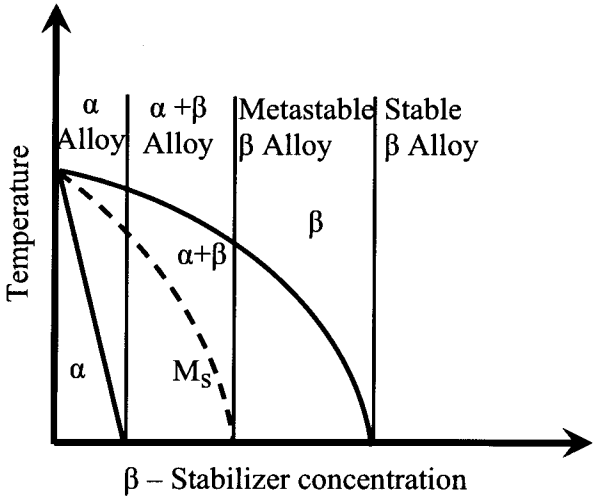

Figure 1.1 Schematic illustration of pseudo-binary section through a β isomorphous phase diagram [2].

The crystal structure of pure titanium at room temperature is hexagonal close packed structure (hcp), called α titanium. At high temperature, the hcp structure changes to the body-centered cubic structure (bcc) which called β titanium. The α/β transformation temperature (β-transus temperature) of pure titanium is approximately 1155±2 K depending on interstitial and substitutional elements and their purity [1-2]. Commercial titanium alloys are classified

into three different groups, i.e., α, α+β and β alloys by determining their position in a pseudo-binary section thorough a β isomorphous phase diagram [2], as shown in Figure 1.1. Commercially pure Ti is classified to α titanium alloys. In addition, the α-titanium alloys can never be heat-treated to improve their mechanical properties, compared to the α+β and β titanium alloys, because they are single-phase alloys [3].

1.2 Strengthening of commercially pure Ti

The improvement of mechanical properties of commercially pure Ti can be achieved by various means, for example, adding alloying elements, grain refinement, precipitation hardening or even dispersion of second phase into Ti matrix [5-7].

1.2.1 Alloying elements

The addition of some substiutional solid solution elements to α-titanium, such as Al, Sn and Zr, which have large atomic size differences to titanium and large solid solubilities in the α-titanium, enables the resultant α-titanium alloys to be heat-treated or processed in the region of α and β phase coexistences [2]. Consequently, the grain size and phase can be controlled by the optimum cooling rate in solidification. Moreover, the solution heat treatment and aging treatment of those structures are also effective to improve its mechanical properties.

Hydrogen, boron, carbon, nitrogen and oxygen are other alloying elements that also formed as interstitial solid solutions because their atomic sizes are very smaller than that of titanium atom. These interstitial elements solid solutions affect the increase of strength which depends on their content and solubility in commercially pure Ti [2, 8-10], in particular the α-titanium grade 2. Most of interstitial elements are α-phase stabilizer except for hydrogen which is β-phase stabilizer. Therefore, the α-phase stabilizing elements are generally used to improve strength of commercially pure Ti.

Among the α-phase stabilizing elements, nitrogen is the most effective to increase strength of commercially pure Ti, compared to carbon and oxygen, while boron fairly shows the improvement. For example, C. Ouchi, *et al.* [9] reported that the increment of tensile

strength per 1 wt.% of the nitrogen, oxygen and carbon doped pure titanium is 2040, 1120 and 1020 MPa, respectively. On the other hand, the improvement by the carbon doping is also included as the effect of Ti grain refinement.

1.2.2 Grain refinement

Grain refinement is a method to improve the strength of polycrystalline metals. The increases of grain boundary are important factors as obstacle to slip of metals. The finer grains, which have many grain boundaries, are stronger than the coarser grain because a higher applied stress is required for slipping. Moreover, the accumulation of dislocations in the finer grains is much higher than coarser grains, so that the required stress to move these dislocations across the grain boundary thus increases with the increasing the grain boundaries. The grains refinement of metals can be obtained using both plastic deformation and thermo-mechanical processing. The plastic deformation is generally used to soft face-centered cubic (fcc) metals such as aluminium and copper because they have higher slip systems than hard hcp metals such as titanium [11]. However, the grain refinement of commercially pure Ti can be achieved by the severe plastic deformation techniques (SPD) such as equal channel angular extrusion (ECAE) and high pressure torsion (HPT) processes [12-14]. The increasing yield stress tendency with decreasing grain size of commercially pure Ti produced via those processes can be expressed by the Hall-Petch relationship [15].

1.2.3 Dispersion strengthening

Dispersion of fine particles is very effective in increasing strength of ductile metals. This technique is widely used to produce high strength composite materials. Generally, the hard particles such as oxides, carbides, nitrides and borides are mixed with metal powder and consolidated by the powder metallurgy process. The dispersed hard particles in ductile metals behave as obstacles to dislocation motion. The dislocation can bow out or cut through the particles which related to the coherency between lattice of particle and matrix [11, 16]. In addition, the increase in strength has directly related to particle size, interparticle distance and volume fraction of second phase [16]. Several other previous reports have shown remarkable improvements in mechanical properties of commercially pure Ti using dispersion of fine particles. D. Handtrack, *et al.* [6] reported that the adding 1.0wt.% Si as second phase

remarkably increased bending strength to 1650 MPa, compared to that of pure Ti at about 874 MPa. Z. F. Yang, *et al.* [17] also showed the adding 1.09 wt.% C was able to increase the tensile strength of commercially pure Ti to 1021 MPa, while K. Kondoh, *et al.* [7] reported that the tensile strength of commercially pure Ti could be remarkably increased to 750 MPa by adding 0.35 wt.% C in the form of carbon nanotubes.

The selection of second phase is important to accommodate the load transfer behavior between metal matrices and second phases [16]. Recently, carbon nanotubes (CNTs) have been considered as promising second phase or reinforcing materials for metal matrices such as magnesium [18-19], aluminium [20-21] and copper [22-23]. The mechanical properties of those metal matrices similar to titanium matrix [7] are significantly improved by adding small amount of CNTs. Those improvements are due to the dramatic properties, especially mechanical properties, of CNTs [24]. However, the dispersion of CNTs in metals has been limited in powder metallurgy process and squeezes casting [25] because of their large difference in density. Conventional casting process is very difficult to achieve uniform dispersion of CNTs in molten metals because CNTs have low density, and trend to separate from the molten metals [26]. Therefore, grinding or mechanical alloying process such as ball milling could be achieved more homogenous dispersion of CNTs in the metal matrices than casting process [21, 26].

1.3 Carbon nanotubes

In 1991, Iijima [27] reported the arc-discharge synthesis and high-resolution electron micrographs of '*helical microtubules of graphitic carbon*' which later known as '*carbon nanotube*' (CNTs). CNTs can exist as single tube which called single-walled nanotubes (SWCNT) or in the form of concentric tubes which called multi-walled nanotubes (MWCNT) [28]. There are many methods to synthesize MWCNTs such as arc-discharge processes, chemical vapor deposition and electrochemical deposition. Their diameter can be varied in the range of 0.37-100 nm, while their length can also be varied from a few hundred nanometers to several hundred microns, depending on the synthesis methods [28].

Moreover, MWCNTs have been shown dramatic properties, especially mechanical properties, as well as electrical and thermal conductivities [29-32]. They have high Young's modulus of approximately 1 TPa [24] and a low density of 1300 $kg.m^{-3}$, which make them preferable for composites materials with improved mechanical properties. However, the uniform dispersion of CNTs has remained an important problem during mixing with metal powders. This is due to that fact that the CNTs have tremendous surface area of up to 200 $m^2.g^{-1}$ [26] which leads to their bundles due to the van der Waals forces [28] between carbon atoms of the nearest-neighbour nanotube. These bundles of CNTs have resulted in the lower mechanical properties of composites because they would behave as the stress concentration points. Hence, a homogeneous dispersion of isolated CNT is an important requirement to achieve homogeneous mechanical properties of the composites.

There are many methods to disperse the CNTs in the metal powders before consolidation to final products, for example, ball milling [21, 33], spray drying [34-35], and surfactant-assisted solution dispersion technique [7, 20, 22]. Although, the conventional ball milling can use to highly dispersed MWCNTs on the metal powders surface, but some bundled MWCNTs have detected in their fractured surface [36]. This is because the van der Waals forces in the bundled MWCNTs can not be reduced by the conventional ball milling completely. Moreover, the MWCNTs are also damaged by the impact of medium balls during ball milling processing [37]. However, those problems can be dealt by the use of chemical surfactant solutions. The surfactant-assisted solution dispersion technique is considered to be a suitable method for dispersion of isolated MWCNTs on metal powders surface.

1.4 Surfactant-assisted dispersion of carbon nanotube

The surfactant-assisted solution dispersion technique has been widely used to obtain highly homogeneous dispersion of individual MWCNT on the metal powders surface [7, 20, 22]. The chemical mediums can be either water based solution or organic solvents [38]. In addition, this technique disperses and sonicates the MWCNTs simultaneously. For instance, MWCNTs are dispersed in ethanol, and vibrated by ultrasonic cleaner for a while before pass through next steps [20, 22]. Furthermore, the dipole/dipole electrostatic interactions of

zwitterionic surfactant solution have been utilized to prepare high dispersion of individual MWCNT, which reported by B. Fugetsu, *et al* [39].

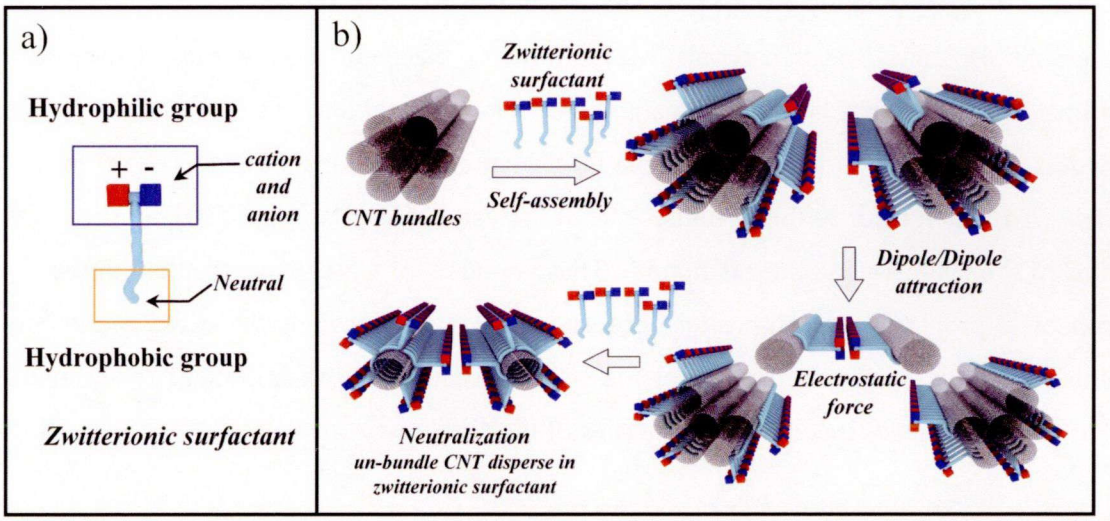

Figure 1.2 Schematic illustrations of a) structure of zwitterionic and b) the disassembling mechanism of CNTs bundles by zwitterionic surfactant.

Schematic illustration of the disassembling mechanism of MWCNTs bundles by zwitterionic surfactant is shown in Figure 1.2. The zwitterionic surfactant solution consists of both hydrophobic and hydrophilic groups. The electrostatic forces, which have larger attractive forces than van der Waals forces between bundled MWCNTs, are generated at the hydrophilic groups because of the associated positive and negative charges, while the hydrophobic group will simultaneously penetrate and coat on the outer surface of the MWCNTs. Consequently, the individual MWCNT will be disassembled and suspended homogeneously in the zwitterionic surfactant solution.

In addition, this technique has the advantages over prior technique as it can prepare a large quantity of individual MWCNTs in zwitterionic surfactant solution within one time preparation, and this solution can be used directly for coating on metal powders without the assistance of sonication method [40]. Therefore, the combination of the advantages of the homogeneously dispersed MWCNTs in zwitterionic surfactant solution and the powder metallurgy route can improve the mechanical properties of commercially pure Ti powder materials.

1.5 Objective of this research

The objective of this research is to investigate the combination effects of surfactant-assisted solution dispersion carbon nanotubes technique and powder metallurgy processing. An effective coating of the individually dispersed MWCNT on commercially pure titanium powders will contribute to the improvement of mechanical properties of the pure titanium matrix composites (TMCs). The concept behind mechanical properties improvement of TMCs is to homogeneously disperse the individual MWCNT on the titanium powders surface via the assistance of zwitterionic surfactant solution, and select the suitable powder metallurgy process parameters to achieve the best conditions for fabrication. However, this research is mainly focused on the mechanical properties response of TMCs when fabricated using the successive processes of spark plasma sintering (SPS) and conventional hot extrusion.

1.6 Research content

The present research is composed of 7 chapters. Firstly, general introduction has been present in this chapter 1. The research flow chart is also shown in Figure 1.3. Chapter 2 provides the detailed description of the experimental procedures employed in this research. In chapter 3, the processing parameters, i.e., debinding temperature and atmosphere for the powder preparation are primarily determined and the characteristics of the commercially pure Ti coated with MWCNTs are subsequently investigated. The effects of thermo-mechanical parameters on the microstructures and the static mechanical properties at room temperature of the extruded commercially pure Ti reinforced with MWCNT composites are described in chapter 4. The fatigue strength and the static stability of the extruded Ti reinforced with MWCNTs composites at elevated temperature, including tensile and hardness properties are evaluated in chapter 5. Chapter 6 introduces the effectiveness of the solution-coating technique for coating nano carbon materials on the commercially pure Ti powders. Finally, the entire research works are summarized in chapter 7.

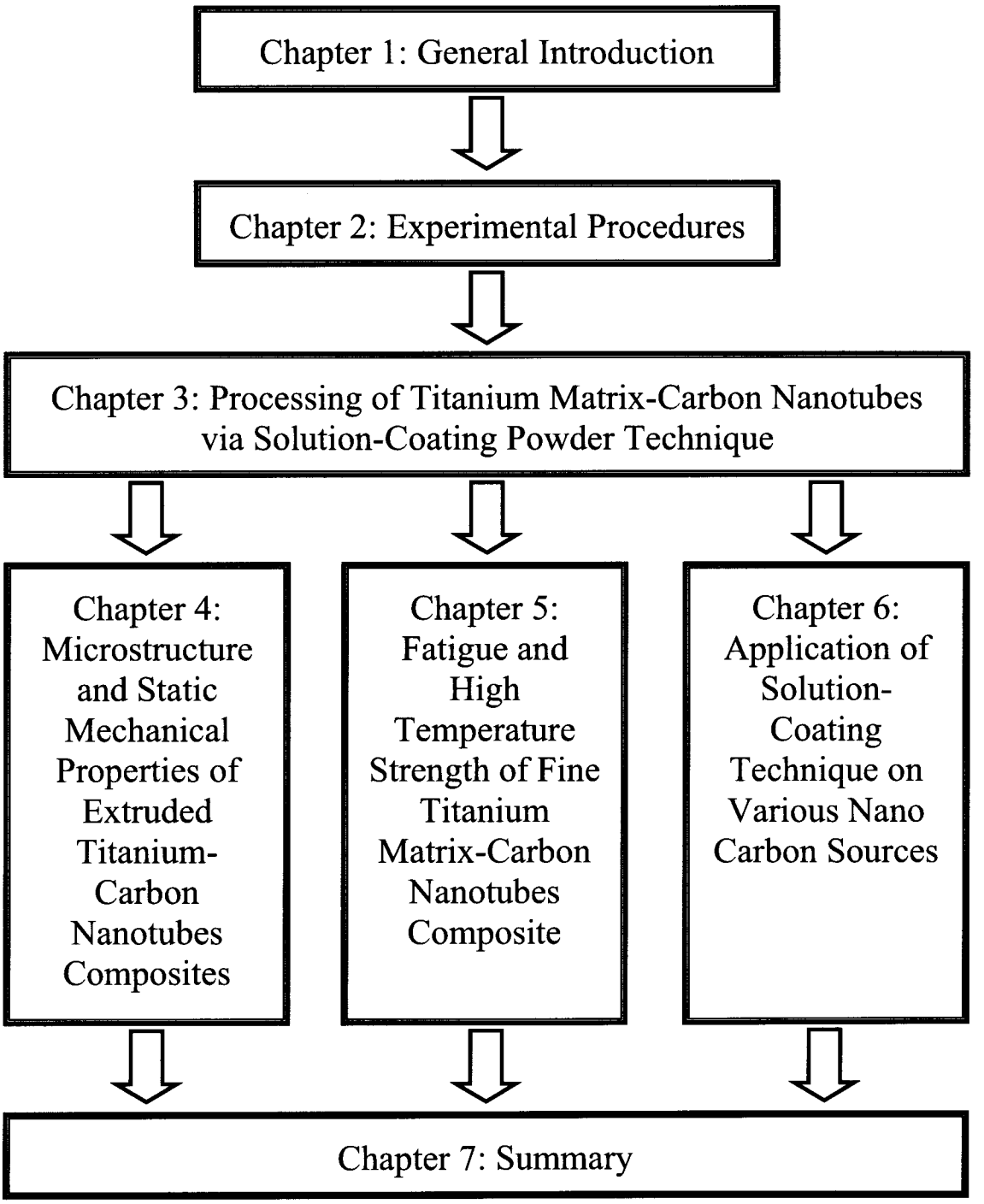

Figure 1.3 Research flow chart of this study.

References

1. C. Leyens and M. Peters, *Titanium and Titanium alloys*, Wiley-VCH, Germany (2003).
2. G. Lütjering and J.C. Williams, *Titanium*, 2nd ed., Springer-Verlag, Germany (2007).
3. M. J. Donachie, Jr., *Titanium: A Technical Guide*, 2nd ed., ASM International, (2000).
4. J. C. Williams, E. A. Starke, Jr., "Progress in Structural Materials for aerospace Systems" *Acta Materialia*, 51 (2003) 5775-5799.
5. Y. Liu, L. F. Chen, H. P. Tang, C. T. Liu, B. Liu and B. Y. Huang, "Design of Powder Metallurgy Titanium alloys and Composites", *Materials Science and Engineering A*, 418 (2006) 25-35.
6. D. Handtrack, F.Despang, C. Sauer, B. Kieback, N. Reinfried and Y. Grin, "Fabrication of Ultra-Fine Grained and Dispersion-Strengthened Titanium Materials by Spark Plasma Sintering", *Materials Science and Engineering A*, 437 (2006) 423-429.
7. K. Kondoh, T. Threrujirapapong, H. Imai, J. Umeda and B. Fugetsu, "Characteristics of Powder Metallurgy Pure Titanium Matrix Composite Reinforced with Multi-Wall Carbon Nanotubes", *Composites Science and Technology*, 69 (2009) 1077-1081.
8. H. Conrad, "Effect of Interstitial Solutes on The Strength and Ductility of Titanium", *Progress in Materials Science*, 26 (1981) 123-403.
9. C. Ouchi, H. Iizumi and S. Mitao, "Effect of Ultra-High Purification and Addition of Interstitial Element on Properties of Pure Titanium and Titanium Alloy", *Materials Science and Engineering A*, 243 (1998) 186-195.
10. J. J. Xu, H. Y. Cheung and S. Q. Shi, "Mechanical Properties of Titanium Hydride", *Journal of Alloys and Compounds*, 436 (2007) 82-85.
11. W. F. Hosford, *Mechanical Behavior of Materials*, Cambridge University Press, UK (2005).
12. V. V. Stolyarov, Y. T. Zhu, T. C. Lowe, R. K. Isalamgaliev and R. Z. Valiev, "A Two Step SPS Processing of Ultrafine-Grained Titanium", *NanoStructured Materials*, vol. 11, 7 (1999) 947-954.

13. V. V. Stolyarov, Y. T. Zhu, I. V. Alexandrov, T. C. Lowe, and R. Z. Valiev, "Grain Refinement and Properties of Pure Ti Processed by Warm ECAP and Cold Rolling", *Materials Science and Engineering A*, 343 (2003) 43-50.
14. X. Zhao, W. Fu, X. Yang and T. G. Langdon, "Microstructure and Properties of Pure Titanium Processed by Equal-Channel Angular Pressing at Room Temperature", *Scripta Materialia*, vol. 59, 5 (2008) 542-545.
15. W. Pachla, M. Kulczyk, M. Sus-Ryszkowska, A. Mazur and K. J. Kurzydlowski, "Nanocrystalline Titanium Produced by Hydrostatic Extrusion", *Journal of Materials Processing Technology*, 205 (2008) 173-182.
16. G. E. Dieter, *Mechanical Metallurgy*, SI Metric ed., McGraw-Hill (1988).
17. Z. F. Yang, W. J. Lu, D. Xu, J. N. Qin and D. Zhang, "In situ Synthesis of Hybrid and Multiple-Dimensioned Titanium Matrix Composites", *Journal of Alloy and Compounds*, 419 (2006) 76-80.
18. C. S. Goh, J. Wei, L. C. Lee and M. Gupta, "Simultaneous Enhancement in Strength and Ductility by Reinforcing Magnesium with Carbon Nanotubes", *Materials Science and Engineering A*, 423 (2006) 153-156.
19. C. S. Goh, J. Wei, L. C. Lee and M. Gupta, "Ductility Improvement and Fatigue Studies in Mg-CNT Nanocomposites", *Composites Science and Technology*, 68 (2008) 1432-1439.
20. R. George, K. T. Kashyap, R. Rahul and S. Yamdagni, "Strengthening in Carbon Nanotube/Aluminium (CNT/Al) Composites", *Scripta Materialia*, 53 (2005) 1159-1163.
21. A. M. K. Esawi and M. A. El Borady, "Carbon Nanotube-Reinforced Aluminium Strips", *Composites Science and Technology*, 68 (2008) 486-492.
22. P. Quang, Y. G. Jeong, S. C. Yoon, S. H. Hong and H. S. Kim, "Consolidation of 1 vol.% Carbon Nanotube Reinforced Metal Matrix Nanocomposites via Equal Channel Angular Pressing", *Journal of Materials Processing Technology*, 187-188 (2007) 318-320.

23. W. M. Daoush, B. K. Lim, C. B. Mo, D. H. Nam and S. H. Hong, "Electrical and Mechanical Properties of Carbon Nanotube Reinforced Copper Nanocomposites Fabricated by Electroless Deposition Process", *Materials Science and Engineering A*, 513-514 (2009) 247-253.
24. J.-P. Salvetat, J.-M. Bonard, N.H. Thomson, A. J. Kulik, L. Forró, W. Benoit, L. Zuppiroli, "Mechanical Properties of Carbon Nanotubes", *Applied Physics A*, 69 (1999) 255-260.
25. H. Uozumi, K. Kobayashi, K. Nakanishi, T. Matsunaga, K. Shinozaki, H. Sakamoto, T. Tsukada, C. Masuda and M. Yoshida, "Fabrication Process of Carbon Nanotube/Light Metal Matrix Composites by Squeeze Casting", *Materials Science and Engineering A*, 459 (2008) 282-287.
26. S. R. Bakshi, D. Lahiri and A. Agarwal, "Carbon Nanotube Reinforced Metal Matrix Composites – A Review", *International Materials Reviews*, vol. 55, 1 (2010) 41-64.
27. S. Iijima, "Helical Microtubules of Graphitic Carbon", *Nature*, vol. 354 (1991) 56-58.
28. S. V. N. T. Kuchibhatla, A. S. Karakoti, D. Bera and S. Seal, "One Dimensional Nanostructured Materials", *Progress in Materials Science*, 52 (2007) 699-913.
29. R. S. Ruoff and D. C. Lorents, "Mechanical and Thermal Properties of Carbon Nanotubes", *Carbon*, vol. 33, 7 (1995) 925-930.
30. J. Hone, M. C. Llaguno, M. J. Biercuk, A. T. Johnson, B. Batlogg, Z. Benes and J. E. Fischer, "Thermal Properties of Carbon Nanotubes and Nanotube-based Materials", *Applied Physics A*, 74 (2002) 339–343.
31. J. Che, T. Çağin and W. A. Goddard III, "Thermal Conductivity of Carbon Nanotubes", *Nanotechnology*, 11 (2000) 65-69.
32. V. N. Popov, "Carbon Nanotubes: Properties and Application", *Materials Science and Engineering R*, 43 (2004) 61-102.
33. L. Wang, H. Choi, J. M. Myoung and W. Lee, "Mechanical Alloying of Multi-Walled Carbon Nanotubes and Aluminium Powders for The Preparation of Carbon/Metal Composites", *Carbon*, vol. 47, 15 (2009) 3427-3433.
34. S. R. Bakshi, V. Singh, S. Seal and A. Agarwal, "Aluminum Composite Reinforced with Multiwalled Carbon Nanotubes from Plasma Spraying of Spray Dried Powders", *Surface & Coating Technology*, 203 (2009) 1544-1554.

35. S. R. Bakshi, A. K. Keshri, V. Singh, S. Seal and A. Agarwal, "Interface in Carbon Nanotube Reinforced Aluminum Silicon Composites: Thermodynamic Analysis and Experimental Verification", *Journal of Alloys and Compounds*, 481 (2009) 207-213.
36. H. Kwon and A. Kawasaki, "Effect of Spark Plasma Sintering in Fabricating Carbon Nanotube Reinforced Aluminum Matrix Composite Materials" in Book Chapter 15, *Advances in Composite Materials for Medicine and Nanotechnology*, InTech, (2011), Open book access, ISBN 978-953-307-235-7.
37. A. Kukovecz, T. Kanyó, Z. Kónya and I. Kiricsi, "Long-Time Low-Impact Ball Milling of Multi-wall Carbon Nanotubes", *carbon*, 43 (2005) 994-100.
38. L. Vaisman, H. D. Wagner and G. Marom, "The Role of Surfactants in Dispersion of Carbon Nanotubes", *Advances in Colloid and Interface Science*, 128-130 (2006) 37-46.
39. B. Fugetsu, W. Han, N. Endo, Y. Kamiya, and T. Okuhara, "Disassembling Single-Walled Carbon Nanotube Bundles by Dipole/Dipole Electrostatic Interactions", *Chemistry Letters*, 34 (2005) 1218–1219.
40. T. Yamamoto, Y. Miyauchi, J. Motoyanagi, T. Fukushima, T. Aida, M. Kato and S. Maruyama, "Improved Bath Sonication Method for Dispersion of Individual Single-Walled Carbon Nanotubes Using New Triphenylene-Based Surfactant", *Japanese Journal of Applied Physics*, vol. 47, 4 (2008) 2000-2004.

Chapter 2

Experimental Procedures

2.1 Raw materials

2.1.1 Titanium powders

Two kinds of commercially pure sponge and fine titanium powders have been used as the starting materials in this study. The sponge titanium powders, having mean particle size of 686 μm, are produced by the Kroll process [1], while the fine titanium powders with mean particle size of 30 μm are produced by Hydrogenation/Dehydrogenation (HDH) process [1]. Both sponge and fine titanium powders are supplied by TOHO TITANIUM Co., Ltd. The sponge titanium powders show much more irregular shape than that of fine titanium powders, which is due to the difference of their production process. The powder size and shape have affected the distribution of the nano carbon reinforcing materials on the Ti surface [2-3]. The chemical compositions and morphology of those starting titanium powders are shown in Table 2.1 and Figure 2.1, respectively.

High oxygen content [4-5] in the fine titanium powders could lead to stronger mechanical properties, compared to the sponge Ti powders. High chlorine content in the sponge Ti powders leads to the decrease of mechanical properties because it can easily form intermetallic compounds, for example $MgCl_2$, with other alloying elements during consolidation and hot extrusion process [2]. However, the focus on those two kinds of sponge and fine titanium is to study and implement the solution-coating technique in the commercial Ti powders without any changes of their original chemical compositions.

Table 2.1 Chemical compositions of starting Ti powder used in this study (wt.%).

Materials	Purity	Fe	Cl	Mg	Si	N	C	O	Ti
Sponge Ti	>97	0.01	0.07	0.03	<0.01	<0.01	0.01	0.069	Bal.
Fine Ti	>95	0.03	<0.002	<0.001	0.01	0.02	<0.01	0.21	Bal.

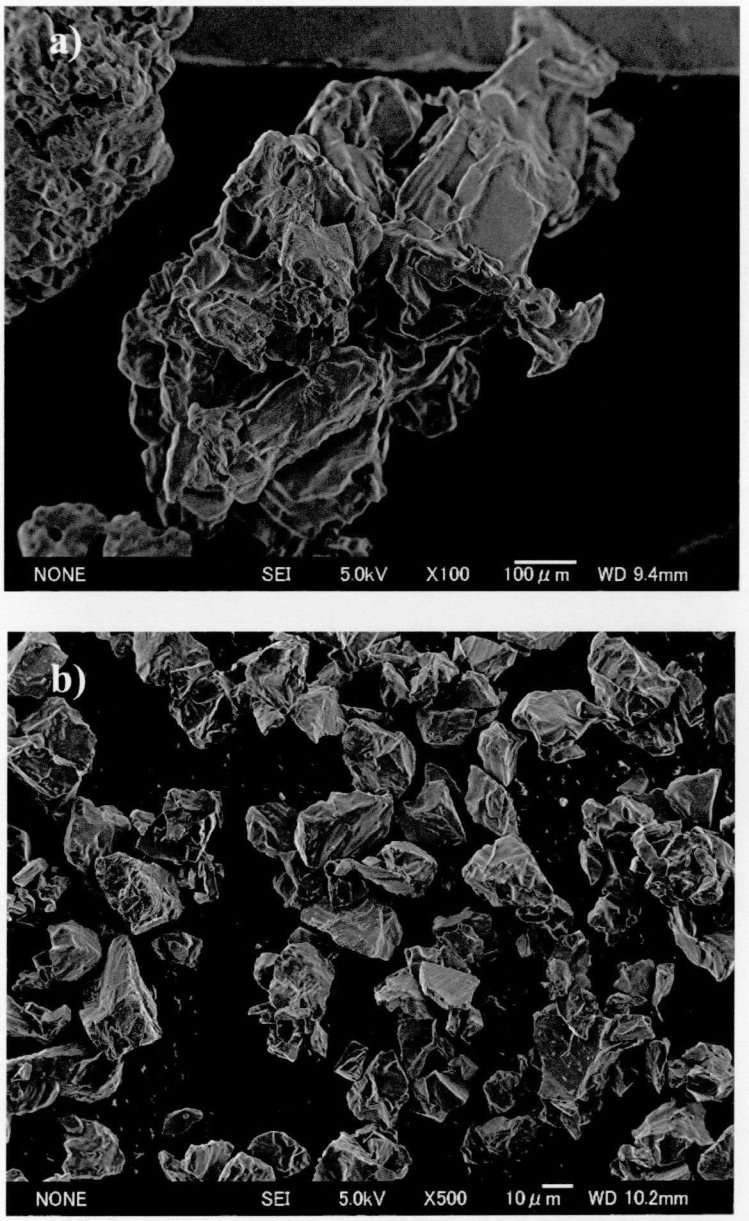

Figure 2.1 Commercially pure a) sponge and b) fine Ti powders used in this study.

2.1.2 Carbon reinforcing materials

The elemental carbon has many allotropes with various structures such as graphite, diamond and fullerene [6]. In this study, multi-wall carbon nanotubes (MWCNTs) are mainly used as the reinforcing material because of their ultra-high strength and modulus [7-8]. The MWCNTs with about 20 nm in diameter and 1 ~ 10 μm in length are produced by Bayer Material Science. The morphology of the multi-wall carbon nanotubes is shown in Figure 2.2.

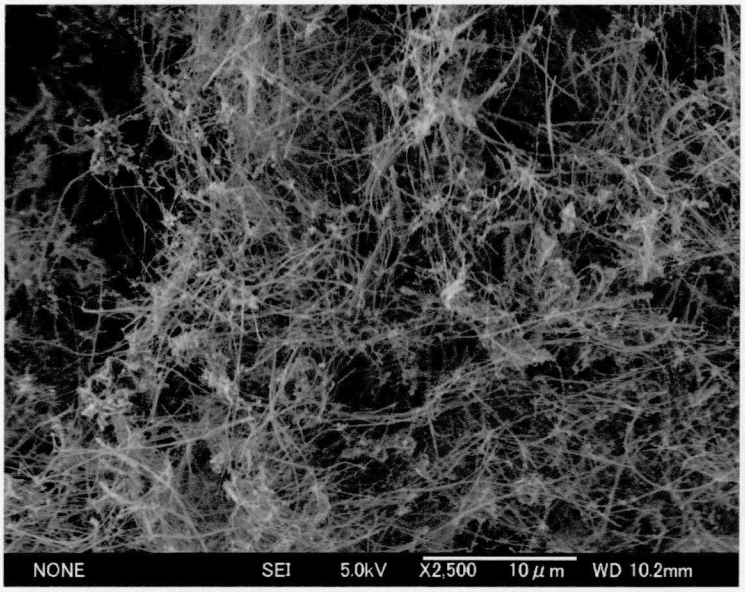

Figure 2.2 Bundled multi-wall carbon nanotubes (MWCNTs) with a diameter of about 20 nm.

In order to investigate the applicability of the solution-coating technique with various kinds of nano carbon materials for coating on Ti powder surfaces, the commercially carbon reinforcing materials, e.g., carbon black, acetylene black and graphene are also used in this study.

2.2 Solution-coating technique

The solution-coating technique consists of two simple processing steps: primary coating by zwitterionic surfactant solution containing nano carbon reinforcing materials and secondary drying step. The solution-coating steps are illustrated in Figure 2.3

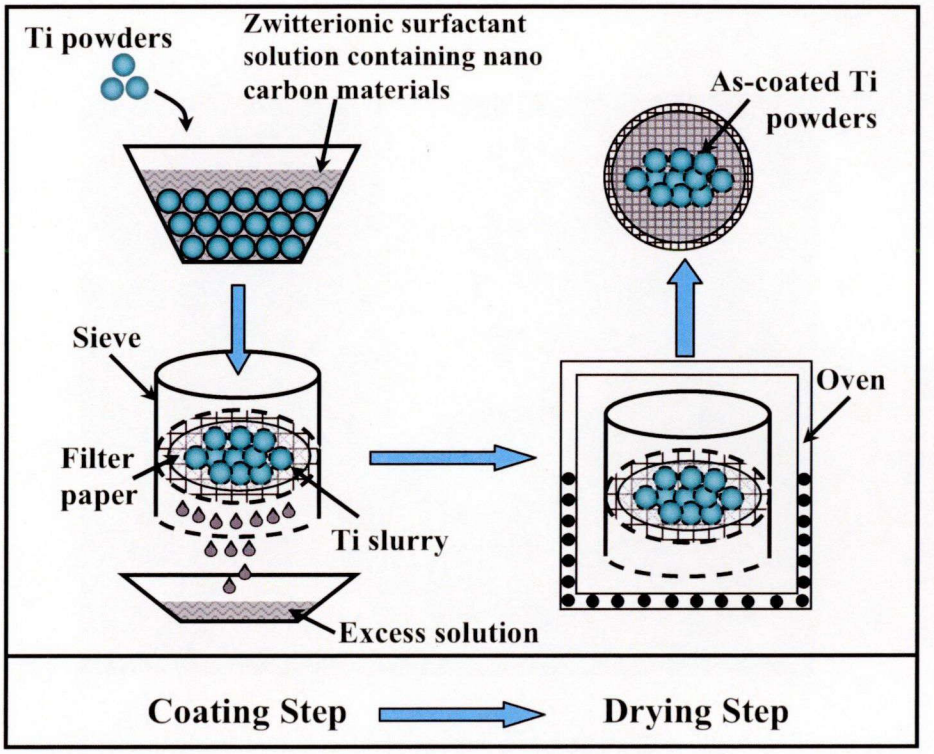

Figure 2.3 Solution-coating technique: coating step and drying step.

In the primary coating step, 130 g of Ti powders is immersed into 60 g of the nano carbon/zwitterionic surfactant solution and subsequently mixed in the solution. The mixture is poured into a sieve with < 46 μm mesh size to drain excess solution. The CNTs coated Ti powders are obtained in the slurry form. The secondary drying step is carried out subsequently. The slurry of the coated Ti powders is dried in an oven at 373 K for 10.8 ks. During the drying step, the solid zwitterionic substances are formed on the Ti powder surface. These substances would behave as an impurity in the composite material and should be removed before consolidation because they would otherwise change to gasses at temperature above 773 K [9]. The CNTs coated Ti composite powders with residual solid zwitterionic

substances are heated again in a horizontal tube furnace at 873 K for 3.6 ks under an Ar protective atmosphere. Detail on the elimination of residual solid zwitterionic substances is discussed in the following chapter 3.

2.3 Characterization of residual solid zwitterionic substance

The residual solid zwitterionic substances could be considered as a binder in the powder metallurgy (P/M) process. The thermal decomposition of the binder has been widely used in P/M industry. Therefore, a proper debinding temperature should be determined using the Thermo-Gravitational Analyzer (TG-DTA, Shimadzu: DTG-60). The zwitterionic surfactant solution with and without nano carbon materials are completely dried as thin film in an oven at 373 K and subjected to the TG-DTA using heating rate 10 K/min, at room temperature up to 873 K under an Ar gas atmosphere. 30 mg of alumina (α-Al_2O_3) powder is used as the reference material.

2.4 Characterization of coated titanium powders

2.4.1 Thermal analysis measurement

Differential Thermal Analysis (DTA) and Thermo-Gravitational Analysis (TGA) are simultaneously used to investigate the thermochemical reactions of the coated Ti powders. The measurement uses the same device (DTA/TG, Shimadzu: DTG-60) as mentioned in the previous section 2.3. An amount of about 50 mg of the CNTs coated Ti powders is put into an alumina pan along with 30 mg of alumina powder as the reference material in another pan. Both the sample and the reference material are heated to 1273 K with a heating rate of 10 K/min. Atmosphere in the chamber is controlled by feeding of Ar gas at a rate of 150ml/min.

2.4.2 Morphology and phase characterization

The coated Ti powders of both before and after debinding step are investigated to understand the complete removal of residual solid zwitterionic, the distribution of nano carbon materials and any reaction occurred at the interface of nano carbon and Ti powder surface using Scanning Electron Microscope equipped with an Energy Dispersive Spectrometer (SEM-EDS, JEOL: JSM-6500F).

In order to investigate the compound formation of the coated Ti powders at elevated temperature, high temperature X-ray diffraction (XRD) analysis is carried out at the temperature ranges from 723 – 1273 K with a step size of 50 K and the scanning ranges of 2θ from 20 – 50 deg. under an Ar gas atmosphere. The investigation is performed using an X-ray diffractometer (XRD, Shimadzu: XRD-6100) with a wavelength of 1.54060 Å of Cu-Kα radiation. Furthermore, the XRD analysis at room temperature of the coated Ti powders is also carried out. The scanning range of 2θ is 30 – 80 deg. The results of the high temperature XRD analysis clearly show the thermochemical reaction sequence, which can be used to determine the suitable sintering temperature.

2.5 Consolidation of coated Ti powders

2.5.1 Spark plasma sintering

The Spark Plasma Sintering (SPS), schematically illustrated in Figure 2.4, is used to primary consolidate the CNTs coated Ti composite powders for preparation of the sintered Ti composite billets. The sintered billets show the relative density of over 96%, compared to pure Ti ($\rho = 4500$ kg/m^3) [10]. Approximately 130 g of the coated Ti powder is poured into a graphite die with a diameter of 42 mm. The SPS is carried out at various temperatures in the range of 873 – 1573 K and different sintering times from 600 – 1800 s under vacuum atmosphere (<4 Pa). The heating rate is 20 K/min and the applied pressure during the SPS process is 30 MPa.

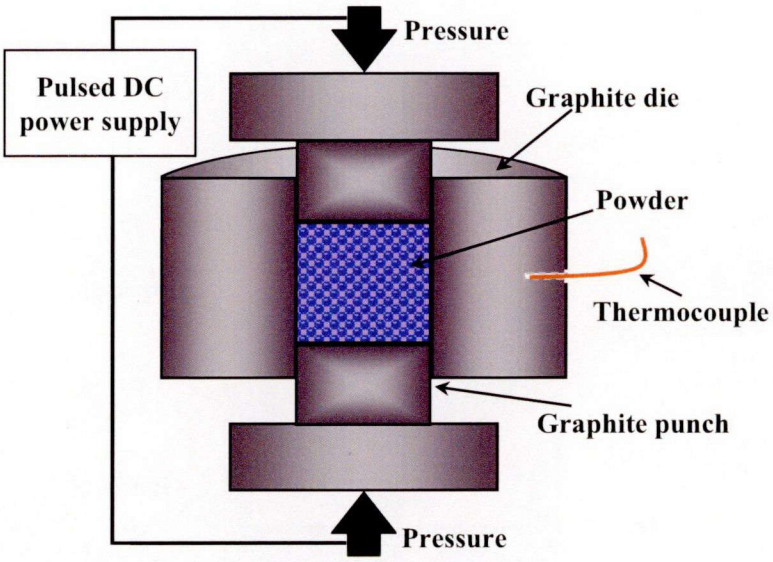

Figure 2.4 Schematic illustration of the Spark Plasma Sintering (SPS) process.

2.5.2 Hot extrusion

A final consolidation by hot extrusion is necessary to make a full density and shaping of the SPSed Ti composite billet as a rod. Figure 2.5 shows a drawing of diagram of the extrusion die sets used in this experiment. The SPSed Ti billet with 42 mm diameter and about 22 mm height is heated in a ULVAC infrared gold image furnace which heat from the heat source is reflected to the billet in a silica tube. The target heating temperature can be accelerated in a few minutes. The heating rate of 2 K/s is used to heat the SPSed Ti composite billet at the various temperatures from 773 – 1273 K with 180s-holding under an Ar protective atmosphere. After the heating step, the heated Ti composite billet is immediately extruded using a 2000 kN hydraulic press machine. To prevent heat loss of the heated Ti composite billet during extrusion, the extrusion die sets, die, container and dummy plate, are heated at 673 K in a muffle furnace for at least two hours before start of the extrusion process. Both the extrusion speeds of 3 and 6 mm/s are used in this experiment. The extrusion ratio of 37 is used to produce an extrusion rod of 7.0 mm diameter and approximately 800 mm in length.

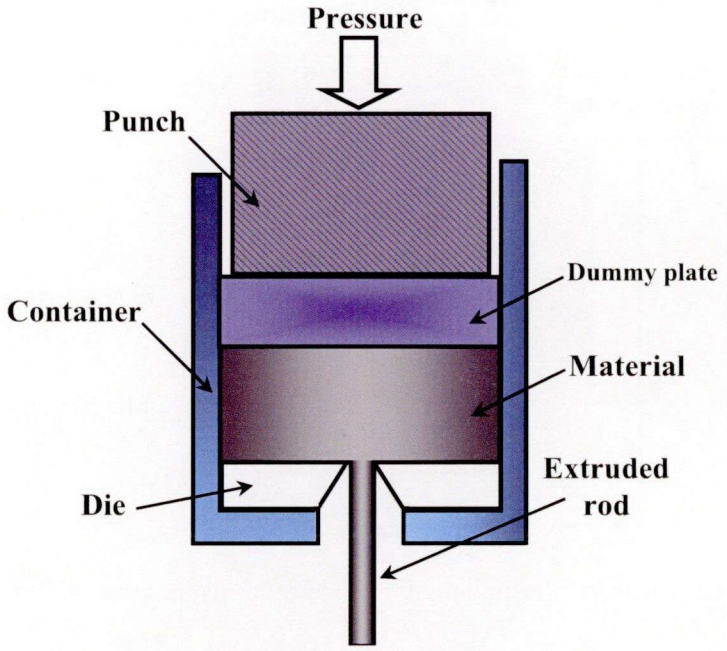

Figure 2.5 Drawing diagram of hot extrusion process.

2.6 Characterization of extruded titanium composites

Microstructure and phase characterization of the extruded Ti composites containing nano carbon materials are investigated by optical microscope, SEM-EDS and XRD technique. The extruded rod is cut in the extrusion direction and grinded with SiC abrasive paper from 240 up to 2000 grit, and then polished using 0.3 and 0.05 μm alumina suspension, respectively. Finally, microstructure is developed by Kroll's reagent (1.5mL HF + 4mL HNO_3 + 94mL H_2O) microetchant. Grain sizes of the extruded Ti composite materials, as well as the *in-situ* formed TiC particles, are evaluated using the image analysis software (Image-Pro Plus 4.0.0.11). SEM and EDS are used to investigate the microstructures at high magnification and analyze the chemical compositions of the dispersed intermetallic compounds. XRD analysis is used to investigate and confirm the phases existing in the extruded Ti composite materials. Furthermore, the Cohen's method of least square analysis [11] is used to analyze the change of lattice constants, a and c axes, of the extruded Ti composite materials.

2.7 Mechanical properties evaluation

2.7.1 Room temperature tensile and hardness test

Tensile test is performed using a universal testing machine (Shimadzu: Autograph AG-X 50 KN) under a strain rate of 5×10^{-4} s^{-1} at room temperature. The extruded Ti composite rods with 7 mm diameter are machined into tensile specimen bars of 3.0 mm in diameter and 20 mm in gauge length according to ASTM E8M standard [12]. The average tested result of three tensile specimens for each Ti composite and their processing conditions are reported. The fractured surfaces of tensile tested samples are also investigated using SEM-EDS.

Hardness of the extruded Ti composite materials is measured by a micro-Vickers hardness tester (Shimadzu: HMV-2T) with an applied load of 0.49 N. The average value of 30 indentations is introduced.

2.7.2 Fatigue Test

In order to evaluate the strength of the extruded Ti composite materials in dynamic mode, the fatigue test is performed using a servo-hydraulic axial fatigue testing machine (Shimadzu: Servopulser E100KN). The extruded Ti composite rods of 13.3 mm in diameter and approximately 1000 mm in length are primarily fabricated and then machined to fatigue specimen of 5.0 mm in diameter with a continuous radius between ends according to ASTM E466 standard [13]. The drawing of fatigue specimen is shown in Figure 2.6.

The size of fatigue specimen is bigger than that of tensile specimen. The objectives in increasing specimen size are to prove the applicability of the solution-coating technique and to scale up the productivity of this technique for industrial implementation. Detail on the scaling up of the Ti coated with MWCNTs via solution-coating technique is discussed in the chapter 5.

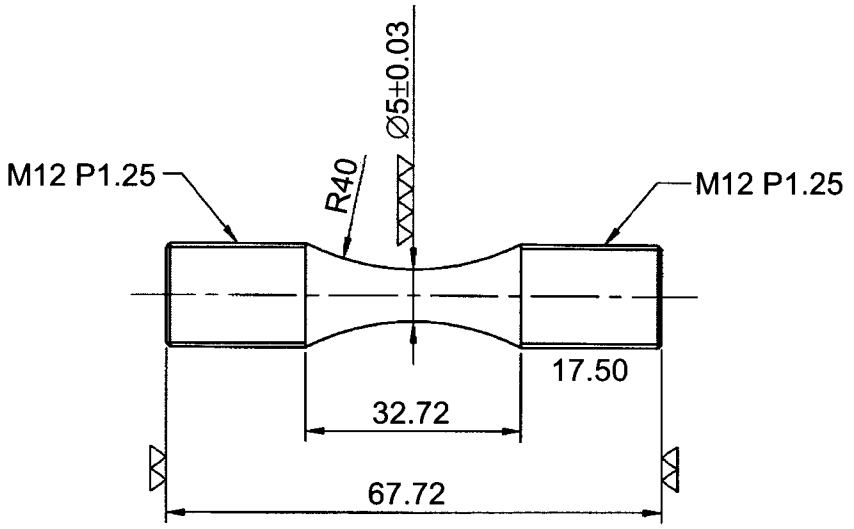

Figure 2.6 Drawing of fatigue specimen (unit: mm.).

2.7.3 High temperature tensile and hardness test

The mechanical stability of the extruded Ti composite materials at elevated temperature is evaluated in order to understand the effect of temperature on their mechanical response. The high temperature tensile properties are evaluated using a horizontal high temperature tensile testing machine (Yonekura: 5KN) as shown in Figure 2.7. In order to reduce a residual strain, the extruded Ti composite rod with a diameter of 7.0 mm is annealed at 473 K for 360 ks (100 hours.) in a muffle furnace under an Ar gas atmosphere with a flow rate of 0.5 l/min. After the annealing process, the annealed sample is machined to tensile specimen bars of 3.0 mm in diameter and 20 mm in gauge length. The tensile specimen is heated to 473, 573 and 673 K, respectively, with a heating rate of 2 K/s and kept at each temperature for 300 s before start of testing. The temperature in the testing chamber is constantly kept using an infrared gold image heater until the end of the test

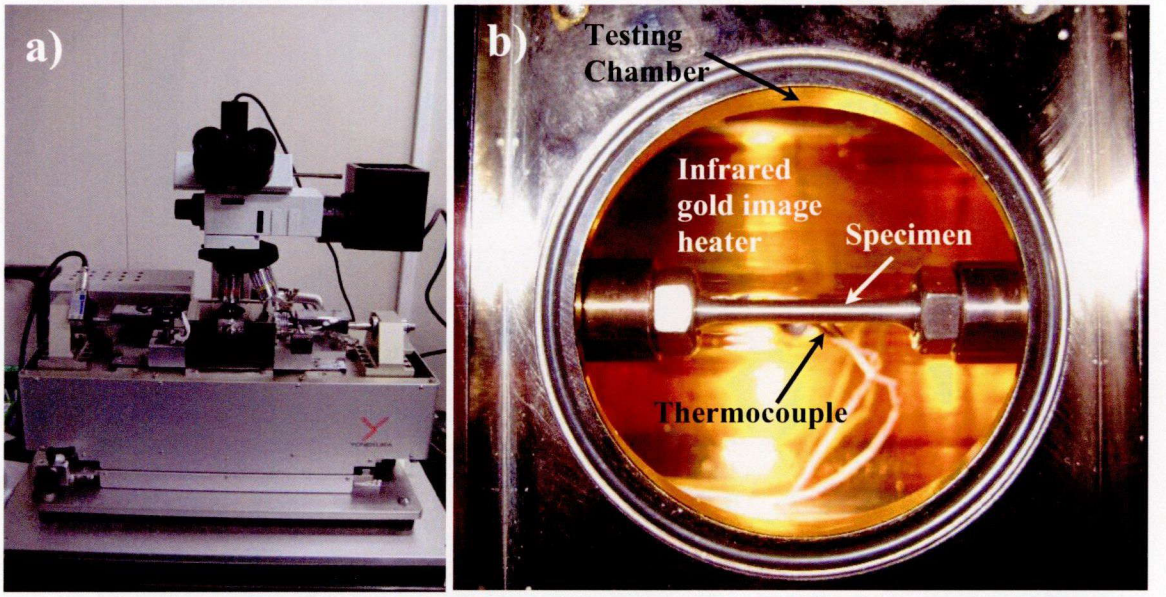

Figure 2.7 Horizontal high temperature tensile testing machine, a) overview and b) inside testing chamber.

High temperature hardness test is also evaluated using homemade heating equipment attached to a micro-Vickers hardness tester. The extruded Ti composite materials are cut in transversal direction of extrusion direction with a thickness of about 5 mm. and annealed using the same condition as mentioned above. The annealed sample is fixed with the heater which is attached to the Vickers hardness tester, shown in Figure 2.8. The measurement is started from room temperature 323 K until 573 K with an increasing step of 50 K. The test sample is kept at the testing temperature for 300 s before start of the test. The number of test, testing load and time are 5, 0.245 N and 10 s, respectively.

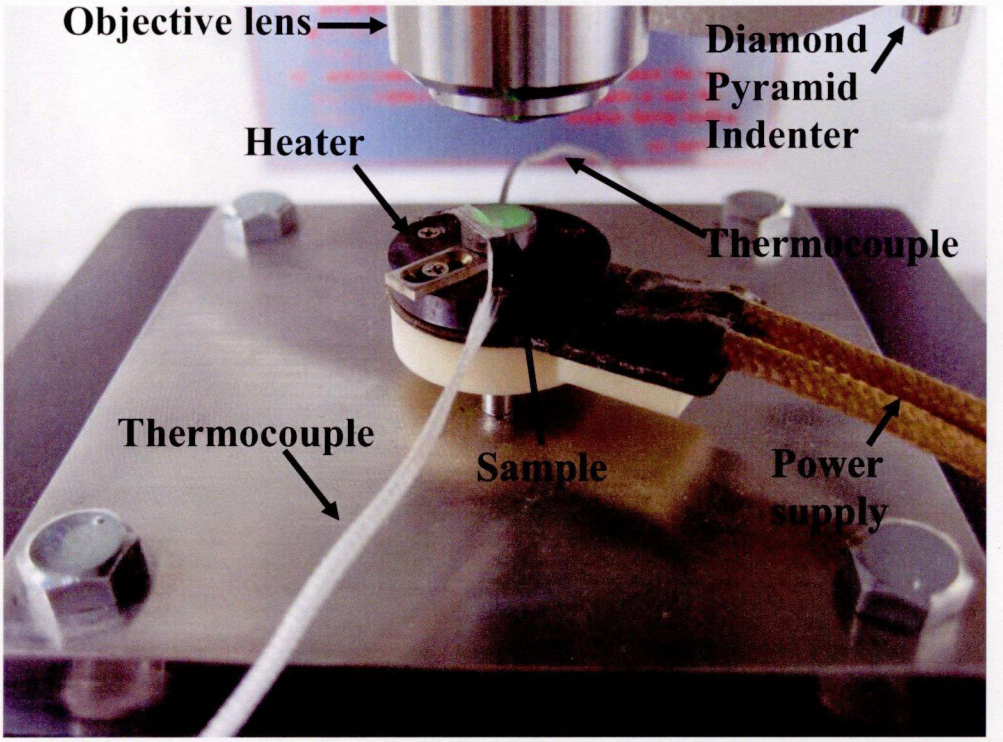

Figure 2.8 Homemade heating equipment attached to a micro-Vickers hardness tester.

References

1. G. Lütjering and J.C. Williams, *Titanium*, 2nd ed., Springer-Verlag, Germany (2007).
2. T. Threrujirapapong, K. Kondoh, H. Imai, J. Umeda and B. Fugetsu, "Mechanical Properties of A Titanium Matrix Composite Reinforced with Low Cost Carbon Black via Powder Metallurgy Processing", *Materials Transactions*, 50 (2009) 2757-2762.
3. T. Threrujirapapong, K. Kondoh, H. Imai, J. Umeda and B. Fugetsu, "Hot Extrusion of Pure Titanium Reinforced with Carbon Nanotubes", *Steel Research International*, 81 (2010) No. 9, 1320-1323.
4. H. Conrad, "Effect of Interstitial Solutes on The Strength and Ductility of Titanium", *Progress in Materials Science*, 26 (1981) 123-403.
5. C. Ouchi, H. Iizumi and S. Mitao, "Effect of Ultra-High Purification and Addition of Interstitial Element on Properties of Pure Titanium and Titanium Alloy", *Materials Science and Engineering A*, 243 (1998) 186-195.
6. H. O. Pierson, *Handbook of Carbon, Graphite, Diamond, and Fullerenes: Properties, Processing, and Applications*, Noyes Publications, New Jersey, USA (1993).
7. S. Iijima, C. Brabec, A. Maiti, and J. Bernholc, "Structural Flexibility of Carbon Nanotubes", *Journal of Chemical Physics*, 104 (1996) 2089–2092.
8. M. R. Falvo, G. J. Clary, R. M. Taylor II, V. Chi, F.P. Brooks Jr, S. Washburn and R. Superfine, "Bending and Buckling of Carbon Nanotubes under Large Strain", *Nature*, 389 (1997) 582–584.
9. K. Kondoh, H. Fukuda, H. Imai and B. Fugetsu: In proceeding of the TMS annual meeting and exhibition: Magnesium Technology, New Orleans, USA, (2008) 289-291.
10. C. Leyens and M. Peters, *Titanium and Titanium alloys*, Wiley-VCH, Germany (2003).
11. B. D. Cullity and S.R Stock, *Elements of X-Ray Diffraction*, 3rd ed., Prentice Hall, USA, (2001).
12. ASTM E8M: Standard Test Methods for Tension Testing of Metallic Materials [Metric], ASTM international, West Conshohocken, PA, USA (2001).
13. ASTM E466: Standard Practice for Conducting Force Controlled Constant Amplitude Axial Fatigue Test of Metallic Materials, ASTM international, West Conshohocken, PA, USA (1996).

Chapter 3

Processing of Titanium Matrix-Carbon Nanotubes via Solution-Coating Powder Technique

In this chapter, the thermal characteristics of both solid zwitterionic substances with and without MWCNTs existing on the powder surface are firstly investigated by the DTA analysis because their thermal behaviors at elevated temperature play an important role in determination of the starting temperature of the debinding process. Debinding atmosphere is another important factor in controlling mechanical properties of the final product. The selection of the suitable debinding atmosphere is done by comparison between the reducing atmosphere and inert atmosphere. Furthermore, the DTA and the high temperature XRD analyses are also used to investigate the formation and identification of the intermetallic compounds on the Ti powder coated with MWCNTs. The debinded Ti powders coated with MWCNTs are consolidated by the spark plasma sintering, and subsequently extruded by hot extrusion process. The extrusion load characteristics of the sintered Ti billets are evaluated in the last section.

3.1 Thermal analysis of solid zwitterionic substance

In order to determine the debinding temperature for the coated Ti powders, the zwitterionic surfactant solution with and without MWCNTs are completely dried in an oven. The thermal resolution of thin films of those dried solid zwitterionic substances is analyzed by the weight loss during heating using the thermal-gravitational analyzer (TGA). The TGA results are plotted in Figure 3.1. In the case of dried solid zwitterionic substances, the weight loss starts at 539 K and obviously occurs until 700 K. The rate in weight change becomes very small and constant after 873 K. This means that the solid zwitterionic substances are completely burned and thermally decomposed over 873 K. In the case of dried solid zwitterionic substances containing MWCNTs, the weight loss quickly starts at 503 K and terminates at about 773 K. The weight change rate is extremely small compared to that of the substances without MWCNTs because CNTs are never burned during heating until 773 K in

TGA evaluation. According to the results of thermal gravimetric analysis, the suitable debinding temperature should be selected at the temperature of 873 K or more.

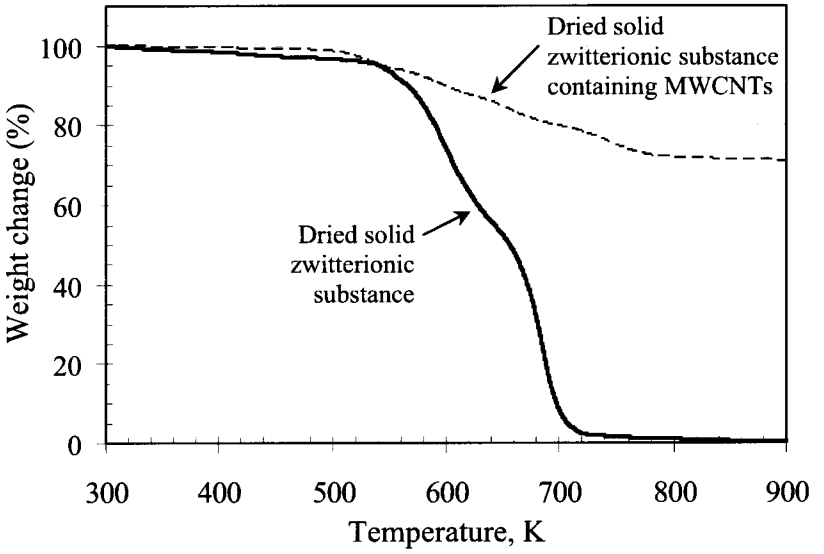

Figure 3.1 Weight change percentage of the dried solid zwitterionic substances containing MWCNTs.

3.2 Selection of debinding atmosphere

In the P/M process, the debinding atmosphere is very important to control and reduce contaminations on the powder surface. Generally, thermal debinding is carried out in either vacuum or an atmosphere of air, hydrogen, nitrogen, argon or mixed atmosphere depending on the final purpose. Pure hydrogen is an excellent reducing gas which can effectively reduce oxides and contaminations on the metal powder surface [1-2]. In this experiment, the hydrogen-argon mixed gases and pure argon gas are used to compare their effect for debinding the surfactant films. The effect of the debinding atmosphere is indirectly investigated by the microstructure observation and mechanical response of the extruded fine Ti powder material with no reinforcement. The fine Ti powders are coated by the zwitterionic solution and subsequently dried at 373 K for 1.8 ks. The coated fine Ti powders with residual solid zwitterionic substances are debinded in a horizontal tube furnace at 873 K for 3.6 ks under the different atmospheres of 10 % hydrogen – 90% argon mixed gases and pure argon gas, respectively. The XRD patterns of the debinded pure Ti powders are shown

in Figure 3.2. The results clearly show the formation of TiH_2 compound which corresponds to the previous reports [3-5].

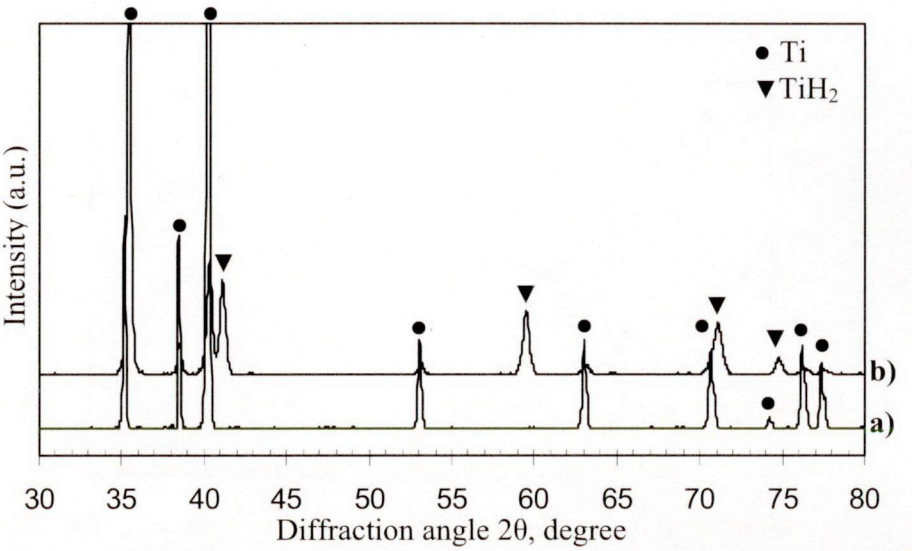

Figure 3.2 XRD patterns of the debinded fine Ti powders using a) argon gas and b) hydrogen-argon mixed gases.

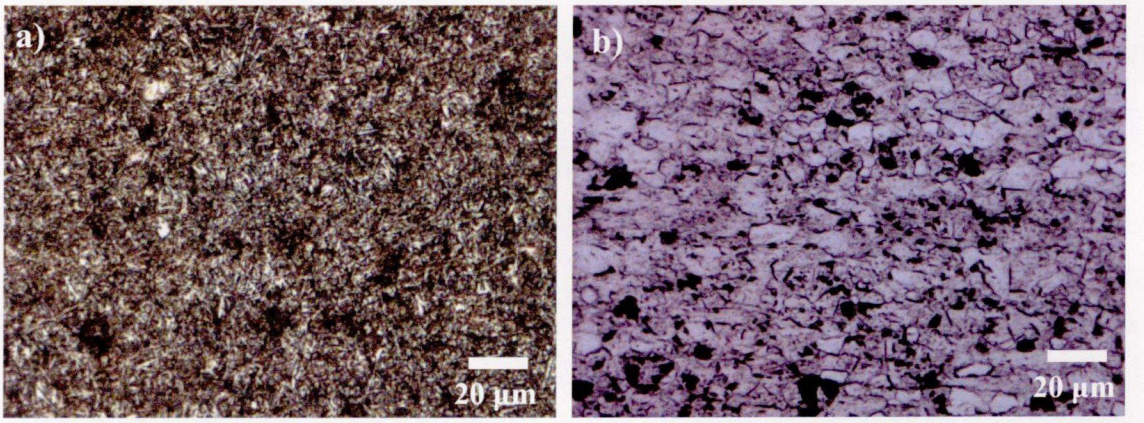

Figure 3.3 Microstructure of the extruded fine Ti composites debinded by a) hydrogen-argon mixed gases and b) argon gas.

The optical microstructures of the extruded fine Ti powder composites debinded by hydrogen-argon mixed gases and argon gas are shown in Figure 3.3. For the hydrogen-argon mixed gases in Figure 3.3 (a), the microstructure reveals the martensitic structure as a result of the interstitial solid solution of H atoms. The martensitic structure has much stronger than

the normal alpha grains, but the elongation is generally much lower than that of alpha grain in Figure 3.3 (b) [6-7]. The mechanical properties of those extruded materials are listed in Table 3.1. It indicates that the extruded fine Ti powder composite debinded by hydrogen-argon mixed gases has no ductility because of the formation and existence of TiH_2 brittle compounds in Ti matrix. Therefore, argon gas should be selected in the debinding step.

Table 3.1 The mechanical properties of the extruded fine Ti composites debinded by hydrogen-argon mixed gases and argon gas.

Debinding atmosphere	YS [MPa]	TS [MPa]	Elongation [%]	HV0.05
Hydrogen-Argon mixed gases	704.76	709.50	0.10	367
Pure argon gas	509.62	675.67	31.23	273

3.3 Characteristic of coated Ti powders

3.3.1 Thermal analysis of Ti powders coated with carbon nanotubes

According to the determination of the debinding temperature in the section 3.1, the fine Ti powders coated with zwitterionic surfactant films using the solution containing 1.0, 2.0 and 3.0 wt.% of MWCNTs are debinded at 873 K for 3600 s under an Ar atmosphere. The debinded Ti powders are subsequently investigated the thermochemical reactions upon heating by the DTA equipment. The DTA profiles are shown in Figure 3.4. The formation of intermetallics can be identified by an exothermic peak in DTA analysis. The DTA profiles of the debinded fine Ti powders which coated with zwitterionic solution containing 1.0 and 2.0 wt.% MWCNTs almost show the same pattern. The first exothermic peaks of them are detected at 1157 and 1152 K, respectively, while the debinded fine Ti powders coated with zwitterionic solution containing 3.0 wt.% MWCNTs show the first exothermic peak at 1008 K. It should be noted that the faster exothermic peak, in the case of 3.0 wt.% MWCNTs, is related with the amount of the MWCNTs which are deposited on the Ti surface. For further understanding, high temperature XRD analysis of the debinded fine Ti powders is performed.

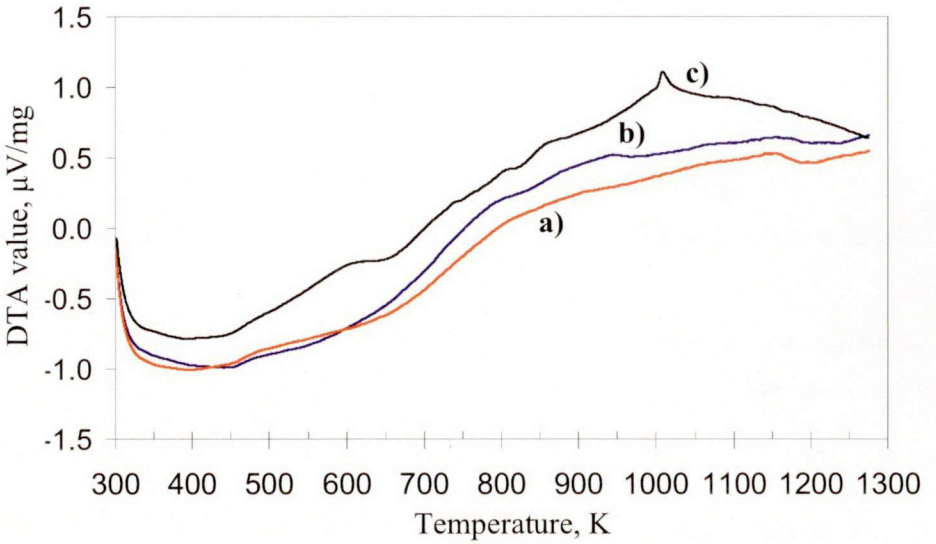

Figure 3.4 DTA profiles of the debinded fine Ti powders coated with zwitterionic solution containing a) 1.0 b) 2.0 and c) 3.0 wt.% MWCNTs.

3.3.2 Phase identification

The debinded fine Ti powders coated with 3.0wt.% MWCNTs/zwitterionic solution are used as a representative sample because it clearly shows an exothermic peak according to the DTA results. Figure 3.5 shows the high temperature XRD patterns of the representative sample at temperature in the range of 723 to 1273 K. The results indicate that the onset temperature of the TiC intermetallic compounds is 923 K. TiC intermetallic compounds continue growth until the temperature of 1273 which is indicated by the increase of its peak intensity. Moreover, the results also indicate the formation of TiO_2 and Fe_3C at 973 and 1223 K, respectively. Both reactions of TiO_2 and Fe_3C formation are spontaneously caused by the thermal activation at high temperature according to thermodynamics data [8-10]. The formation of TiO_2 can be accounted for by insufficient protection of the tested sample by flowing Ar gas during measurement, while the Fe_3C compound is caused by the reaction between C and Fe atoms which are originated from MWCNTs and alloying element in Ti powders, respectively.

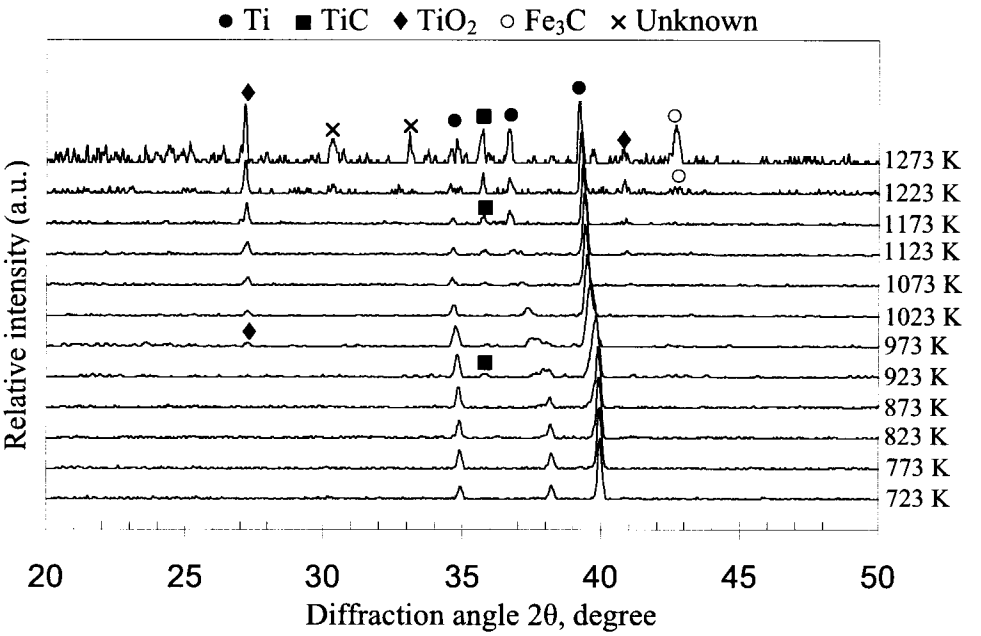

Figure 3.5 XRD patterns of the debinded fine Ti powders coated with 3.0wt.% MWCNTs/zwitterionic solution at various temperatures.

According to the thermal analysis result of solid zwitterionic substance in the section 3.1 and the high temperature XRD results, the optimal temperature for the debinding step is selected at 873 K. Moreover, the high temperature XRD results can be used to determine the thermal processing condition for the next process, especially consolidation temperature. To prevent the formation of Fe_3C and TiO_2 intermetallic compounds, the consolidation temperatures should be selected in the range of 923 K to 1173 K with a controlled atmosphere [1-2].

3.3.3 Morphology

The morphologies of sponge and fine Ti powders coated with MWCNTs after debinding process are observed by SEM. The MWCNTs are individually distributed on the Ti powder surface as a result of high dispersion of individual MWCNT in zwitterionic solution [11]. In the case of sponge Ti powders, the distribution of MWCNTs mainly consists of local deposition on the facet of the powder as shown in Figure 3.6 (a). Due to the sponge powder has many facets as shown in Figure 2.1 (a), the MWCNTs prefer deposition at the

edge of powder than in the other areas of the Ti surfaces. The ideal dispersion of individual MWCNT is also found as shown in Figure 3.6 (b). In the case of fine Ti powders, the distribution of MWCNTs reveals homogenous dispersion on the Ti surface as shown in Figure 3.7. The difference of the deposited quantity of MWCNTs in each area on the Ti powder surface causes the varying in morphology of the TiC particles during the sintering.

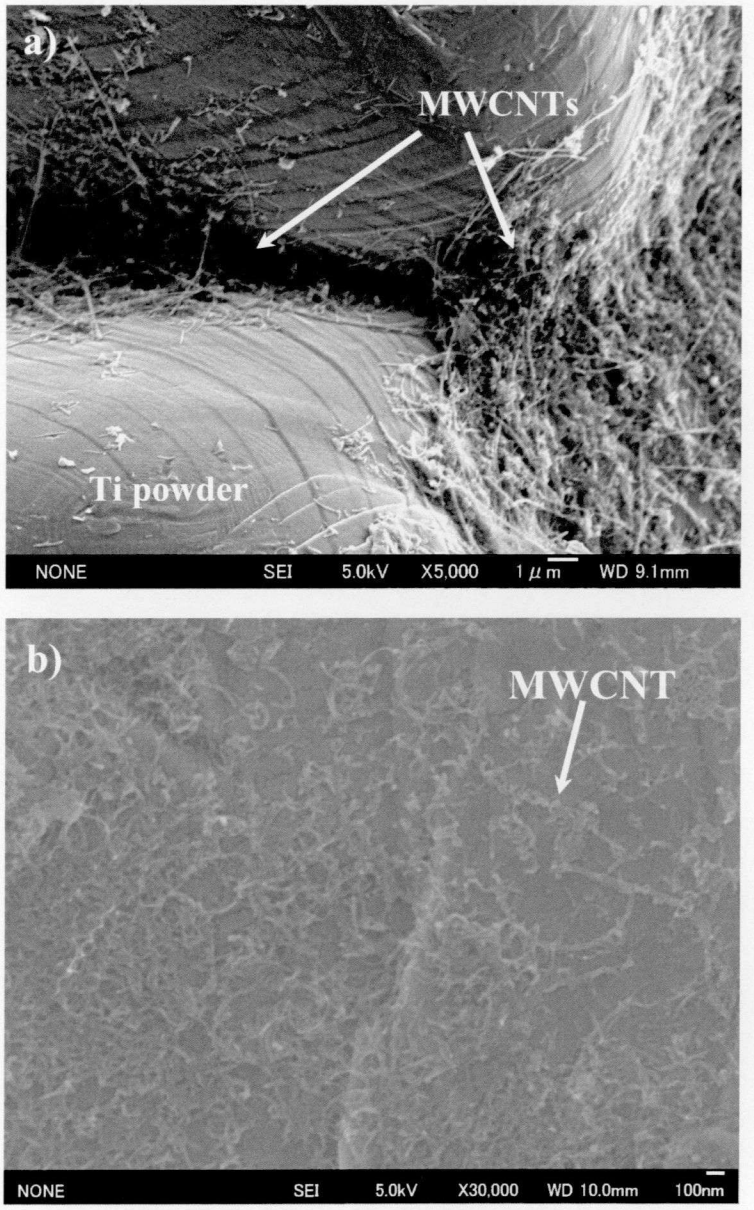

Figure 3.6 Sponge Ti powder coated with MWCNTs a) locally deposited on facet and b) individually dispersed on Ti surface.

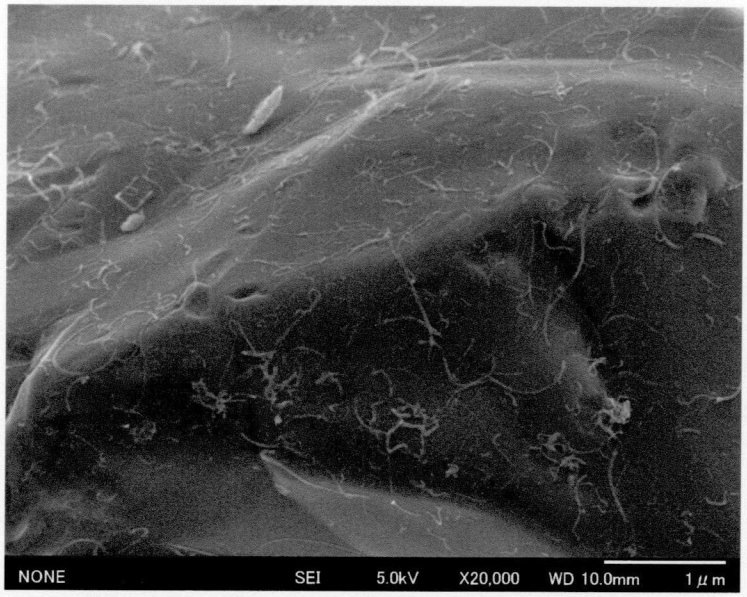

Figure 3.7 Homogeneous distribution of individual MWCNT on surface of fine Ti powder.

3.3.4 Quantity of deposited MWCNTs on Ti powders

In the solution-coating technique, the amounts of deposited MWCNTs are generally less than those of original concentration in the solution because they can flow with the solution during the drain of excess solution. The carbon content analysis of the final product is used to reflect the actual amount of deposited MWCNTs on the Ti powder surface. Therefore, the carbon contents in the extruded sponge and fine Ti powder composites coated with 1.0, 2.0 and 3.0 wt.% MWCNTs are measured. By subtracting the carbon content in the starting materials, the actual deposited MWCNTs will be obtained as shown in Figure 3.8.

The results indicate that the amount of deposited MWCNTs on each Ti powder surface increases with increasing MWCNTs concentration in zwitterionic solution. MWCNTs can be deposited on the fine Ti powders higher than the sponge Ti powders. This is due to the fact that fine Ti powders, which have a smaller size compared to sponge Ti powders, exhibit a higher specific surface area than sponge Ti powders. Hence, at the same amount of powder, fine Ti powder has a higher probability of being coated with MWCNTs than sponge Ti powder. Furthermore, the results suggest that the solution-coating technique

can not linearly control the deposition of MWCNTs on Ti powders by adjusting their concentration in zwitterionic solution.

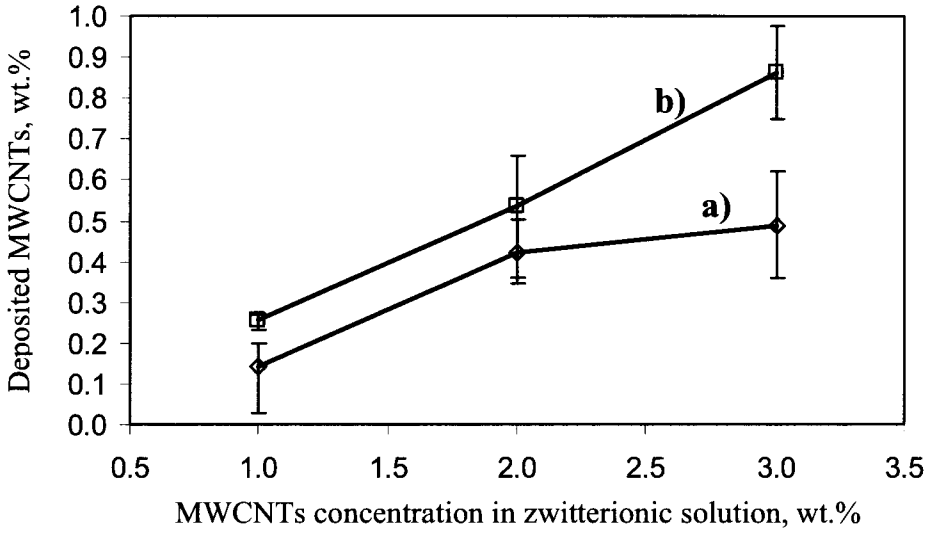

Figure 3.8 Amount of deposited MWCNTs on a) sponge and b) fine Ti powders.

3.4 Consolidation of coated Ti powders

The consolidation of the debinded Ti powders can be divided into two steps: primary consolidation by SPS process and secondary consolidation by conventional hot extrusion process. The objective of the SPS process is to consolidate the debinded Ti powders with a proper high density, and also to induce the formation of titanium carbide (TiC) compounds. The sintering temperature and time of the SPS process are basically followed by the conventional sintering process of Ti powder [1]. Moreover, the SPS process can provide more uniform density and high metallurgical bonding between powder particles with short time sintering. The sintered Ti composite billets coated by solution-coating technique show a very high relative density (at least 96%), compared to the sintered pure Ti, depending on the amount of MWCNTs coated on the Ti surface. The formation and growth of TiC compound simultaneously occur during SPS process. The effect of SPS temperatures and times on the microstructure and mechanical response of the extruded Ti composite will be discussed in the chapter 4.

To fabricate a full density material, the secondary consolidation after sintering process is performed by hot extrusion process. The formability of the sintered Ti composites in the hot extrusion process is more important to investigate than that in SPS process because the materials finally need to form to a required shape. Furthermore, the obtained information from the investigation can be used to design some of optimum parameters in extrusion for an industrial approach. The sponge Ti powders coated with MWCNTs are used as a representative sample to investigate the extrudability because they have a lower quantity of MWCNTs on their surface. The investigation result, which can be considered as the lower boundary of extrudability of Ti coated with MWCNTs, is shown in Figure 3.9.

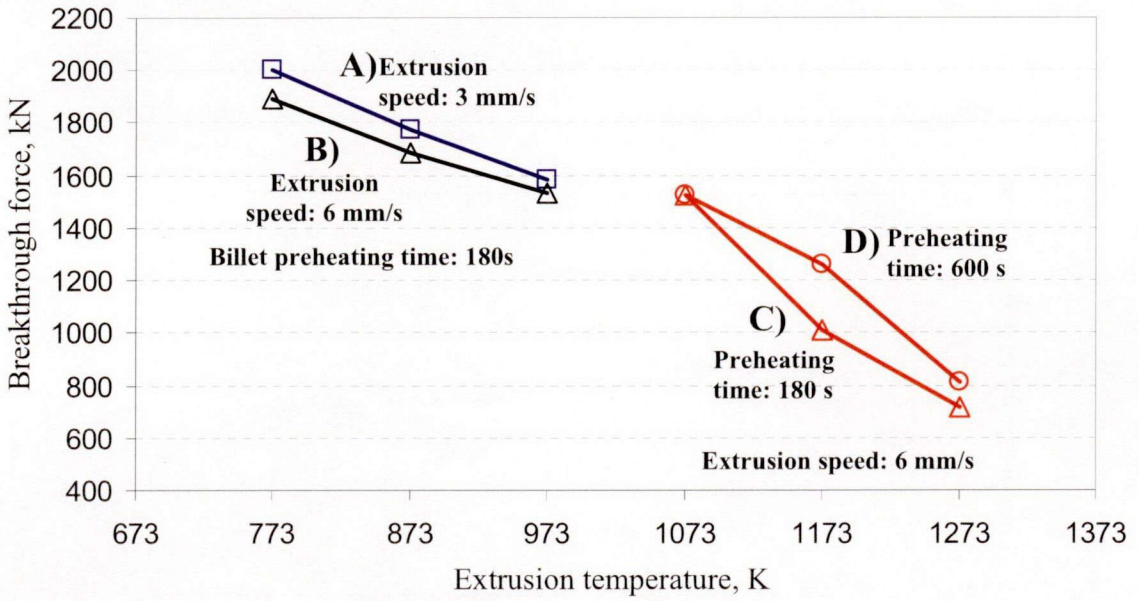

Figure 3.9 Influence of extrusion temperature (billet temperature) on the breakthrough force of the sponge Ti composites. A) and B) 1.0wt. % coated MWCNTs + SPSed 873 K for 600 s. C) and D) 2.0wt. % coated MWCNTs + SPSed 1273 K for 600 s.

Regardless of the effect of MWCNTs, the higher extrusion temperature causes the decrease of breakthrough force of Ti composite billet. This is because the softening phenomenon [12] highly occurs in the Ti billet at the higher extrusion temperature. The observed results are divided into 4 cases, as indicated by A, B, C and D in Figure 3.9. The first two cases, A and B, are coated with 1.0 wt.% MWCNTs/zwitterionic solution and subsequently SPSed at 873 K for 600 s, which are extruded with different speeds (3mm/s and

6mm/s) The last two cases, C and D, are coated with 2.0 wt.% MWCNTs/zwitterionic solution and subsequently SPSed at 1273 K for 600 s, which are extruded with a preheating time of Ti billet at 180 s to 600 s, respectively.

The effect of extrusion speed on breakthrough force indicates that the higher extrusion speed, in the case of B, causes a slight decrease in the breakthrough force. The increase extrusion speed leads to the higher extrusion force which contributes to the decrease in the breakthrough force. In other words, the input extrusion energy of the case B is larger than that of case A, so that the material can be conveniently extruded. It is noted that the extrusion speed of 3 mm/s, in the case of A, at the extrusion temperature of 773 K yields a few centimeters of extruded rod. That can be accounted for an insufficient input energy which is limited by the maximum capability of the extrusion machine in this study.

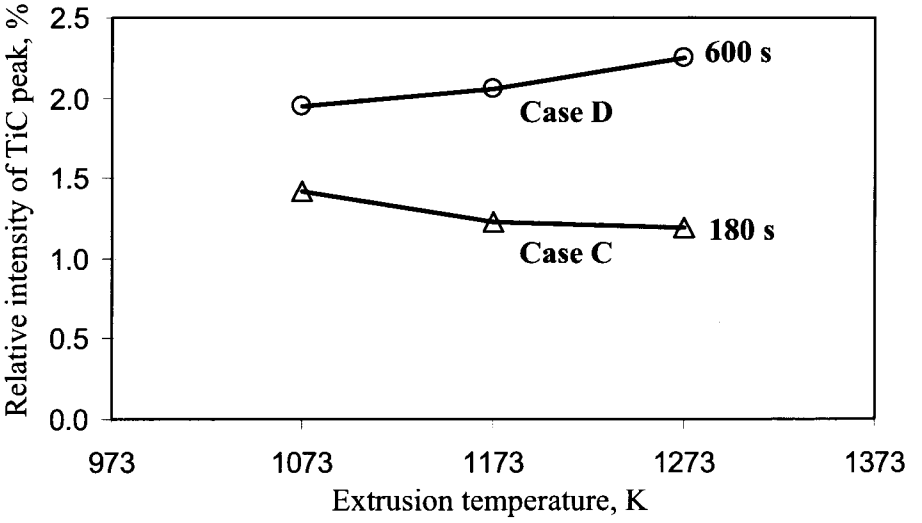

Figure 3.10 Maximum relative intensity of TiC peak of the case C and D in Figure 3.9.

The effect of preheating time on the breakthrough force indicates that a longer preheating time at the higher temperature, in the case of D, results in increasing breakthrough force, especially at 1173 and 1273 K. In general, the increase of preheating time causes the lower breakthrough force as same as the effect of the extrusion temperature, but in the case of D indicates an adverse result because the TiC dispersoids existing in Ti billet are higher than those of the case C as a result of the longer preheating time used at high temperature. The

higher TiC dispersoids in the case D are confirmed by the relative intensity of TiC peak in the XRD results as shown in Figure 3.10. The maximum relative intensity of TiC peak in the case D is higher than that of the case C. It means that the Ti composite billet in the case of D contains high TiC dispersoids which are hardly deformed during hot extrusion, resulting in the increase of the breakthrough force.

3.5 Conclusions

The thermal characteristic of the solid zwitterionic substances and the Ti powders coated with MWCNTs via the solution-coating technique were investigated to determine the suitable thermal parameters for the fabrication of the MWCNTs reinforced Ti composites. The conclusions of this chapter are as follows.

(1) The solid zwitterionic substance with and without MWCNTs completely burned at 773 and 873 K, respectively, and the debinding temperature for the Ti powder coated with MWCNTs via the solution-coating technique was selected at the temperature of 873 K.

(2) The formation of TiC particle via reaction between MWCNTs and Ti powders was significantly detected at 923 K.

(3) The inert Ar atmosphere used for the debinding process yielded superior ductility for the extruded Ti composites. H_2 gas caused to synthesize TiH_2 brittle compounds, and resulted in the poor ductility of the composite.

(4) Solution-coating technique was effective to uniformly coat individual MWCNTs on the surface of sponge and fine Ti powders.

(5) The amount of deposited MWCNTs on the fine Ti powder was larger than that of the sponge Ti powder because the fine Ti powder had a higher specific surface area than sponge Ti powder. The solution-coating technique could not linearly control the amount of deposited MWCNTs on Ti powder by adjusting MWCNTs concentration in zwitterionic solution.

(6) Extrusion speeds of 3 and 6 mm/s were selected to produce the Ti reinforced with MWCNTs composites in this study.

(7) Long preheating of Ti composite billet led to the increase of TiC particle existing in the billet which was difficult to extrude.

References

1. G. S. Upadhyaya, *Powder Metallurgy Technology*, 1st ed., Cambridge International Science Publishing, UK (2002).
2. ASM Handbook vol. 7, *Powder Metal Technologies and Applications*, ASM International, (1998).
3. J. J. Xu, H. Y. Cheung, S. Q. Shi, "Mechanical Properties of Titianium Hydride", *Journal of Alloy and Compounds*, 436 (2007) 82-85.
4. Y. Furuya, A. Takasaki, K. Mizuno and T. Yoshiie, "Hydrogen Desorption from Pure Titanium with Different Concentration Levels of Hydrogen", *Journal of Alloy and Compounds*, 446-447 (2007) 447-450.
5. P. E. Kalita, A. L. Cornelius, K. E. Lipinska-Kalita, C. L. Gobin and H. P. Liermann, "In situ Observations of Temperature- and Pressure-Induced Phase Transitions in TiH2: Angle-Dispersive and Synchrotron Energy-Dispersive X-ray Diffraction Studies", *Journal of Physics and Chemistry of solids*, 69 (2008) 2240-2244.
6. C. Leyens and M. Peters, *Titanium and Titanium alloys*, Wiley-VCH, Germany (2003).
7. G. Lütjering and J.C. Williams, *Titanium*, 2nd ed., Springer-Verlag, Germany (2007).
8. O. Kubaschewski, C.B. Alcock, P. J. Spencer, *Materials Thermo-chemistry*, 6th ed., Pergamon Press, England, (1993).
9. R. Habu and W. Yamada, "Ostwald Growth of Fe_3C and Distributions of Carbon Atoms in α-Iron Annealed under A Constant Temperature Gradient", *Materials Transactions, JIM*, vol 41, 7 (2000) 877-879.
10. K. Lenik, M. Pashechko, A. Kondry, L. Bohun and Z. Lenik, "Calculation of Phase Equilibrium in Fe-B-C-O System", *Archives of Materials Science and Engineering*, vol. 28, 8 (2007) 483-488.
11. B. Fugetsu, W. Han, N. Endo, Y. Kamiya, and T. Okuhara, "Disassembling Single-Walled Carbon Nanotube Bundles by Dipole/Dipole Electrostatic Interactions", *Chemistry Letters*, 34 (2005) 1218–1219.
12. B. Verlinde, J. Driver, I. Samajdar and R. D. Doherty, *Thermo-Mechanical Processing of Metallic Materials*, 1st ed., Pergamon, Netherlands (2007).

Chapter 4

Microstructure and Static Mechanical Properties of Extruded Titanium-Carbon Nanotubes Composites

In this chapter, the effects of thermo-mechanical processing parameters on the microstructures and mechanical properties of the extruded Ti powder composites reinforced with MWCNTs are discussed. Furthermore, the estimation of the incremental yield stress of the extruded Ti composites will be discussed at the end of this chapter

4.1 Microstructure and tensile properties of extruded sponge Ti reinforced with MWCNTs

4.1.1 Effect of MWCNT contents on microstructure

The sponge Ti powders coated with 1.0, 2.0 and 3.0wt.% MWCNTs/zwitterionic solution are consolidated at 1073 K for 1.8 ks by SPS process. The extrusion of those SPSed billets is subsequently preformed at 1273 K. The optical microstructure observation at a plane normal to the extrusion direction of all extruded Ti composites is shown in Figure 4.1. The microstructure reveals the presence of fine TiC particles and Ti matrix, which are confirmed by XRD analysis as shown in Figure 4.2. TiC particles are distributed throughout the Ti matrix, which can account for the high dispersion of MWCNTs on the Ti powder surface during solution-coating step. The grain size measurements of all extruded Ti composites, which are calculated by using the image analysis software, indicate the average value of 7.0, 6.4 and 6.5 μm for the use of 1.0, 2.0 and 3.0wt.% MWCNTs/zwitterionic solution, respectively, while the TiC particles almost show the same size of 2.4 μm, approximately.

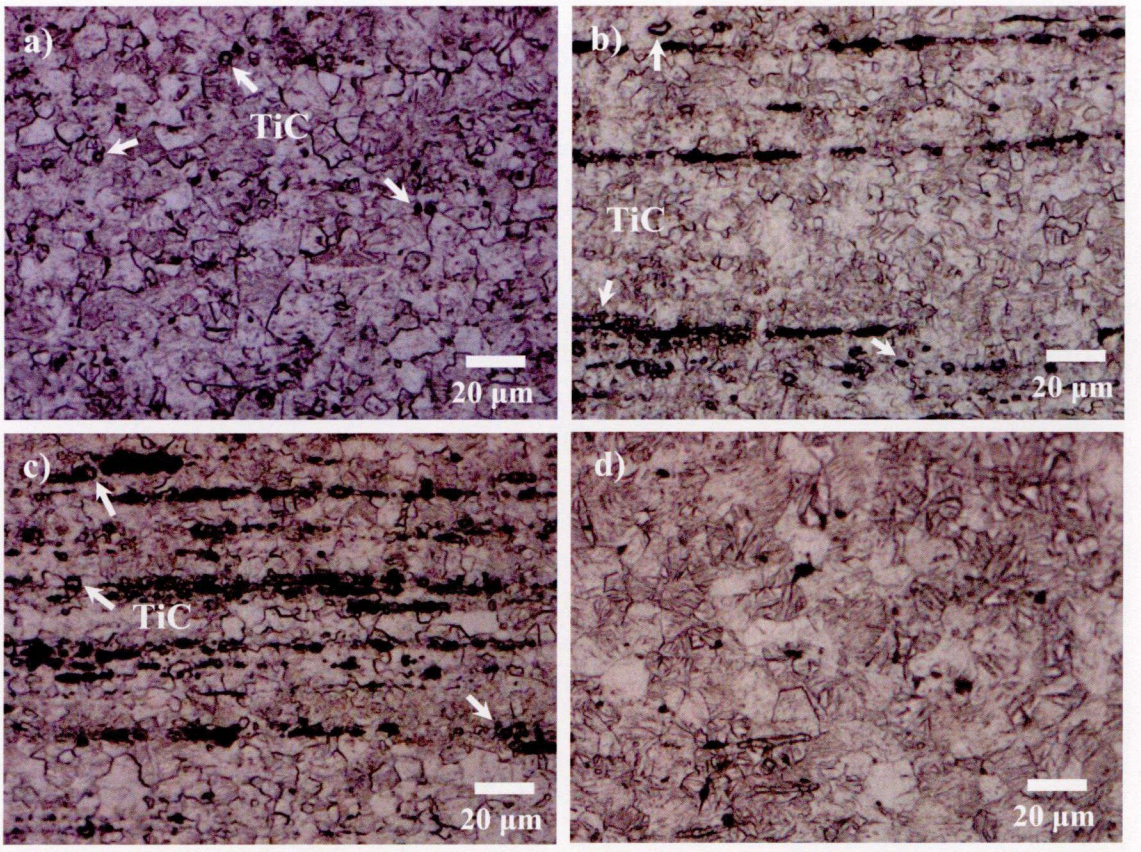

Figure 4.1 Microstructure of the extruded sponge Ti composite coated by the solution-coating technique containing a) 1.0, b) 2.0, c) 3.0 wt.% MWCNTs and d) extruded sponge Ti composite without any reinforcements.

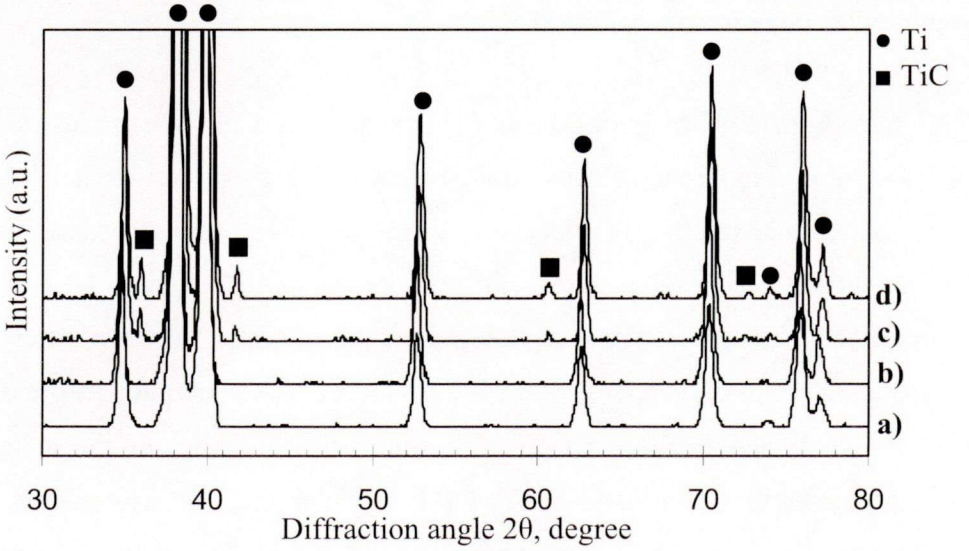

Figure 4.2 XRD patterns of the extruded sponge Ti composites, a) without reinforcement, coated by b) 1.0, c) 2.0 and d) 3.0 wt.% MWCNTs/zwitterionic solution.

The amount of TiC particles existing in the Ti matrix increases with increasing the MWCNTs content corresponding to the TiC peak intensity of the XRD results in Figure 4.2. Furthermore, the fractional amount of TiC particles can be estimated by comparison the strongest relative peak intensity of TiC of each extruded rod in the XRD results with the calibration curve. The TiC calibration curve used for the estimation of TiC fraction can be found later in the section 4.3.2. The amount of TiC particle of each extruded Ti composite using 1.0, 2.0 and 3.0wt. % MWCNTs is 0.125, 1.169 and 1.199 wt.%, respectively.

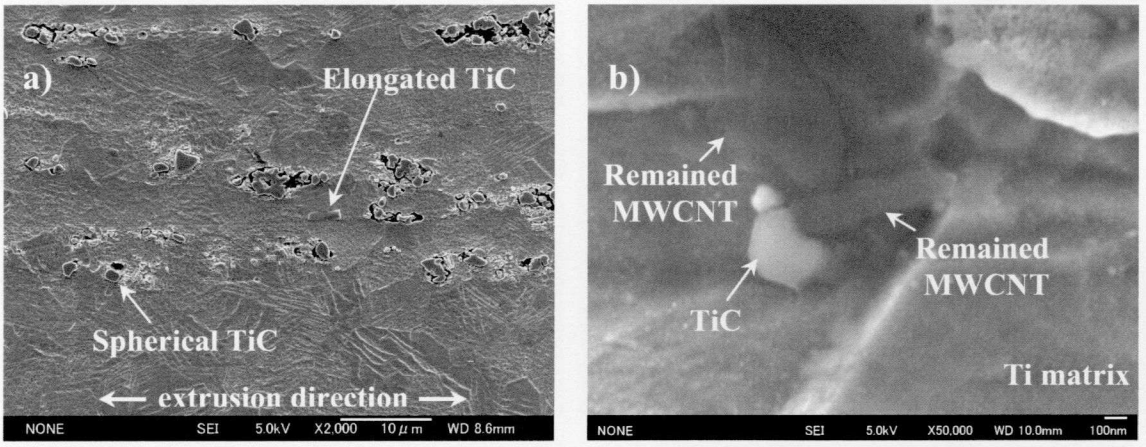

Figure 4.3 SEM images of the extruded sponge Ti composite prepared by 1.0 wt.% MWCNT via solution-coating technique, a) overview image indicating elongated and spherical TiC particle, b) high magnification image showing remained MWCNTs.

High magnification images of the extruded sponge Ti composite are also observed by SEM as shown in Figure 4.3. The extruded sponge Ti composite coated by 1.0wt.% MWCNTs/zwitterionic solution is selected as a representative sample because it shows the same microstructure as the other except for the amount of TiC. Figure 4.3 (a) shows the morphologies of TiC particles. The morphologies of TiC particles have two different shapes, i.e., elongated and spherical shapes. The elongated TiC particles, having a length of about 10 μm or less, are aligned in the extrusion direction. The formation of the elongated TiC particles is presumed that the individual MWCNT at Ti surface as shown in Figure 3.6 (b) or Figure 3.7 is recombined and formed into the elongated shape of TiC particle during the SPS sintering process. The elongated TiC particles possibly position in any direction existing in

the SPSed billet. However, their orientations are adjusted in the extrusion direction due to the shear force in the plastic flow of the softer Ti matrix during hot extrusion. On the other hand, the formation of a spherical shape supposes that the agglomerated MWCNTs at the edge of the Ti powder, shown in Figure 3.6 (a), are recombined and formed into such a coarse TiC particle. Furthermore, the microstructure observation at higher magnification reveals the incredible evidence of remained MWCNTs as shown in Figure 4.4 (a). This evidence can also be detected in the extruded Ti composite coated 2.0 and 3.0wt.% MWCNTs/zwitterionic solution as shown in Figure 4.4 (b) and Figure 4.5, respectively.

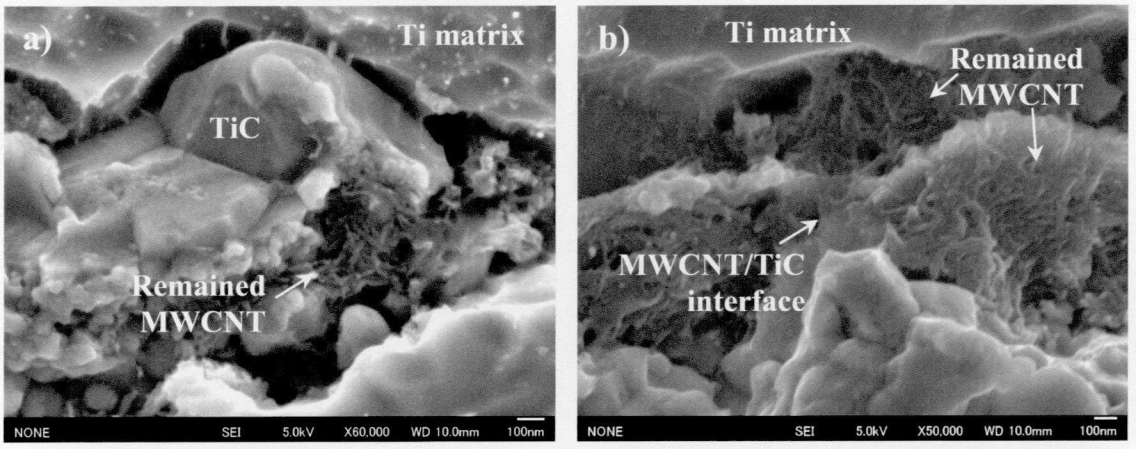

Figure 4.4 SEM images of extruded sponge Ti composites prepared by a) 1.0 and b) 2.0 wt.% MWCNTs via solution-coating technique.

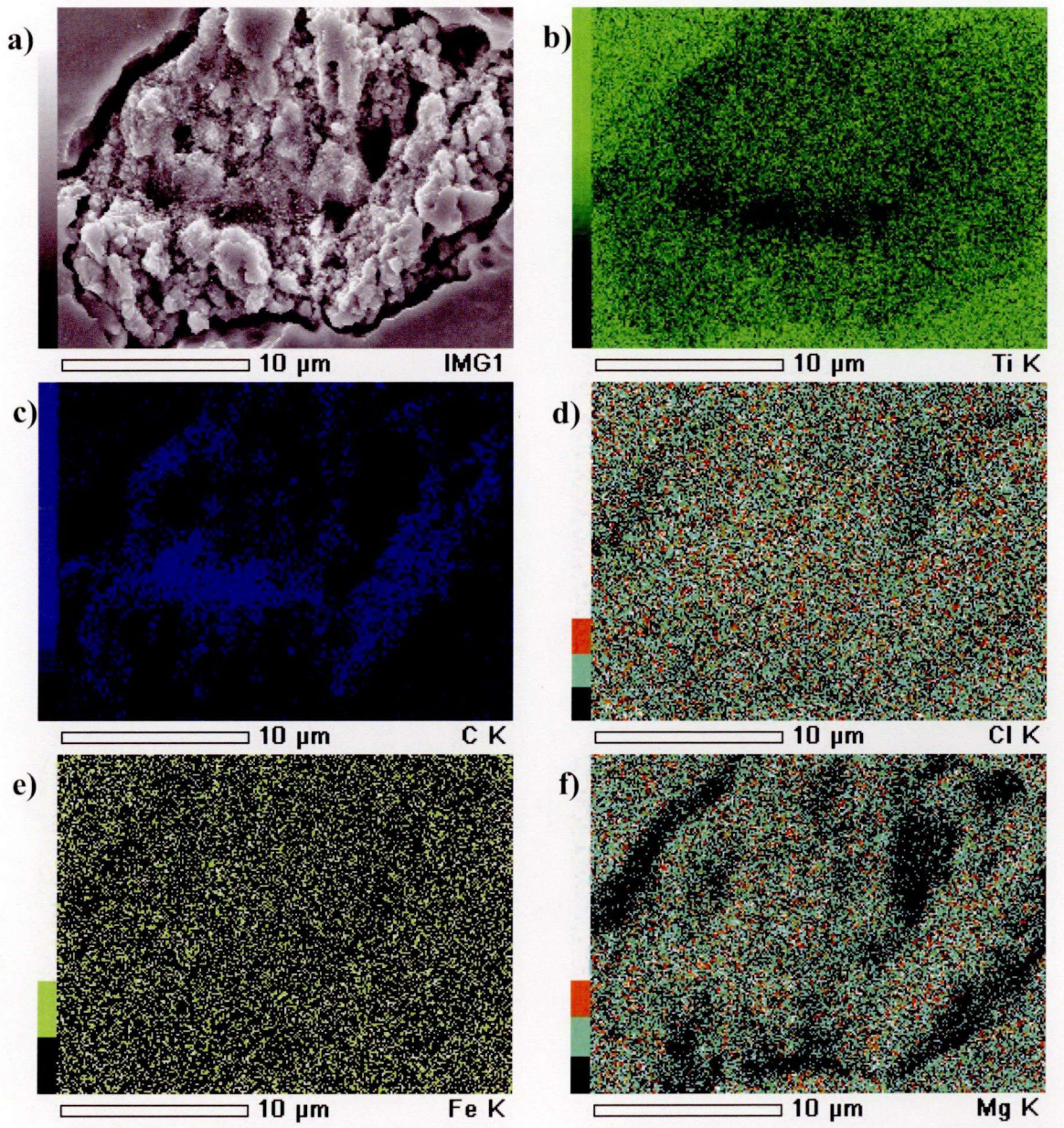

Figure 4.5 EDS mapping images of a) SEI, b) Ti, c) C, d) Cl, e) Fe and f) Mg of the extruded Ti composite prepared by 3.0 wt.% MWCNTs/zwitterionic solution.

Figure 4.5 shows EDS analysis results of the extruded Ti composite prepared by 3.0 wt.% MWCNTs/zwitterionic solution, where the remained MWCNTs can be detected. The ESD results confirm the presence of the remained MWCNTs surrounded TiC particle as shown in Figure 4.5 (a)-(c), and also indicate the homogeneous distribution of elemental

chlorine, magnesium and iron in the Ti matrix. These elements are the main alloying elements of the starting material according to Table 2.1. The remained MWCNTs in the microstructure suggest that the sintering temperature of 1073 K for 1.8 ks is insufficient to complete the TiC formation. However, they show superior enhancement in mechanical properties, especially tensile properties, because they possess a Young's modulus of approximately 1 TPa [1] and show good bonding with Ti matrix via the TiC interface [2-3].

4.1.2 Effect of MWCNT contents on mechanical properties

The stress-strain curves of all extruded sponge Ti composites prepared by 1.0, 2.0 and 3.0 wt.% MWCNTs/zwitterionic solution are shown in Figure 4.6, compared to stress-strain curve of extruded sponge Ti with no reinforcement. The average tensile test results of all test samples and the carbon content analysis results are listed in Table 4.1.

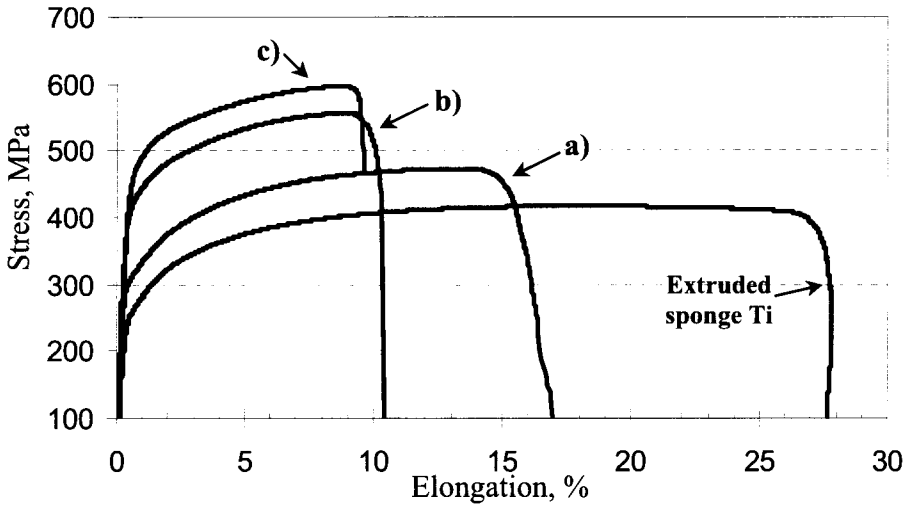

Figure 4.6 Stress-stain curves of the extruded sponge Ti composites prepared by solution-coating of a) 1.0, b) 2.0 and c) 3.0 wt.% MWCNTs, compared to the extruded sponge Ti matrix.

Table 4.1 Average mechanical properties of the extruded sponge Ti prepared by the solution- coating of 1.0, 2.0 and 3.0 wt.% MWCNTs.

Extruded sponge Ti composites	YS, MPa	TS, MPa	e_l, %	HV	Grain size, μm	TiC size, μm	TiC fraction, (wt.%)	Carbon content, (wt.%)
Extruded sponge Ti	247	412	25.4	171	5.0	-	-	0.013
1wt.%MWCNTs	317	484	17.6	195	7.0	2.4	0.125	0.041
2wt.%MWCNTs	430	564	12.9	232	6.4	2.3	1.169	0.360
3wt.%MWCNTs	462	596	9.9	248	6.5	2.5	1.199	0.636

The yield stress (YS) and tensile strength (TS) values of the extruded Ti composite prepared by 1.0 wt.% MWCNTs/zwitterionic solution are increased by 28.3% and 17.5%, compared to the extruded Ti without any reinforcement. In the case of 2.0 wt.% MWCNTs/zwitterionic solution, the increases in YS and TS are 74.1% and 36.9%, respectively, while the increases in YS and TS of the case 3.0 wt.% MWCNTs/zwitterionic solution are remarkably elevated by 87.0% and 44.7%, respectively. The dependence of tensile properties on the MWCNTs content is also shown in Figure 4.7.

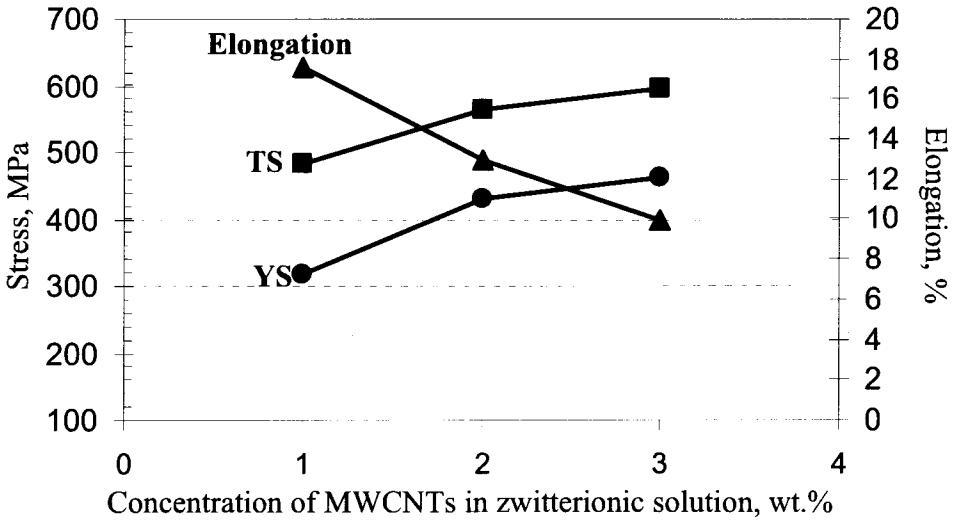

Figure 4.7 Dependence of tensile properties of the extruded sponge Ti composites on concentration of MWCNTs in zwitterionic solution.

It clearly shows the increase of YS and TS with increasing MWCNTs content. The elongation of the extruded Ti composites indicates a straightforward decrease in ductility with increasing MWCNTs content. However, the ductility of the extruded Ti composites coated with 1.0 and 2.0 wt.% MWCNTs is high enough to be considered for the applications.

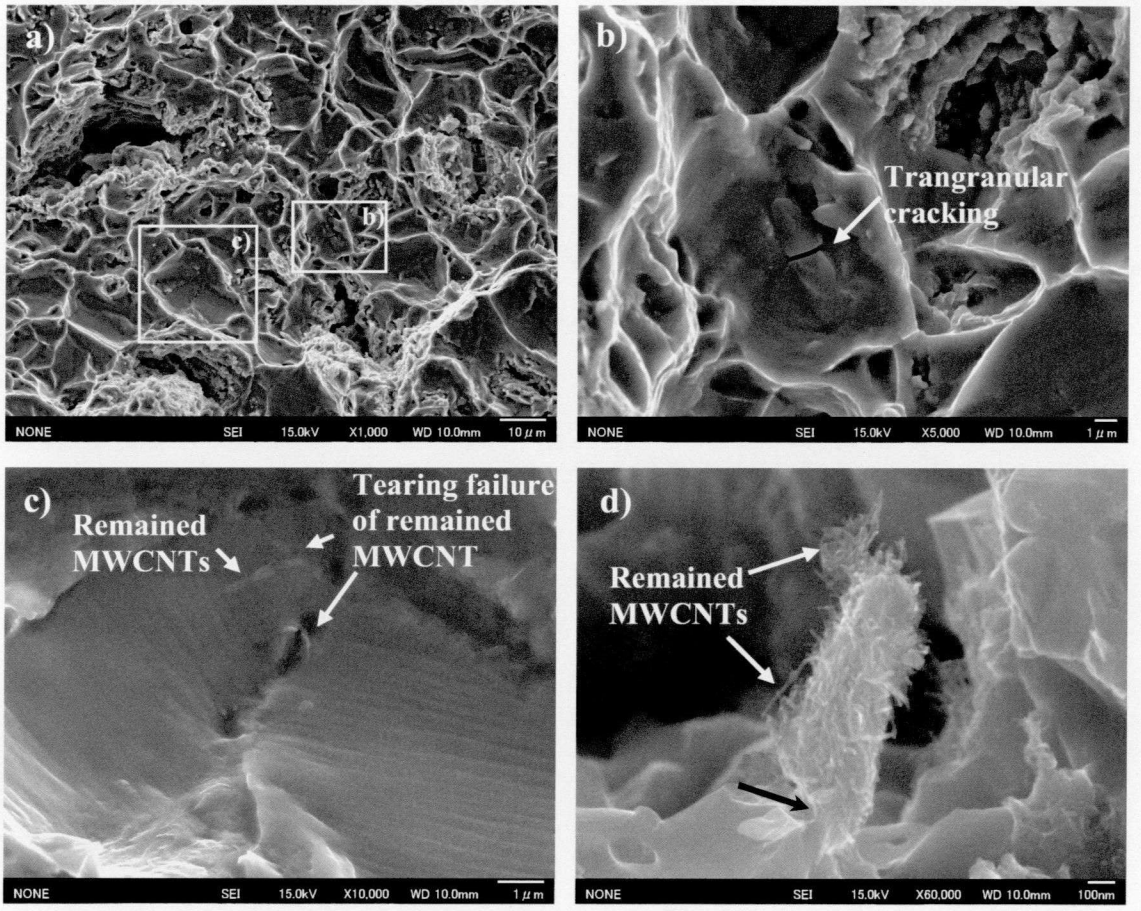

Figure 4.8 Fractography of tensile test sample of extruded sponge Ti composite coated by 2.0wt.% MWCNTs shows a) typical ductile failure, b) transgranular cracking of TiC particle, c) fiber-tear failure of MWCNT and d) remained MWCNTs.

Fractography of the fractured tensile test specimens of Ti composites coated by 2.0 and 3.0 wt.% MWCNTs is further investigated to understand the increasing in strength and decreasing in ductility. Figure 4.8 reveals the fractured surface of Ti composite coated by 2.0wt.% MWCNTs. A typical fractograph of ductile fracture in general Ti material and the intergranular fracture of TiC particles show in Figure 4.8 (a).

This means that the sintering at 1073 K for 1.8 ks is high enough to allow bonding of Ti powders and also this sintering condition can simultaneously synthesize and bond TiC particles completely as shown in Figure 4.8 (b). Transgranular fracture occurred at the TiC particle, which is confirmed an excellent bonding between TiC and Ti matrix [2-3] that stresses can be highly transferred to the stronger TiC particles, and eventually, increase the tensile strength. Furthermore, the fiber-tear failure mode of MWCNTs is also detected as indicated by arrows in Figure 4.8 (c). That evidence strongly confirms the excellent adhesive behavior of MWCNTs [4] and Ti matrix, which contributes to the increase in the tensile strength. Figure 4.8 (d) is another evidence of the good interfacial bonding and the excellent adhesion of MWCNTs as indicated by black arrows.

The same fracture behavior can also be observed in the case of 3.0wt.% MWCNTs, but its fractograph evidently reveals the formation of $MgCl_2$ and TiFe intermetallic compounds as shown in Figure 4.9. The formation of those intermetallic compounds is possible and consistent with both theoretical thermodynamics and experimental data [5-7], but the sequence of reactions are still unclear because there are many alloying elements in the starting sponge Ti powder, which are associated with the reactions. To prevent those reactions, the effects of thermal processing, in particular the lower sintering and extrusion temperatures, on the mechanical properties response are investigated in the next section.

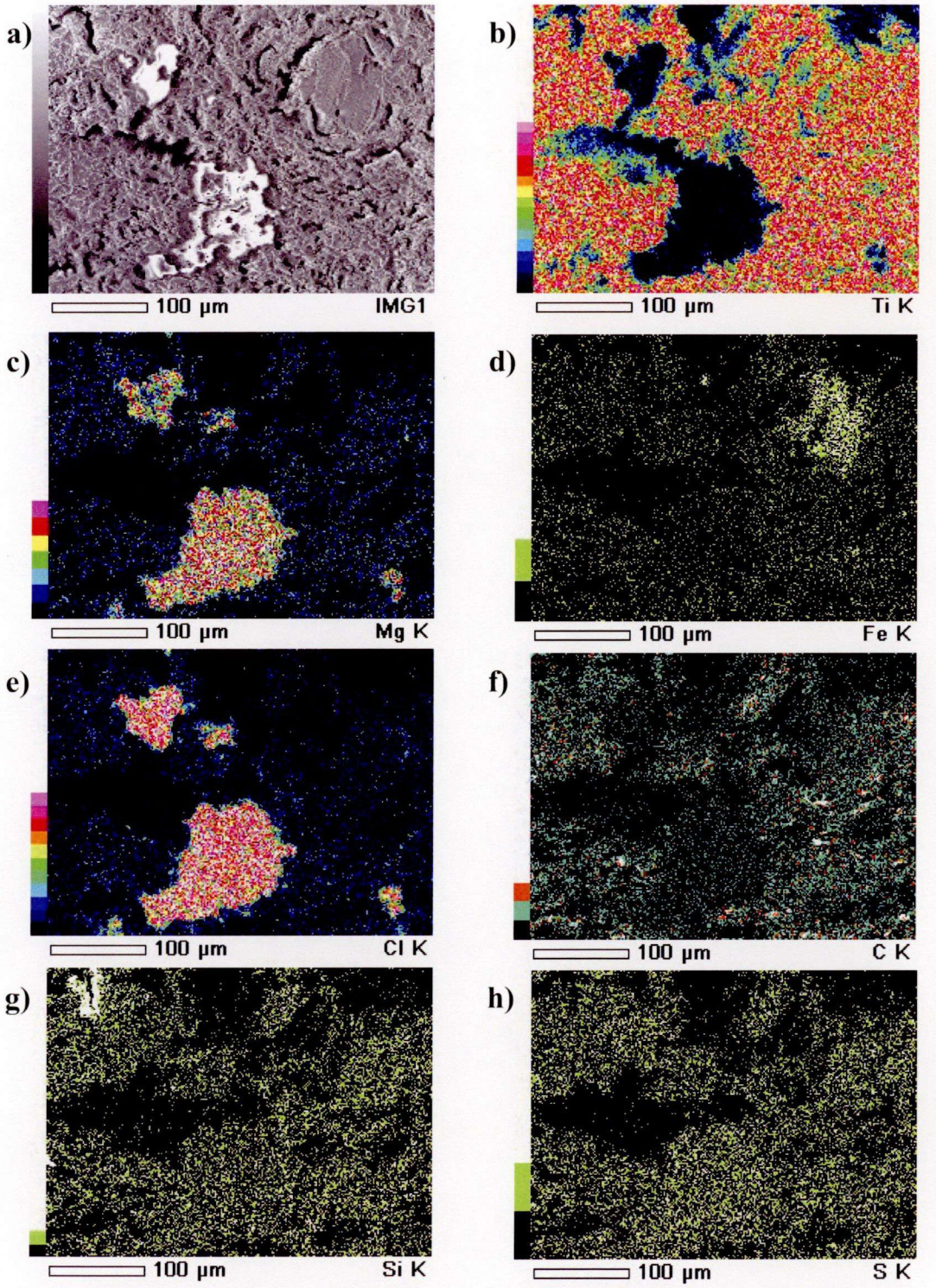

Figure 4.9 EDS mapping images of a) SEI, b) Ti, c) Mg, d) Fe, e) Cl, f) C, g) Si and h) S of extruded Ti composite prepared by 3.0 wt.% MWCNTs/zwitterionic solution.

4.1.3 Effect of low temperature in SPS and hot extrusion

The effect of lower sintering and extrusion temperature on the mechanical properties is investigated. The objective of this sintering and extrusion at low temperature is to control, not only $MgCl_2$ and TiFe, but also TiC particle formation during SPS and hot extrusion process. In addition, the experiment needs to maintain the remained MWCNTs [8] as high as possible to investigate their effect on the strength and ductility of the extruded Ti composite.

The sponge Ti powders coated with 1.0wt.% MWCNTs/zwitterionic solution are prepared. Before the SPS consolidation process, all debinded Ti powders are mixed together to form homogeneous powders. The SPS consolidation is preformed at 873 K for 600 s. The SPSed billets are preheated to the hot extrusion temperature at 773, 873 and 973 K, respectively, with the preheating time of 180 s for each billet. The hot extrusion of the preheated billets is subsequently preformed with extrusion speed (ram speed) of 3 and 6 mm/s. Unfortunately, one of extruded Ti composite, which is preheated at 773 K and extruded with 3 mm./s, can not be extruded as shown in Figure 4.10. This is due to an insufficient input energy which is limited by the maximum capability of the extrusion machine.

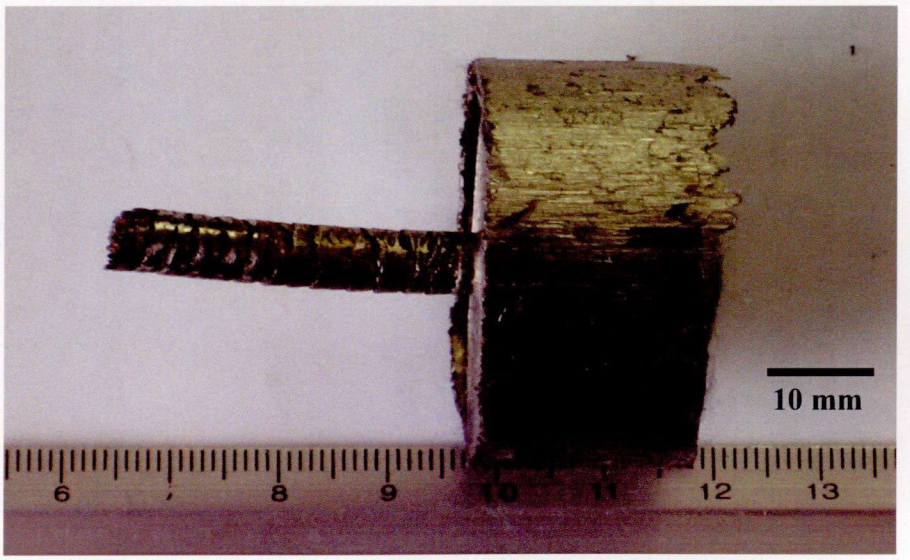

Figure 4.10 Unsuccessful extruded billet of sponge Ti coated with 1.0wt.% MWCNTs/zwitterionic solution.

The optical microstructure observation shows a microstructure similar to that of the extruded sponge Ti composites which described in the section 4.1.1. The TiC particles can rarely be detected corresponding to the XRD results. The amount of TiC particles is also estimated using the same comparison with the TiC calibration curve. The grain size and amount of TiC with the average value of mechanical properties of all extruded Ti composites are listed in Table 4.2. The carbon content of each extruded Ti composite indicates in the range of 0.183 to 0.196 wt.%, which corresponds to the results in Figure 3.8. That shows the characteristic of the MWCNTs coating the sponge Ti powder via the solution-coating technique.

Table 4.2 Average grain size, amount of TiC and the average value of mechanical properties of the extruded sponge Ti coated by 1.0wt.% MWCNTs/zwitterionic solution.

Extrusion speed	Extrusion temperature, K	YS, MPa	TS, MPa	e_f, %	HV	Grain size, μm	TiC fraction, (wt.%)
3 mm/s	773	N/A	N/A	N/A	N/A	N/A	N/A
	873	296	411	6.5	176	8.8	0.109
	973	372	518	14.5	174	8.7	0.105
6 mm/s	773	334	505	11.6	175	8.0	0.104
	873	295	487	10.5	176	8.8	0.109
	973	342	543	13.1	172	8.0	0.104

Figure 4.11 shows the dependence of mechanical properties on the low extrusion temperatures at different extrusion speeds for the extruded sponge Ti composites. Generally, the lower extrusion temperature causes the increasing in yield stress, tensile strength and hardness because the strain hardening occurs during plastic deformation of the extrusion process. This strain hardening effect is also induced to the extruded material by the increasing extrusion speed during low temperature extrusion. In the case of 6 mm/s extrusion speed, the tensile strength shows slightly higher than that of the extrusion at 3mm/s because of the effect of strain hardening. However, the stain hardening occurred in both of 3 and 6 mm/s does not show large differences in the mechanical properties because those values are close together as shown in Table 4.2.

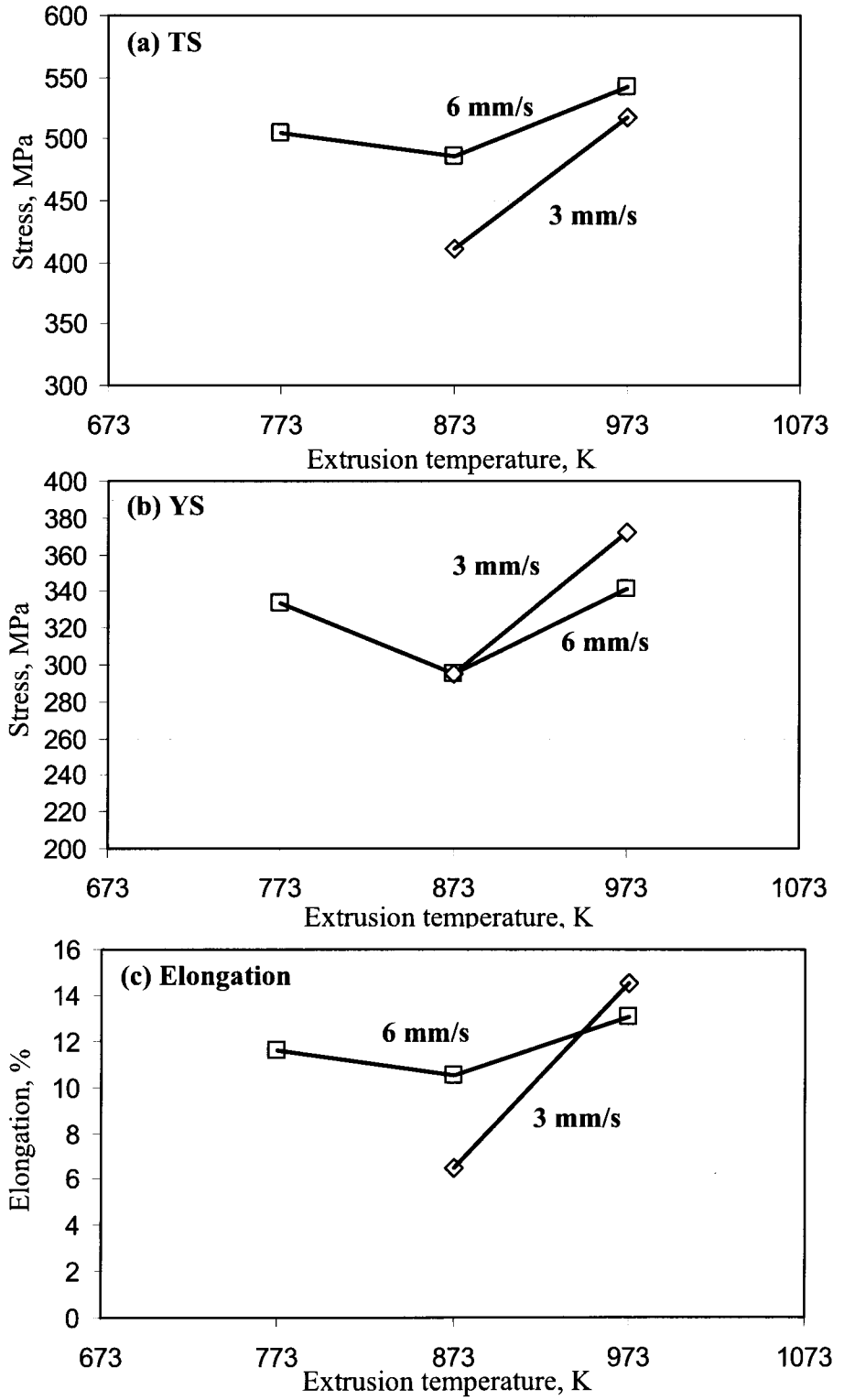

Figure 4.11 Dependence of mechanical properties on extrusion temperatures at different extrusion speeds of the extruded sponge Ti composites coated by the solution- coating of 1.0 wt.%MWCNTs.

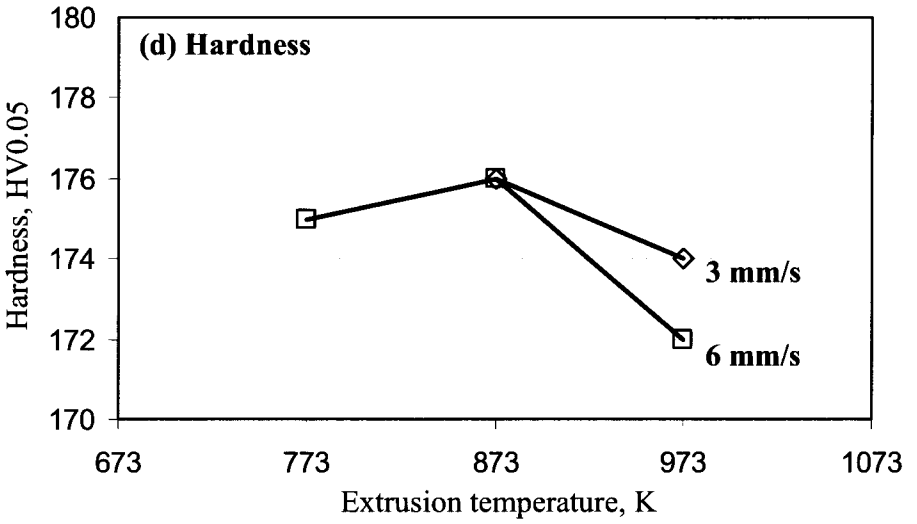

Figure 4.11 (continued) Dependence of mechanical properties on extrusion temperatures at different extrusion speeds of the extruded sponge Ti composites coated by the solution- coating of 1.0 wt.%MWCNTs.

Fractured surfaces show the formation of $MgCl_2$ and TiFe intermetallic compounds as shown in Figure 4.12. Those intermetallic compounds cause the decreasing mechanical properties, especially ductility, of the extrude Ti composites. Although, the lower thermal processing can maintain the remained MWCNTs, but the $MgCl_2$ and TiFe intermetallic compounds are formed. These intermetallic compounds may be uncontrollable factors because those of the reacted elements are already-existing element in the starting sponge Ti powders. Moreover, the results indicate low ductility of the extruded Ti composites, even though the MWCNTs have remained in the matrix, which are affected by low sintering temperature. The effect of the remained MWCNTs on mechanical properties of the extruded sponge Ti has been remained unclear because the mechanical properties are dominated by the effects of $MgCl_2$ and TiFe intermetallic compounds. The higher sintering temperature is one of the effective factors to increase the ductility of Ti composite, even though the $MgCl_2$ and TiFe intermetallic compounds are formed. Hence, the higher sintering temperature with short time is preferably used to produce the sponge Ti composites.

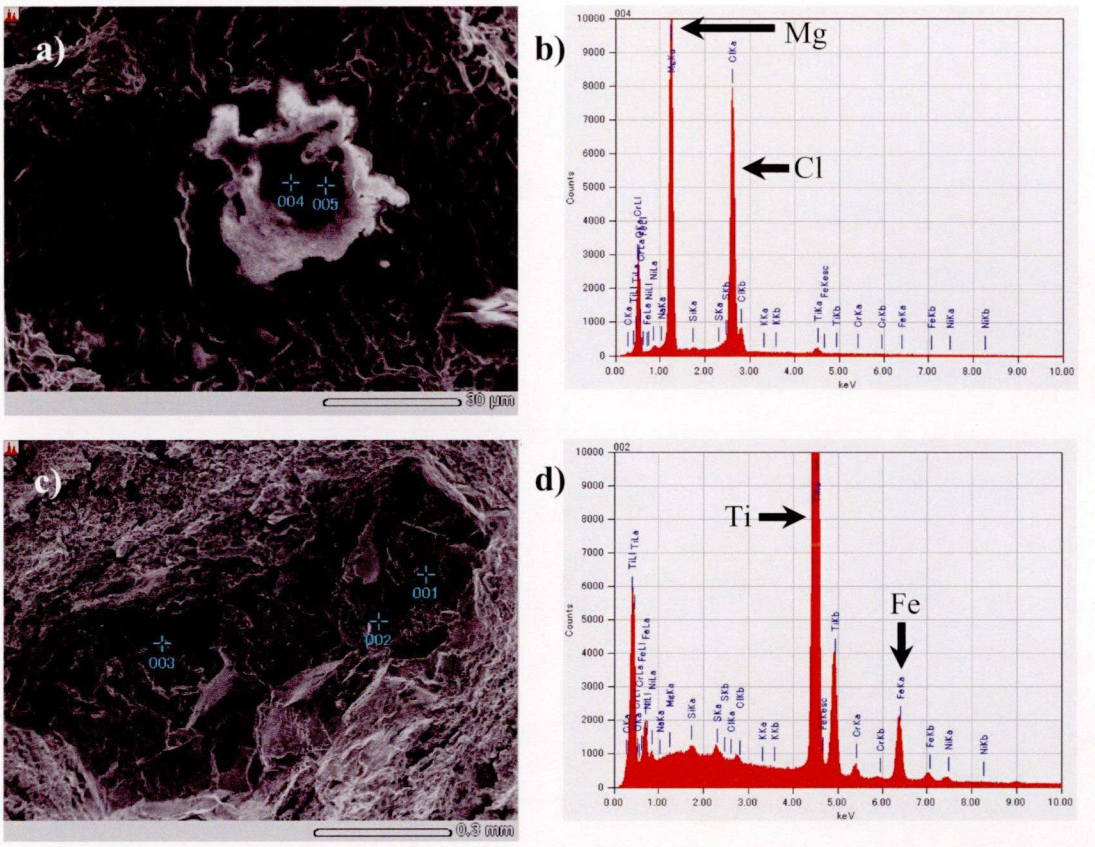

Figure 4.12 EDS point-analysis of a)-b) MgCl2 and c)-d) FeTi of the extruded Ti composite coated by 1.0 wt.% MWCNTs/zwitterionic solution.

4.1.4 Effect of high temperature in SPS and hot extrusion

The effects of higher sintering and extrusion temperature on the mechanical properties response are further investigated. To improve ductility of the extruded Ti composite, the high SPS temperature with short time sintering is employed to fabricate the Ti composites before the extrusion process. The sponge Ti powders coated with 2.0wt.% MWCNTs/zwitterionic solution are prepared. Similar to the previous section, the debinded Ti powders are mixed together to form homogeneous powders before the SPS consolidation. The SPS consolidation is preformed at 1273 K for 600 s. The SPSed billets are preheated to the hot extrusion temperature at 1073, 1173 and 1273 K, respectively, with different preheating times of 180 and 600 s for each temperature. The hot extrusion process is subsequently preformed with extrusion speed (ram speed) of 6 mm/s. The optical microstructure is primarily used to observe microstructure of the extruded Ti composites. Similar to the microstructure in the section 4.1.1, the microstructure indicates α – Ti grains with the distribution of TiC as shown by a representative sample in Figure 4.13. A small number of TiC particles exist inside the Ti grain, as marked by the arrow in Figure 4.13. These TiC particles act as dislocation-moving inhibitors inside Ti grains, while the TiC particles along the grain boundary also act as grain boundary-sliding inhibitors, resulting in increasing tensile strength [9]. The grain size, amount of TiC, carbon content and the average value of mechanical properties of all extruded sponge Ti composites are listed in Table 4.3.

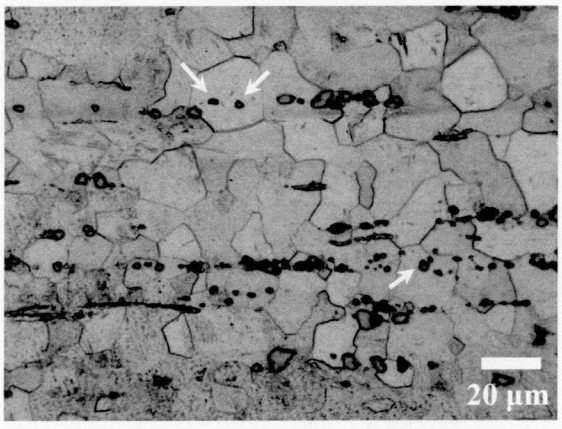

Figure 4.13 Microstructure of sponge Ti composite extruded at 1173 K.

Table 4.3 Average grain size, amount of TiC, carbon content and the average value of mechanical properties of the extruded sponge Ti coated by 2.0wt.% MWCNTs/zwitterionic solution.

Preheating time	Extrusion temperature, K	YS, MPa	TS, MPa	e_l, %	HV	Grain size, μm	TiC size, μm	TiC fraction, (wt.%)	Carbon content, (wt.%)
180 s	1073	427	564	21.1	204	10.9	2.6	1.225	0.348
	1173	452	587	16.6	221	10.1	2.8	1.222	0.370
	1273	487	606	19.1	205	9.4	2.7	1.187	0.371
600 s	1073	431	573	28.6	232	9.8	2.4	1.648	0.501
	1173	483	611	29.4	217	9.5	2.3	2.051	0.510
	1273	375	533	24.9	202	9.2	2.4	2.245	0.515

Figure 4.14 shows the dependence of mechanical properties on the extrusion temperatures at different preheating times of billet. Both yield stress and tensile strength of the samples heated at 1073 and 1173 K for 600 s are slightly higher than those of sample heated with 180 s at the same temperature because the amounts of TiC particles present in the matrix are higher than those of the case 180 s corresponding to the estimation of their fraction in Table 4.3. In contrast, the yield stress and tensile strength of the sample heated at 1273 K for 600 s suddenly decrease, comparing to those of 180 s preheating time. The long preheating time at high temperature is a severe condition for the sponge Ti coated with MWCNTs because $MgCl_2$ and Fe_3C intermetallics quickly grow in microstructure and change to coarse compounds. Figure 4.15 confirms the formation of $MgCl_2$ and Fe_3C intermetallic compounds existing in the extruded Ti composites. These are inevitable factors for the use of sponge Ti powders.

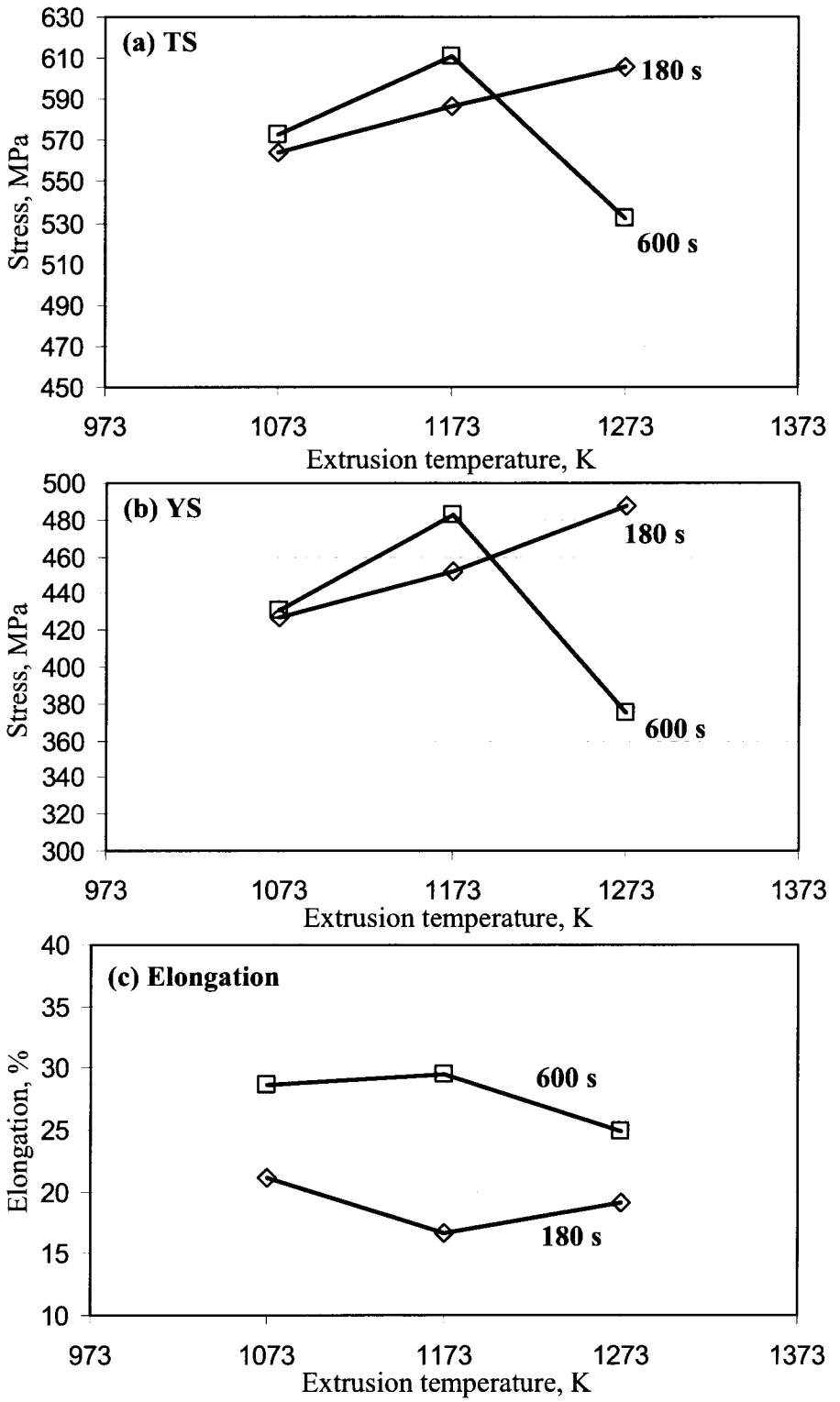

Figure 4.14 Dependence of mechanical properties on extrusion temperatures at different preheating times of the extruded sponge Ti composites prepared by the solution- coating of 2.0 wt.%MWCNTs.

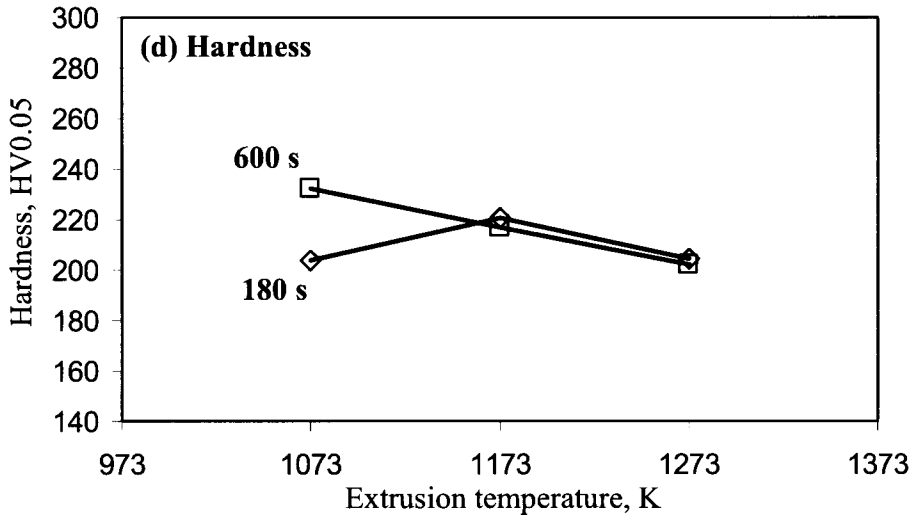

Figure 4.14 (continued) Dependence of mechanical properties on extrusion temperatures at different preheating times of the extruded sponge Ti composites prepared by the solution- coating of 2.0 wt.% MWCNTs.

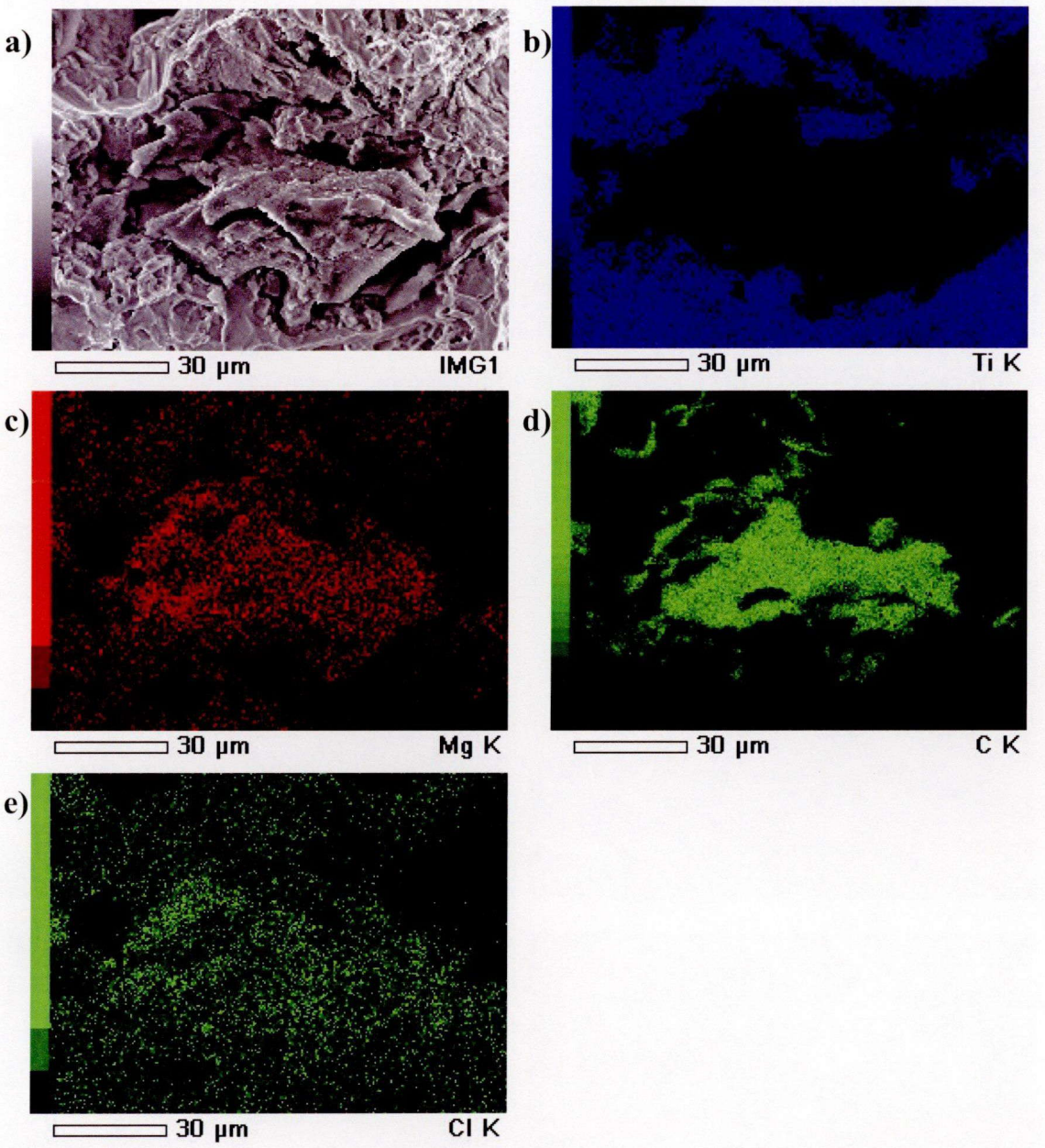

Figure 4.15 EDS mapping images of a) SEI, b) Ti, c) Mg, d) C, and e) Cl of the extruded Ti composite prepared by 2.0 wt.% MWCNTs/zwitterionic solution.

4.2 Microstructure and tensile properties of extruded fine Ti reinforced with MWCNTs

4.2.1 Effect of MWCNT contents on microstructure

The effect of MWCNT contents on the microstructure of extruded fine Ti composites is also investigated. The fine Ti powders coated with 1.0, 2.0 and 3.0wt.% MWCNTs/zwitterionic solution are consolidated at 1073 K for 1.8 ks by SPS process, and subsequently extruded at 1273 K. The optical microscope is primarily used to observe the microstructure of all extruded Ti composites as shown in Figure 4.16.

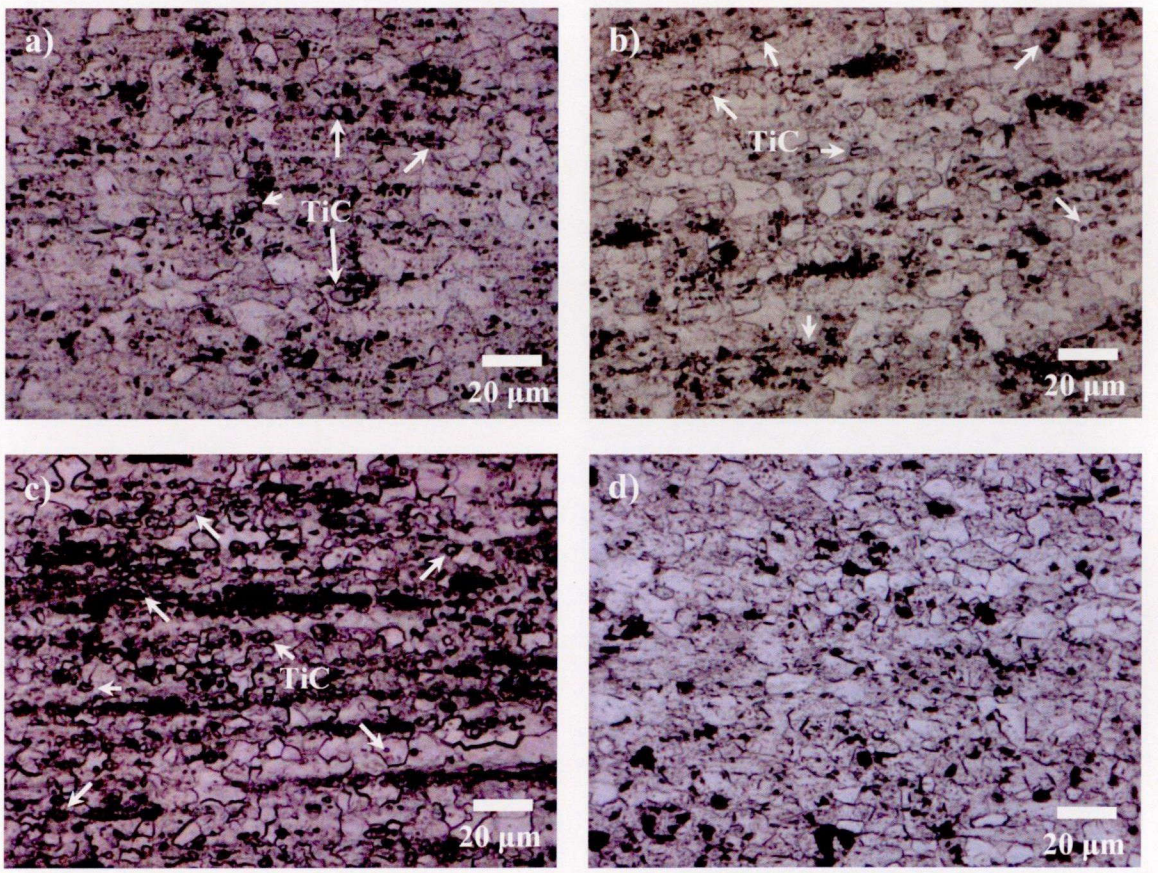

Figure 4.16 Microstructures of the extruded fine Ti composites prepared by zwitterionic solution containing a) 1.0, b) 2.0 and c) 3.0 wt.% MWCNTs and d) extruded fine Ti composite without reinforcement.

The microstructure reveals the same TiC particles and Ti matrix similar to the extruded sponge Ti composites. Those phases are confirmed by the XRD analysis as shown in Figure 4.17. It should be noted that in addition to the formation of TiC particles, the carbon atoms at the outer surface of MWCNTs and/or the carbon atoms from the *in-situ* formed TiC particles possibly diffuse into the Ti matrix during the SPS process, resulting in increase of mechanical properties of the extruded Ti composites. Details of the carbon solid solution effect on the improvement of mechanical properties will be described in the section 4.3.2.

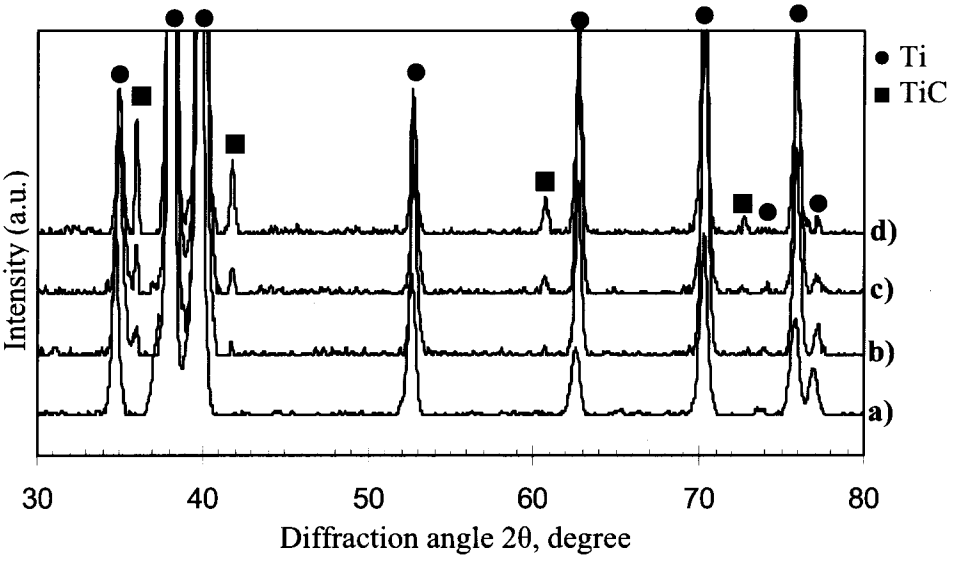

Figure 4.17 XRD patterns of the extruded fine Ti composites, a) without reinforcement, coated by the solution- coating of b) 1.0, c) 2.0 and d) 3.0 wt.% MWCNTs.

The TiC particles size measurements of all extruded fine Ti composites which are prepared by the solution-coating technique containing 1.0, 2.0 and 3.0wt.%MWCNTs, indicate that TiC particles measure 1.4, 1.7 and 1.5 μm, respectively, while the grain size measurements of those extruded fine Ti composites average 6.5, 6.0 and 5.6 μm, respectively.

The distribution uniformity and amount of TiC particles existing in microstructure increase with increasing the MWCNTs content corresponding to the microstructure and the relative intensity of TiC peak in the XRD results as shown in Figure 4.16 and Figure 4.17, respectively. The increased TiC amounts can contribute to the increase in the tensile strength as same as the results of the extruded sponge Ti composites. The fractional TiC amount can

be estimated by comparison the strongest relative intensity of TiC of each extruded rod in the XRD results with the calibration curve. The amount of TiC particle of each extruded fine Ti composite using 1.0, 2.0 and 3.0wt. % MWCNTs is 0.812, 1.267 and 3.322 wt.%, respectively. Similar to the extruded sponge Ti composites, high magnification images of the extruded fine Ti composites are also detected the remained MWCNTs existing in the Ti matrix of all MWCNTs contents used in this experiment. Figure 4.18 shows the SEM images of the extruded fine Ti composite coated with 3.0 wt.% MWCNTs/zwitterionic solution.

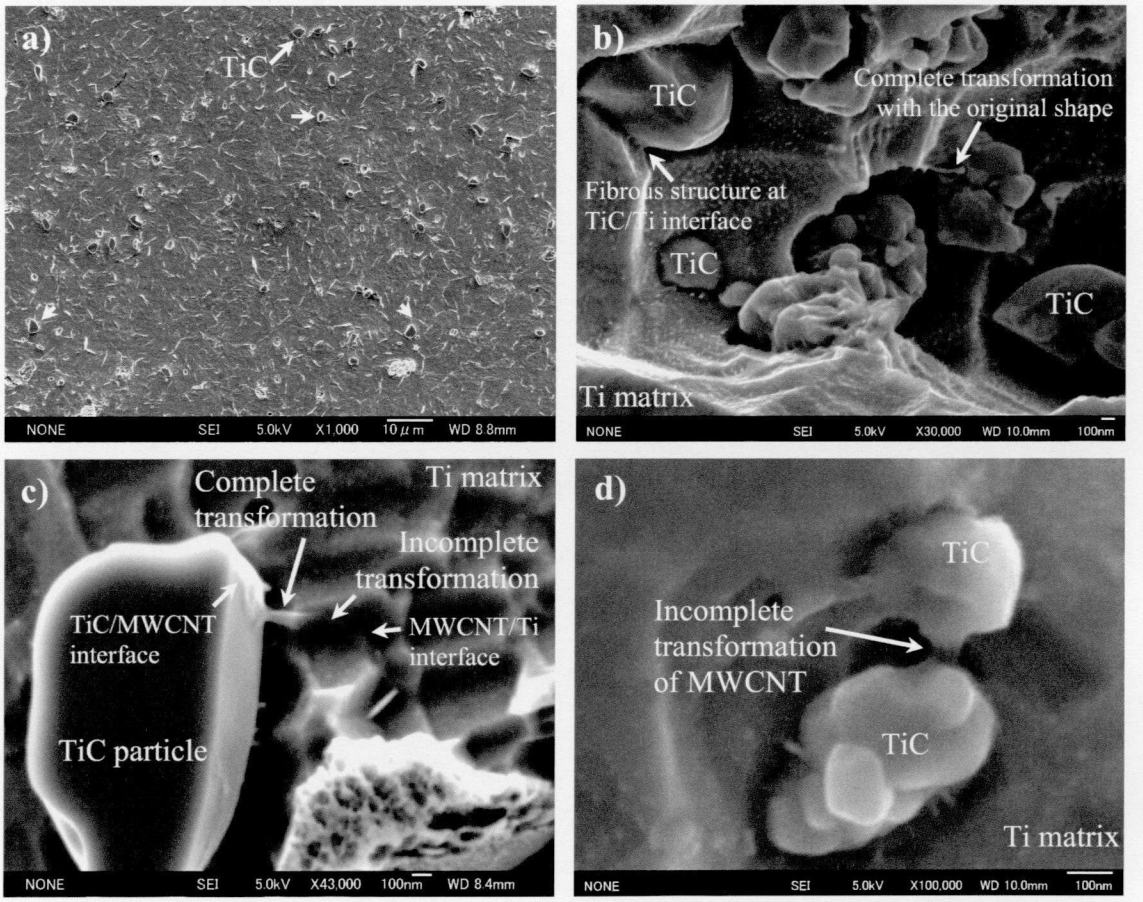

Figure 4.18 Microstructure of extruded fine Ti composite coated by 3.0wt.% MWCNT shows a) overview, b) interface between Ti/TiC, c) and d) incomplete transformation of MWCNT.

Figure 4.18 (a) shows an overview image of the extruded Ti composite, which reveals the elongated and spherical TiC particles. The different in morphologies can be accounted by the same behavior as mentioned in the section 4.1.1. Figure 4.18 (b) shows a close

observation on the fracture of the TiC grain clusters, which reveals not only the interface between TiC particle and Ti matrix, but also the transformation of MWCNTs to TiC as indicated by arrows. Moreover, the higher magnification images also reveal the evidence of reaction at the interfaces between TiC, MWCNT and Ti as shown in Figure 4.18(c) and (d). The incomplete transformation of the remained MWCNTs can help to increase tensile strength by mechanical interlocking feature [8, 10-11].

4.2.2 Effect of MWCNT contents on mechanical properties

Figure 4.19 shows the stress-strain curves of all extruded fine Ti composites prepared by 1.0, 2.0 and 3.0 wt.% MWCNTs/zwitterionic solution, compared to the stress-strain curve of extruded fine Ti with no reinforcement. The grain size, amount of TiC, carbon content and the average value of mechanical properties of all samples are also given in Table 4.4.

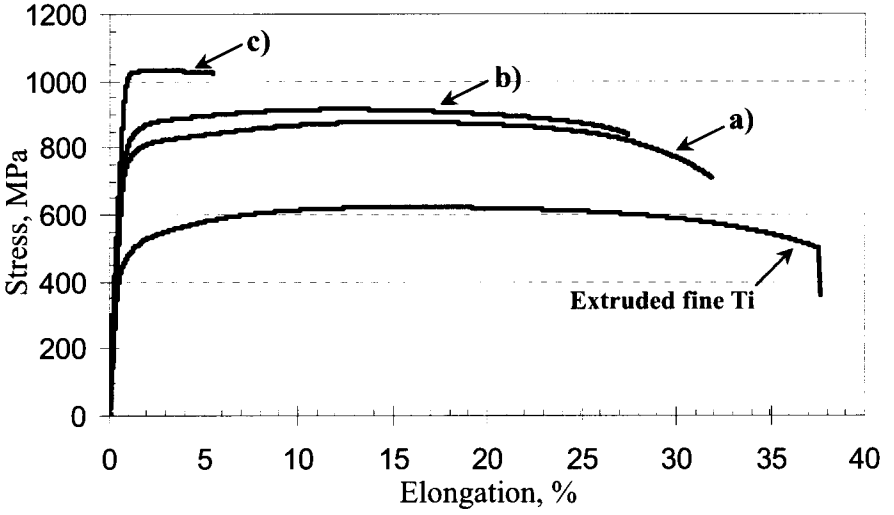

Figure 4.19 Stress-stain curves of the extruded fine Ti composites prepared by the solution- coating of a) 1.0, b) 2.0 and c) 3.0 wt.% MWCNTs, compared the extruded fine Ti matirx.

Table 4.4 Average grain size, TiC size, amount of TiC, carbon content and average mechanical properties of the extruded fine Ti composite prepared by the solution- coating of 1.0, 2.0 and 3.0 wt.% MWCNTs.

Extruded fine Ti composites	YS, MPa	TS, MPa	e_f, %	HV	Grain size, μm	TiC size, μm	TiC fraction, (wt.%)	Carbon content, (wt.%)
Extruded fine Ti	421	625	35.3	261	4.1	-	-	0.012
1wt.%MWCNTs	750	883	29.3	345	6.5	1.4	0.812	0.250
2wt.%MWCNTs	808	918	28.2	370	6.0	1.7	1.267	0.463
3wt.%MWCNTs	1015	1028	5.4	418	5.6	1.5	3.322	0.990

The YS and TS values of the extruded Ti composite prepared by 1.0 wt.% MWCNTs/zwitterionic solution are increased by 78.1% and 41.3%, compared to the extruded Ti without any reinforcement. In the case of 2.0 wt.% MWCNTs/zwitterionic solution, the increases in YS and TS are 91.9% and 46.9%, respectively, while the increases in YS and TS of the case 3.0 wt.% MWCNTs/zwitterionic solution are remarkably elevated by 141.1% and 64.5%, respectively. Hardness of all extruded fine Ti composites are increased by 32.2, 41.8 and 60.2% for 1.0, 2.0 and 3.0 wt.% MWCNTs coating, respectively, compared to the extruded fine Ti composites without reinforcement. The dependence of tensile properties on the MWCNTs contents is also shown in Figure 4.20. The YS and TS have increased with the increasing MWCNTs content. The ductility of the extruded fine Ti composites prepared by 1.0 and 2.0 wt.% MWCNTs/zwitterionic solution shows high elongation of 29.3 and 28.2 %, which can comparable to those of extruded fine Ti without reinforcement in this study or conventional Ti alloys, especially Ti-6Al-4V [12-13].

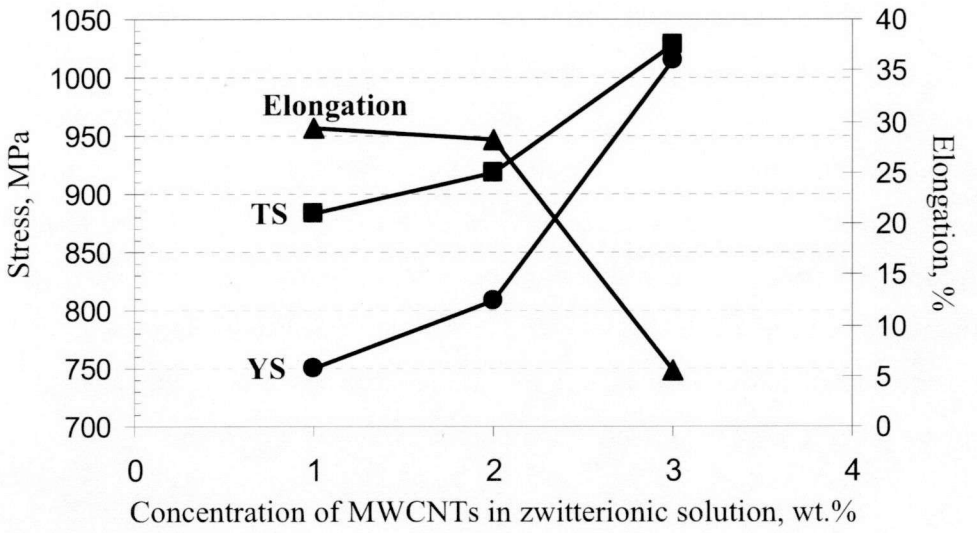

Figure 4.20 Dependence of tensile properties of the extruded fine Ti composites on the concentration of MWCNTs in zwitterionic solution.

Fractography of the fractured tensile test specimens of the extrude fine Ti composites prepared by 1.0 and 2.0 wt.% MWCNTs is further investigated, shown in Figure 4.21. Similar to that of extrude sponge Ti composite, a typical fractograph of ductile fracture mode and the intergranular fracture of TiC particles can be found, which mean that the tensile loading can completely transfer from Ti matrix to TiC particle and/or the remained MWCNTs.

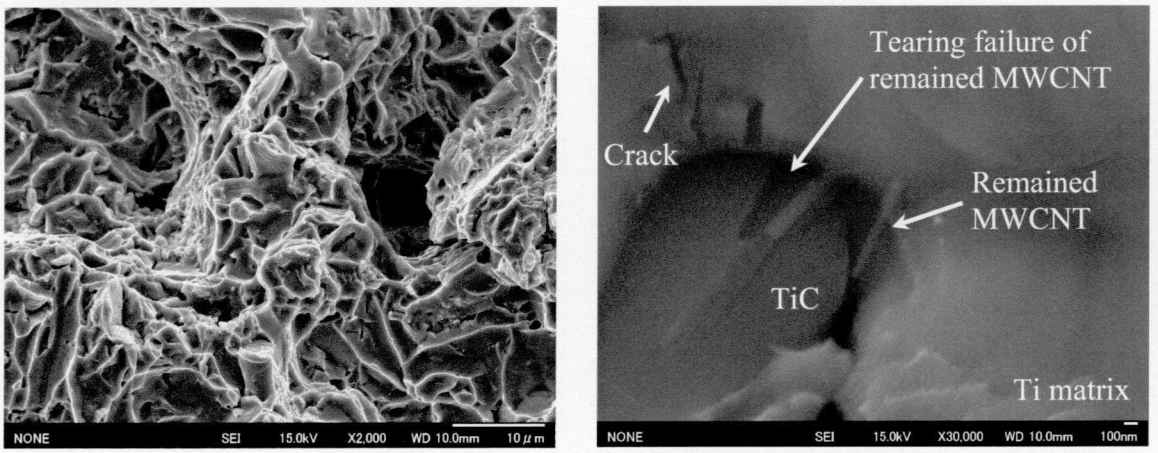

Figure 4.21 Fractography of tensile test sample of extruded fine Ti composite prepared by a) 1.0wt.% MWCNTs, showing a typical ductile failure, and b) 2.0 wt.% MWCNTs.

In the case of fine Ti powders, the formation of $MgCl_2$ and TiFe intermetallic compounds inside Ti matrix during consolidation can not be found in the fractured surface, comparing to the fractured surface of extruded sponge Ti materials. On the other hand, the observation can detect the formation of silicon of all MWCNTs contents used in this study as shown by a representative sample of 3 wt.% MWCNTs in Figure 4.22. The formation of Si probably occurs during SPS consolidation because Si atoms have had sufficient time to diffuse and form a Si particle. However the formation of Si can be considered as a positive factor for the composite because Ti_5Si_3 [12-13] can also be formed and behaved as another second phase particle which is effective to inhibit dislocation movement.

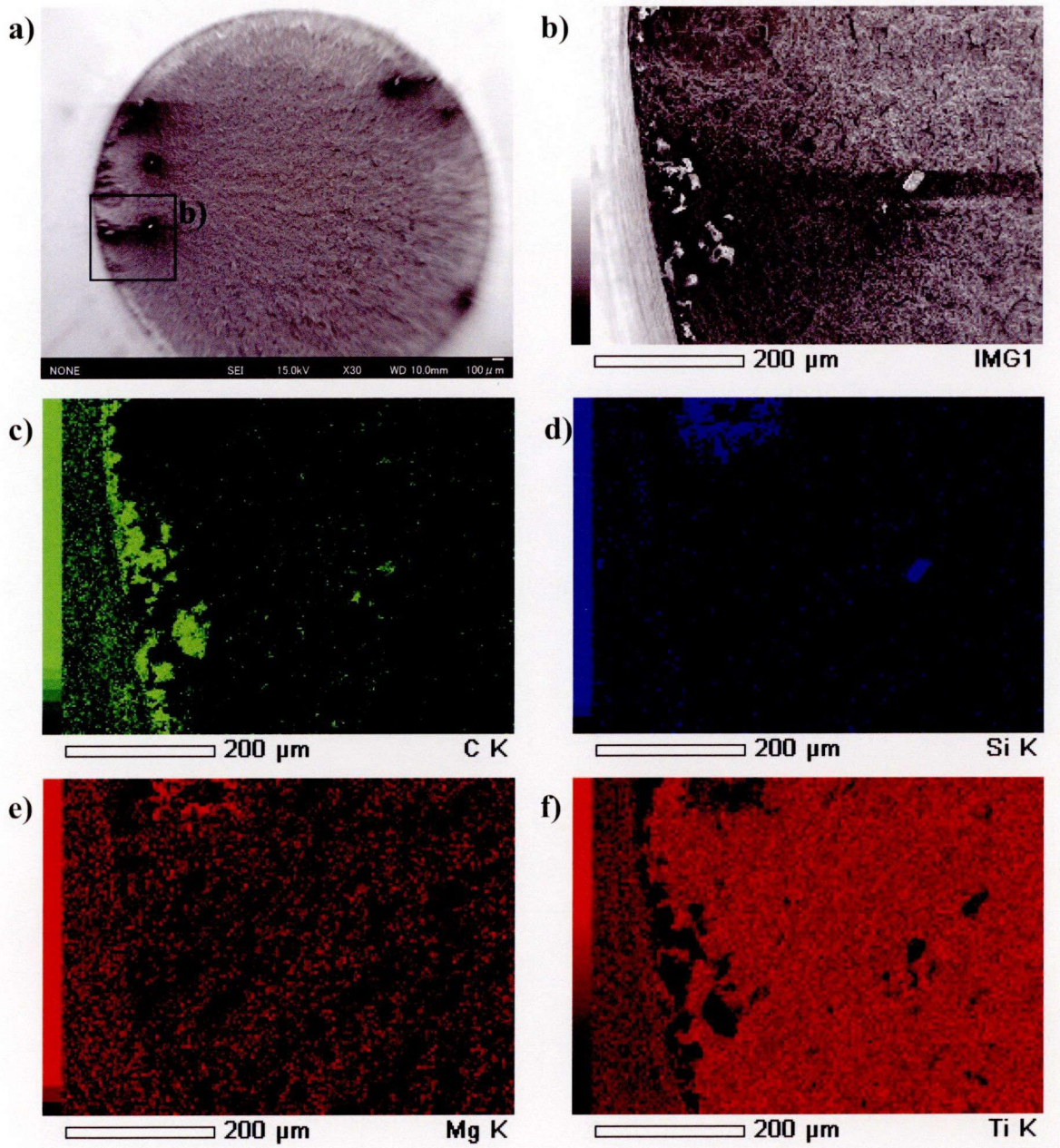

Figure 4.22 Fractography of tensile test sample of extruded fine Ti composite prepared by 3 wt.% MWCNTs/zwitterionic solution a) overview and the EDS mapping images of b) SEI, c) C, d) Si, e) Mg, and f) Ti.

4.2.3 Effect of SPS temperature on mechanical properties

The effect of sintering temperature on the mechanical properties response is investigated using fine Ti powder coated with 2.0wt.%MWCNTs/zwitterionic solution as starting powder. After debinding process at 873 K for 1.8 ks, the SPS consolidation is preformed at 1073 K until 1573 K with interval of 100 K. The consolidation time is fixed at 600 s. Finally, the SPSed billets are preheated to 1273 K for 180 s, and subsequently extruded with extrusion speed of 3 mm/s.

The optical microstructure observation shows the same microstructure of α-Ti grain as the previous results, but the average value of TiC particle size is increased with increasing consolidation temperature. Ti grain size almost shows a small variation in the range of 7 to 10 μm. It should be noted that the higher consolidation temperature strongly affects to the increase of TiC size than Ti grain coarsening. In other words, the distribution of TiC particle size retards the grain growth of Ti during consolidation at high temperature. Table 4.5 is the summarization of the grain size, amount of TiC, carbon content and the average value of mechanical properties of all extruded Ti composites depending on SPS temperature.

Table 4.5 Average grain size, TiC size, amount of TiC, carbon content and average mechanical properties of the extruded fine Ti composites consolidated at elevated temperature.

SPS temperature, K	YS, MPa	TS, MPa	e_f, %	HV	Grain size, μm	TiC size, μm	TiC fraction, (wt.%)	Carbon content, (wt.%)
1073	710	823	18.0	333	8.3	2.3	2.413	0.570
1173	694	820	15.0	327	9.6	2.2	2.802	0.560
1273	695	819	22.2	330	7.4	2.6	4.169	0.562
1373	675	799	19.2	318	7.4	3.0	4.134	0.562
1473	675	796	20.4	301	7.5	4.2	4.020	0.585
1573	655	769	18.2	311	8.4	5.7	4.764	0.569

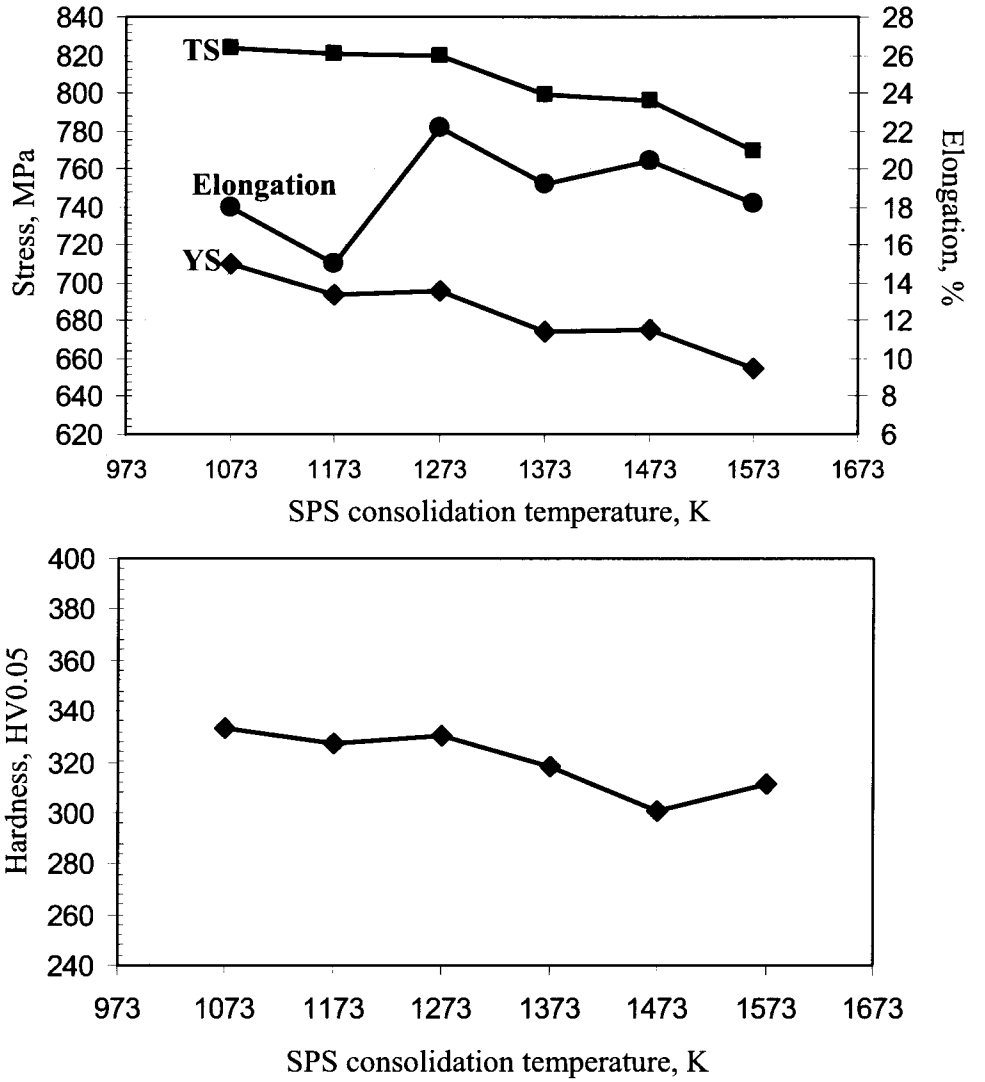

Figure 4.23 Dependence of mechanical properties on SPS consolidation temperatures of the extruded fine Ti composites prepared by 2.0 wt.% MWCNTs/zwitterionicthe solution.

The mechanical properties dependence on the consolidation temperatures of the extruded fine Ti composites is shown in Figure 4.23. The higher SPS temperature causes the lower yield and tensile strength of the extruded fine Ti composite materials. That can be explained by the coarsening of TiC particles as clearly shown in Figure 4.24. The yield and tensile strength decrease with increasing TiC particle size when the sintering temperature increases.

Microstructures of the extruded Ti composites sintered at 1073 and 1573 are the best comparison of the coarsening of TiC particle, shown in Figure 4.25

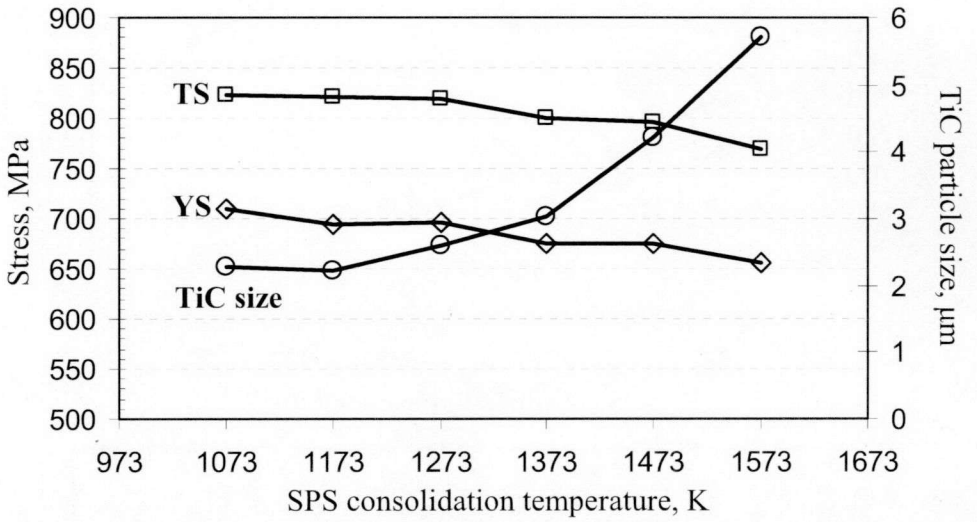

Figure 4.24 Dependence of mechanical properties on the TiC particle size of the extruded fine Ti composites prepared by 2.0 wt.% MWCNTs/zwitterionicthe solution.

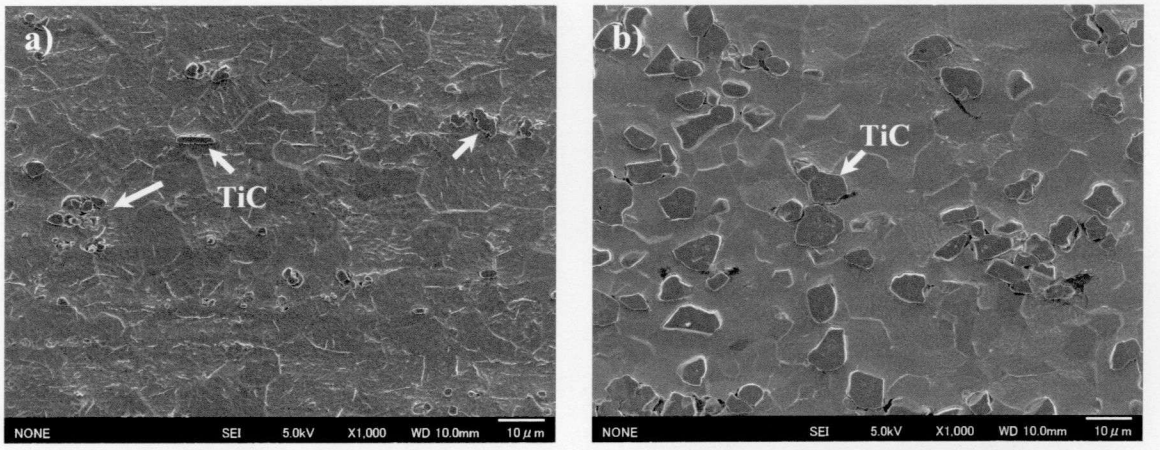

Figure 4.25 Microstructures of the extruded fine Ti composites sintered at a) 1073 K and b) 1573 K.

4.2.4 Effect of SPS time on mechanical properties

The effect of sintering time on the mechanical properties response is further investigated using the same fine Ti powder coated by 2.0 wt.% MWCNTs/zwitterionic solution as starting powder. The SPS consolidation is preformed at the temperatures of 1073, 1173 and 1273 K with different holding times of 600, 1200 and 1800 s, respectively. The SPSed billets are preheated to the hot extrusion temperature at 1273 K with the preheating time of 180 s, and subsequently extruded with the extrusion speed of 3 mm/s.

The microstructure of each extruded fine Ti composite shows the same α-Ti grain as described in the previous section. Ti grain sizes have fluctuated in the range of 7 to 10 μm. It can be inferred from the previous and this experiment that the sintering temperature and time hardly affect to the growth of Ti grains in this study. This is due to the high distribution of fine TiC particles throughout the Ti matrix, in particular at grain boundary, retards the Ti grains coarsening by a pining effect. On the other hand, the higher sintering temperature and time strongly affect to the coarsening of TiC particles. The amounts of TiC particles are also increased as the SPS temperature and time increase corresponding to the relative intensity of TiC peak in the XRD results. Average Ti grain size, TiC particle size and relative intensity of the TiC(111) peak of the all extruded Ti composite materials are summarized in Table 4.6.

Table 4.6 Average Ti grain size, TiC particle size and relative intensity of the TiC(111) peak of the extruded Ti composite materials consolidated at different temperature and time.

SPS temp. K	SPS time: 600 s			SPS time: 1200 s			SPS time: 1800 s		
	Ti grain Size, μm	TiC size, μm	TiC(111) intensity,%	Ti grain size, μm	TiC size, μm	TiC(111) intensity,%	Ti grain size, μm	TiC size, μm	TiC(111) intensity,%
1073	8.3	2.3	2.4151	9.2	2.4	1.1905	7.4	2.6	1.6807
1173	9.6	2.2	2.8053	8.7	2.7	2.4631	8.0	3.4	3.8286
1273	7.4	2.6	4.4944	9.5	2.7	1.0727	7.8	3.0	4.627

The dependence of mechanical properties on the consolidation times of the extruded fine Ti composites is shown in Figure 4.26 and summarized in Table 4.7. The higher SPS temperature causes the lower yield and tensile strength of the extruded fine Ti composite materials. That can be attributed to the coarsening of TiC particles during sintering corresponding to the TiC size analysis. In contrast, the sintering at lower temperature indicates better tensile strength. At sintering temperature of 1073 K with a holding time of 1.8 ks, a good balance between SPS temperature and time can be founded, which yields the highest mechanical properties.

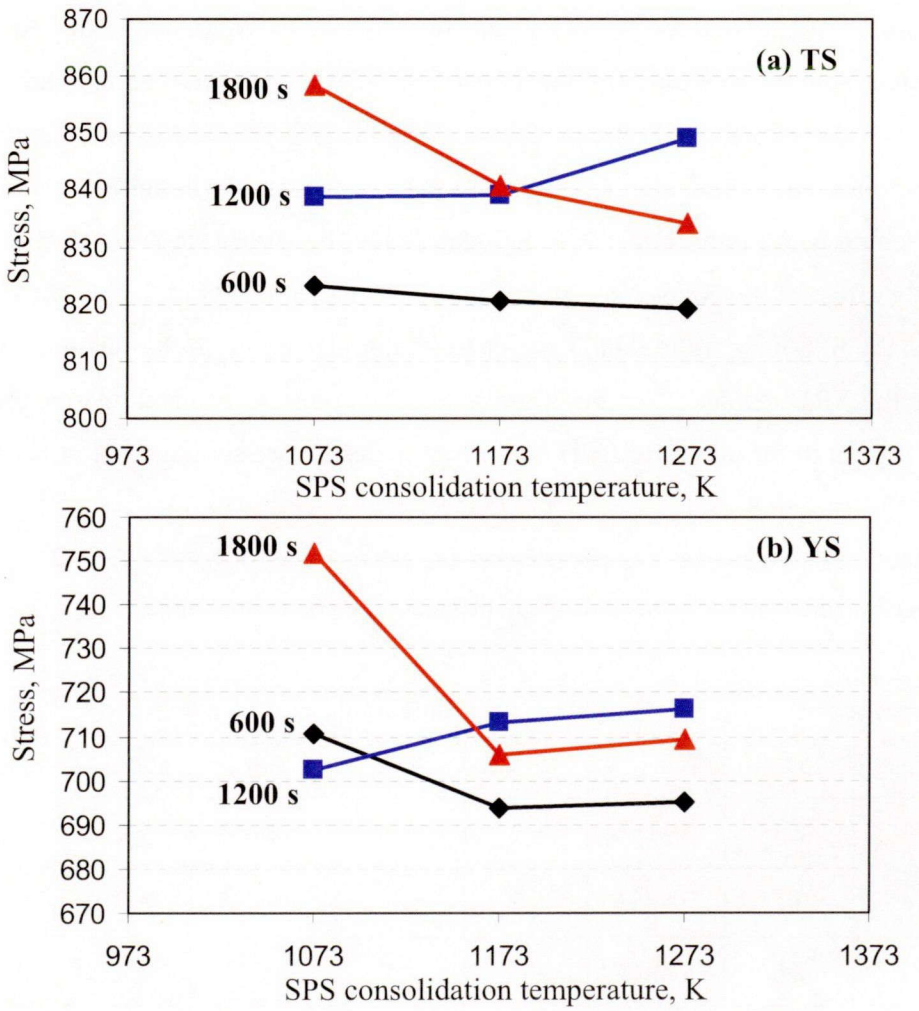

Figure 4.26 Dependence of tensile properties on the consolidation temperatures at various times of the extruded fine Ti composites prepared by 2.0 wt.% MWCNTs/zwitterionic solution.

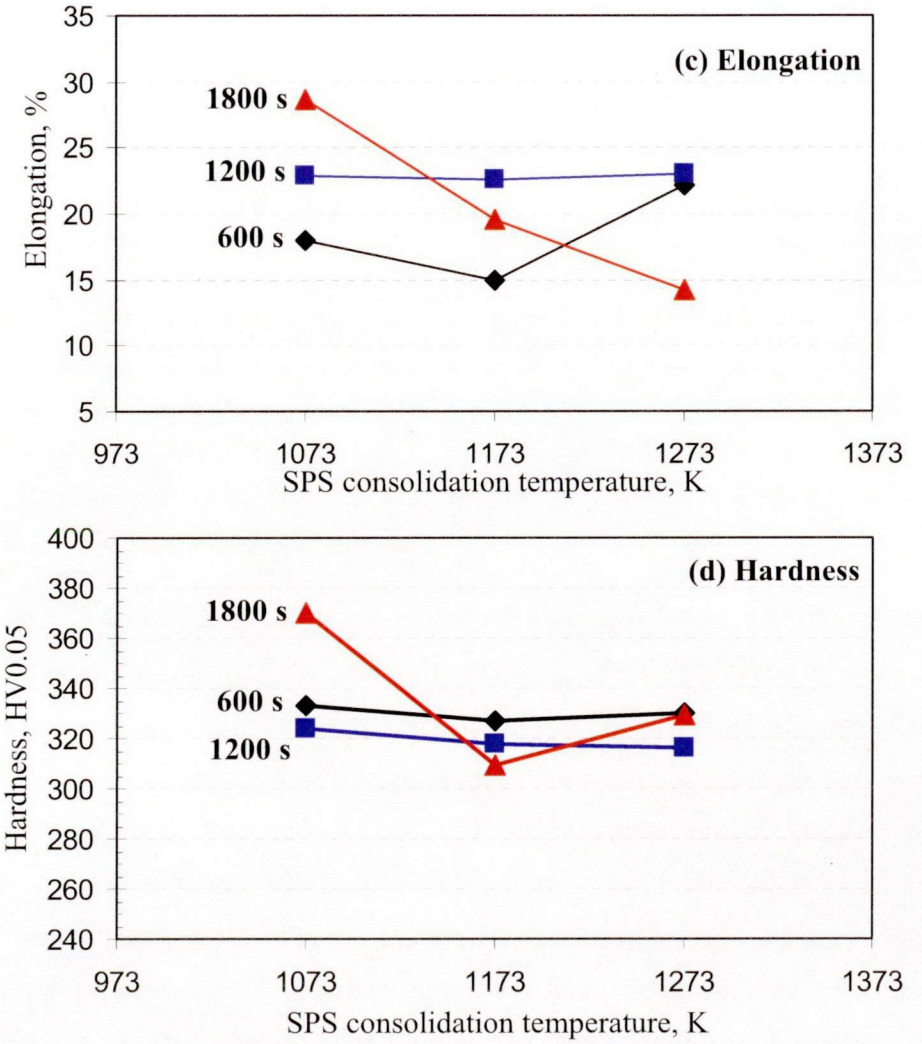

Figure 4.26 (continued) Dependence of tensile properties on the consolidation temperatures at various times of the extruded fine Ti composites prepared by 2.0 wt.% MWCNTs/zwitterionic solution.

Table 4.7 Average mechanical properties of the extruded fine Ti composite materials consolidated at different temperatures and times.

SPS temp. K	SPS time:10 min				SPS time: 20 min.				SPS time: 30 min.			
	YS, MPa	TS, MPa	Elong, %	Hv	YS, MPa	TS, MPa	Elong, %	Hv	YS, MPa	TS, MPa	Elong, %	Hv
1073	711	823	18.0	333	703	839	22.9	324	752	859	28.7	333
1173	694	821	15.0	327	714	839	22.6	318	706	841	19.6	309
1273	695	819	22.2	330	717	849	23.0	316	709	834	14.3	329

The good balance between SPS temperature and time is related to the incomplete transformation of MWCNTs and the *in-situ* formed TiC particle. Although, the reaction kinetics between MWCNTs and Ti have been unknown, but there is generally expected that the reaction will be done when the sintering temperature is increased with a suitable time. Hence, the amounts of the remained MWCNTs, in the case of sintering at 1073 K with holding times of 600 s and 1200 s, are possibly higher than amounts of the *in-situ* formed TiC particles because of short sintering time, while the amounts of the remained MWCNTs and TiC particles are almost equal together in the case of 1800 s sintering time. Furthermore, this balance is also founded in the case of sintering at 1273 K for 1200 s. The sintering time of 600 s at 1273 K shows a lower amount of TiC particles than that of 1200 s sintering time, resulting in lower tensile strength. When the sintering time is changed to 1800 s at 1273 K, the amount of TiC particles is higher than that of 1200 s. In other words, the amount of the remained MWCNTs of 1800 s is lower than those of 1200 s, resulting in decrease of tensile strength. This is due to the higher amounts of TiC particles and their coarsening occurred at sintering temperature of 1273 K. The higher SPS temperature also causes the lower ductility of the extruded fine Ti composite materials. The higher amount of TiC particles is formed as the SPS temperature increases, which causes the decrease in ductility due to their coarsening.

4.3 Estimation of incremental stress

The above results show superior improvement of the mechanical properties of Ti composite reinforced with the *in-situ* formed TiC and some remained MWCNTs. In order to clarify the strength mechanism occurred in the extruded Ti composites, the related strengthening mechanism could be separated into the effects of grain refinement, carbon solid solution and second phase dispersion strengthening [14-15]. Based on the superposition method, the estimation of incremental yield stress by each strengthening mechanism could be considered separately. The extruded fine Ti composites coated with 1.0, 2.0 and 3.0 wt.% MWCNTs are selected as a representative in the estimation.

4.3.1 Grain refinement

Although the previous results have indicated that the effect of grain size does not significantly increase the yield stress of the extruded Ti composites, but the estimation of the incremental yield stress have to consider this effect in the first step because the obtained value will eventually be used as threshold stress for further estimation. The estimation of the threshold stress for all extruded fine Ti composites is followed by Hall-Petch relationship [14-16] as shown below

$$\sigma = \sigma_0 + kD^{-1/2}$$

σ_0 is a constant stress and k is materials constant. D is a mean grain diameter of the Ti matrix. The constant stress and material constant for pure Ti matrix are 172.5 MPa and 18 MPa $\sqrt{mm}$ [17]. In order to verify the validity of the σ_0 and k value, the extruded pure Ti matrix is used to investigate in the first step. By using the grain diameter of 4.1 μm for extruded pure Ti matrix, the calculation shows the σ value of 453 MPa, while the experimental value is 421MPa. The calculation and experimental results show good agreement, therefore the σ_0 and k value can be used to estimate the threshold stress for the extruded fine Ti composites. The estimation results are shown in Figure 4.27 and summarized in Table 4.8. The calculation results confirm that the Ti grain size does not affect to the increase of yield stress in the extruded Ti composites materials in this study. On the other hand, the calculation confirms the effect of grain refinement in the extruded pure Ti without reinforcement. The

obtained results of the incremental yield stress will be used to further estimation of incremental yield stress by the effect of carbon solid solution in the next section.

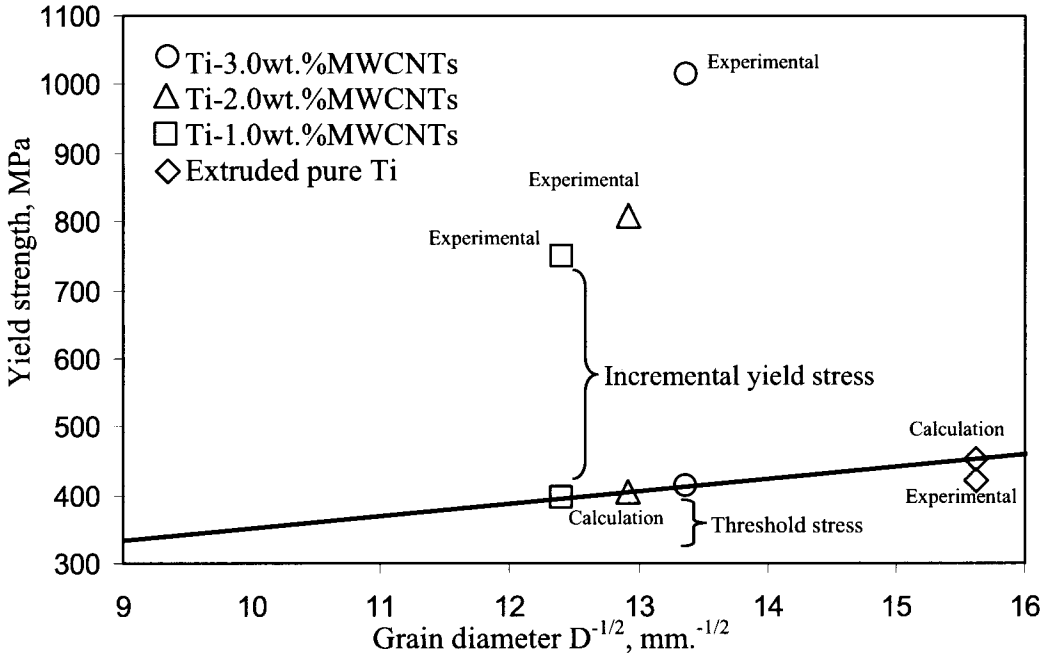

Figure 4.27 Incremental yield stress of the extruded fine Ti composites coated with 1.0, 2.0 and 3.0wt.% MWCNTs/zwitterionic solution.

Table 4.8 Incremental yield stress of the extruded fine Ti composites coated with 1.0, 2.0 and 3.0wt.% MWCNTs/zwitterionic solution.

Extruded fine Ti composites	Grain size, μm	Experimental yield stress, MPa	Calculation yield stress (Threshold stress), MPa	Incremental yield stress, MPa
Extruded fine Ti	4.1	421	453	Good agreement
1wt.%MWCNTs	6.5	750	396	354
2wt.%MWCNTs	6.0	808	405	403
3wt.%MWCNTs	5.6	1015	413	602

4.3.2 Carbon solid solution

The increase of yield stress by the effect of carbon solid solution is also investigated. This is due to carbon atoms at the outer surface of MWCNTs possibly diffuse into the Ti matrix during the SPS process. They will occupy in both *a* and *c* axes of the Ti lattice [18], resulting in expansion of the lattice parameters. Therefore, the XRD analysis and the Cohen's least squares method [19-20] are primarily used to investigate and calculate the expansion of the Ti lattices, compared to the lattice parameters of extruded fine Ti without reinforcement which is the reference material in this investigation. The expanded lattice parameters results will be compared with the master plot which reported by H. Conrad [18] to obtain the amount of carbon solid solution. It should be noted that the master plot can be adjusted by using the ratio of *c*/*a*. The extruded fine Ti composites in the section of 4.3.1 are used as a representative sample again. The carbon solid solution amount of each sample is shown in Figure 4.28 and those of calculation results, i.e., *a*, *c* axis and their ratio, are listed in Table 4.9

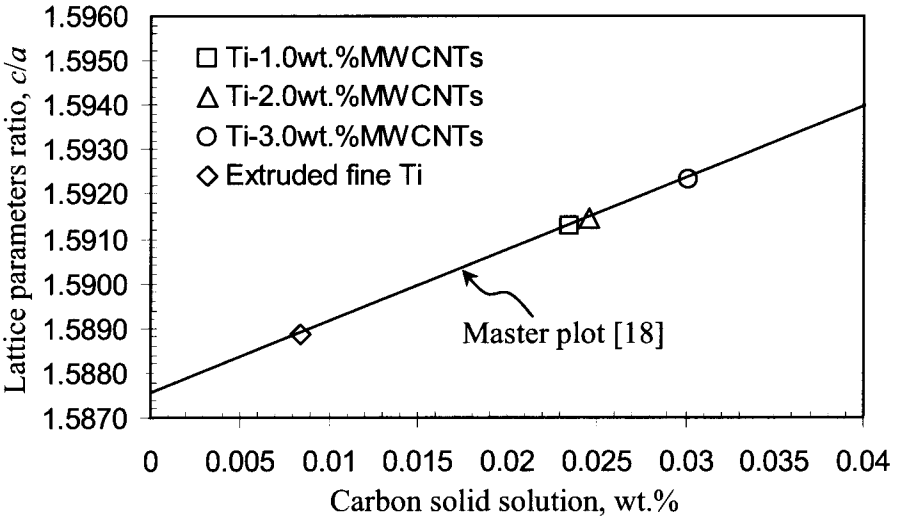

Figure 4.28 Estimation of carbon solid solution amount in the extruded Ti composites coated with 1.0, 2.0 and 3.0wt.% MWCNTs/zwitterionic solution.

Table 4.9 Lattice parameters of the extruded fine Ti composites and amount of carbon solid solution.

Extruded fine Ti composites	Lattice parameters, Å		Expansion of lattice parameter, Å		Ratio of *c*/*a*	Carbon solid solution, wt.%
	a axis	*c* axis	Δa	Δc		
Extruded fine Ti	2.94473	4.67873	0	0	1.58885	0.00840
1wt.%MWCNTs	2.94990	4.69409	0.00052	0.00154	1.59127	0.02350
2wt.%MWCNTs	2.95048	4.69552	0.00057	0.00168	1.59144	0.02457
3wt.%MWCNTs	2.95223	4.70094	0.00075	0.00222	1.59234	0.03015

It is noted that the comparison result of the extruded fine Ti without reinforcement shows the carbon solid solution amount of 0.00840 wt.% which corresponds to the carbon content analysis value of 0.012 wt.% in Table 4.4. This means the calculation of lattice parameters and the comparison can yield good results for further estimation. The increase of yield stress by the effect of carbon solid solution can be obtained by comparing with the relationship between yield stress and carbon solid solution amount, shown in Figure 4.29

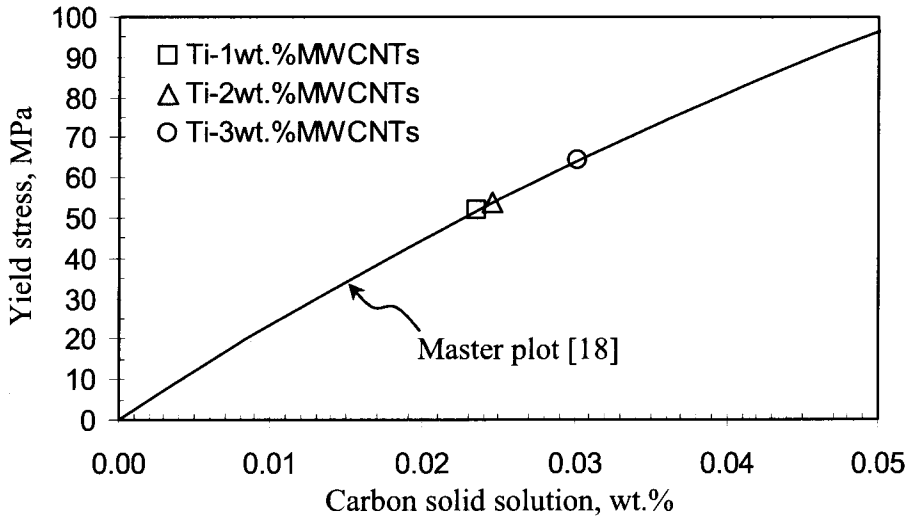

Figure 4.29 Estimation of incremental yield stress by effect of carbon solid solution.

The increase of yield stress by carbon solid solution of the extruded Ti composites coated with 1.0, 2.0 and 3.0 wt.%MWCNTs/zwitterionic solution is 51.8, 53.9 and 64.3 MPa, respectively. Finally, the increased yield stress by the second phases can be obtained by subtracting the summation of the threshold stress in the section 4.3.1 and this estimation from the measured yield stress in the experiment. The summarization of the increased yield stress by each strengthening mechanism is shown in Table 4.10.

Table 4.10 Summarization of the increased yield stress by each strengthening mechanism.

Extruded fine Ti composites	Experimental yield stress, MPa	Threshold stress, MPa	Incremental yield stress, MPa	
			Carbon solid solution	Second phases (TiC+MWCNTs)
1wt.%MWCNTs	750	396	51.8	302.2
2wt.%MWCNTs	808	405	53.9	349.1
3wt.%MWCNTs	1015	413	64.3	537.7

4.3.3 Second phase dispersion strengthening

The strengthening mechanism by the dispersion of *in-situ* formed TiC particles and the remained MWCNTs are clearly shown in Table 4.10. However, the further clarification, concerning the effects of the remained MWCNTs and the dispersed TiC particles, is limited by many reasons, such as volume fraction, dispersion and inter spacing of each remained MWCNTs. These factors directly relate to the *in-situ* formed TiC particles, and they are all interrelated together. For example, at constant particle size, the interparticle distance of TiC decreases with increasing volume fraction. This will be more complicated in the case of remained MWCNTs. In addition, although the volume fraction of TiC particles can be estimated by the metallographic methods, but one of the cases in the section 4.1.3, the TiC particles are rarely detected by microstructure observation. This evidence increases more complication for the estimation of incremental yield stress by the effect of second phases. However, the quantitative measurement of TiC particles in the Ti matrix can be used to reflect the increase of mechanical properties by the balance of TiC and remained MWCNTs as mentioned in the section 4.2.4. Figure 4.30 shows the TiC calibration curve which is prepared by internal standard method [19] to estimation of the TiC content in this study

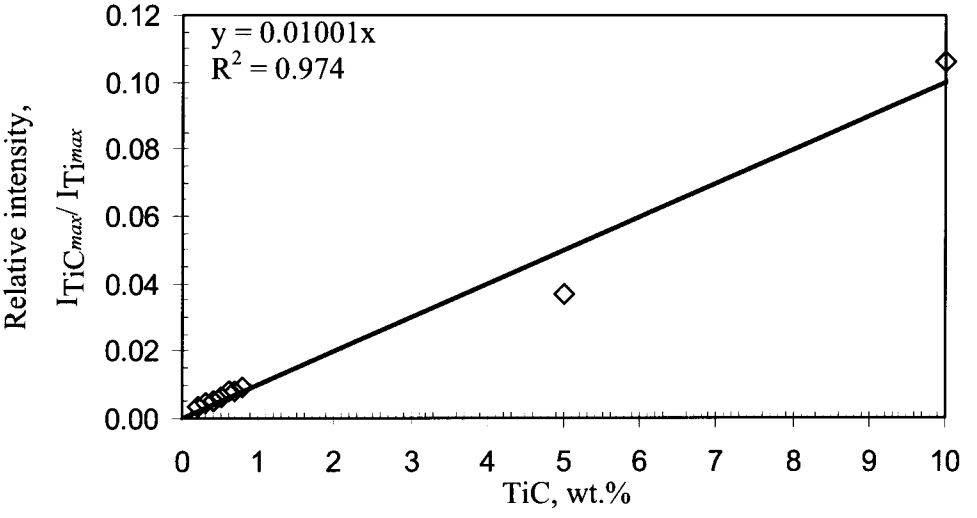

Figure 4.30 Calibration curve of TiC particle in Ti matrix.

4.4 Conclusions

The microstructure and mechanical properties of both extruded sponge and fine Ti composites reinforced with MWCNTs were improved through a combination of solution-coating technique and powder metallurgy process. By adding a small amount of MWCNTs, the yield stress and tensile strength of the extruded Ti composites were tremendously increased. The conclusions of this chapter are as follows.

(1) The yield stress and tensile strength of both extruded sponge and fine Ti composites were increased with the increasing MWCNTs content, while the elongation of those extruded Ti composites were high enough for engineering application.

(2) $MgCl_2$ and TiFe intermetallic compounds were inevitably formed at every thermal parameter used for the sponge Ti powders because of their chemical compositions.

(3) Ti grain size did not significantly affect the increase of mechanical properties of the extruded Ti composite.

(4) The increased yield stress and tensile strength of the extruded Ti composites were mainly due to the dispersion strengthening mechanism of the TiC particles and the remained MWCNTs in the Ti matrix.

(5) Higher SPS consolidation temperature caused the coarsening of TiC particles reducing the mechanical properties of the extruded Ti composites

(6) A good balance between microstructures and mechanical properties of high strength Ti composites could be obtained by SPS consolidation at 1073 K for 1.8 ks.

References

1. J.-P. Salvetat, J.-M. Bonard, N.H. Thomson, A. J. Kulik, L. Forró, W. Benoit, L. Zuppiroli, "Mechanical Properties of Carbon Nanotubes", *Applied Physics A*, 69 (1999) 255-260.
2. Z. X. Guo and B. Derdy, "Chemistry Effects on Interface Microstructure and Reaction in Titanium-based Composites", *Composites*, vol. 25, 7 (1994) 630-636.
3. J. Tanabe, T. Sasaki and S. Kishi, "Diffusion Bonding of Ti/Graphite and Ti/Diamond by Hot Isostatic Pressing Method", *Journal of Materials Processing Technology*, 192-193 (2007) 453-458.
4. Y. Maeno, A. Ishikawa and Y. Nakayama, "Adhesive Behavior of Single Carbon Nanotubes", *Applied Physics Express*, 3 (2010) 065102-1 – 065102-2.
5. O. Kubaschewski, C.B. Alcock and P. J. Spencer, *Materials Thermo-chemistry*, 6th ed., Pergamon Press, England, (1993).
6. C. Robelin, P. Chartrand and A. D. Pelton, "Thermodynamic Evaluation and Optimization of the ($MgCl_2$ + $CaCl_2$ + $MnCl_2$ + $FeCl_2$ +$CoCl_2$ + $NiCl_2$) System", *Journal of Chemical Thermodynamics*, 36 (2004) 793-808.
7. P. Selvam, B. Viswanathan, C. S. Swamy and V. Srinivasan, "X-Ray Photoelectron Spectroscopic Investigations of The Activation of FeTi for Hydrogen Uptake", *International Journal of Hydrogen Energy*, vol. 2, 4 (1987) 245-250.
8. T. Kuzumaki, O. Ujiie, H. Ichinose and K. Ito, "Mechanical Characteristics and Preparation of Carbon Nanotube Fiber-Reinforced Ti Composite", *Advance Engineering Materials*, vol. 2, 7 (2002) 416-418.
9. T. Threrujirapapong, K. Kondoh, H. Imai, J. Umeda and B. Fugetsu, "Hot Extrusion of Pure Titanium Reinforced with Carbon Nanotubes", *Steel Research International*, vol. 81, 9 (2010) 1320-1323.
10. G. S. Upadhyaya, *Powder Metallurgy Technology*, 1st ed., Cambridge International Science Publishing, UK (2002).
11. J. R. Davis, *Metal Handbook*, Desk ed., ASM International, (1998).
12. C. Leyens and M. Peters, *Titanium and Titanium alloys*, Wiley-VCH, Germany (2003).
13. G. Lütjering and J.C. Williams, *Titanium*, 2nd ed., Springer-Verlag, Germany (2007).

14. G. E. Dieter, *Mechanical Metallurgy*, SI Metric ed., McGraw-Hill (1988).
15. W. F. Hosford, *Mechanical Behavior of Materials*, Cambridge University Press, UK (2005).
16. R. M. Aikin, Jr., "The Mechanical Properties of *In-Situ* Composites", JOM, 49, 8 (1997) 35-39.
17. Y. Kobayashi, Y. Tanaka, K. Matsuoka, K. Kinoshita, Y. Miyamoto and H. Murata, "Effect of Forging Ratio and Grain Size on Tensile and Fatigue Strength of Pure Titanium Forgings", *Journal of the Society of Materials Science*, Japan, vol. 54, 1 (2005) 66-72 (In Japanese).
18. H. Conrad, "Effect of Interstitial Solutes on The Strength and Ductility of Titanium", *Progress in Materials Science*, 26 (1981) 123-403.
19. B. D. Cullity and S.R Stock, *Elements of X-Ray Diffraction*, 3rd ed., Prentice Hall, USA, (2001).
20. J. B. Hess, "A Modification of The Cohen Procedure for Computing Precision Lattice Constants from Powder Data", *Acta Crystallographica*, vol. 4, 3 (1951) 209-215.

Chapter 5

Fatigue and High Temperature Strength of Fine Titanium Matrix-Carbon Nanotubes Composite

Based on the results in chapter 4, the mechanical properties of commercially pure titanium are improved tremendously by the application of solution-coating technique in the P/M route. However, those improvements are valid in the static mode. The mechanical evaluation in the dynamic mode of the produced materials is required to determine their performance. In addition, the stability of those produced materials at elevated temperatures is also determined in this chapter.

5.1 Preparation of large-scale materials for fatigue strength evaluation

In order to study the ability to scale up processes from laboratory to industrial scale, large amounts of the fine Ti powders are coated by the developed solution-coating technique. The concentrations of 1.0 and 2.0 wt.% MWCNTs in the zwitterionic solution are selected to use in this experiment because the mechanical properties results as shown in chapter 4 indicate a good balance of high strength and high ductility. 860 g of fine Ti powders are immersed into 400 g of the MWCNTs/zwitterionic solution, compared to laboratory scale of 130g of fine Ti powders and 60 g of solution. The consolidation is performed using the same thermal history of the SPS process at 1073 K for 1.8 ks. The applied pressure during consolidation can not be fixed at 30 MPa because the capability limitation of the SPS machine. Therefore, the consolidation pressure is decreased to the smaller level of 25 MPa.

Dimension and bulk density of the SPS consolidated billet are shown and summarized in Figure 5.1 and Table 5.1. The SPSed billets show the relative density of over 97% which is comparable to that of the SPSed billet produced in laboratory scale. Subsequently, the SPSed billet is extruded by 5000 kN hydraulic press machine installed in the company, but some extrusion parameters used in laboratory are adjusted to suit the industrial equipment. The

extrusion ratio is changed from 37 to 26. The heating rate of billet is also changed from 2 K/s to approximately 1.6 K/s corresponding to the type of industrial furnace and size of billet.

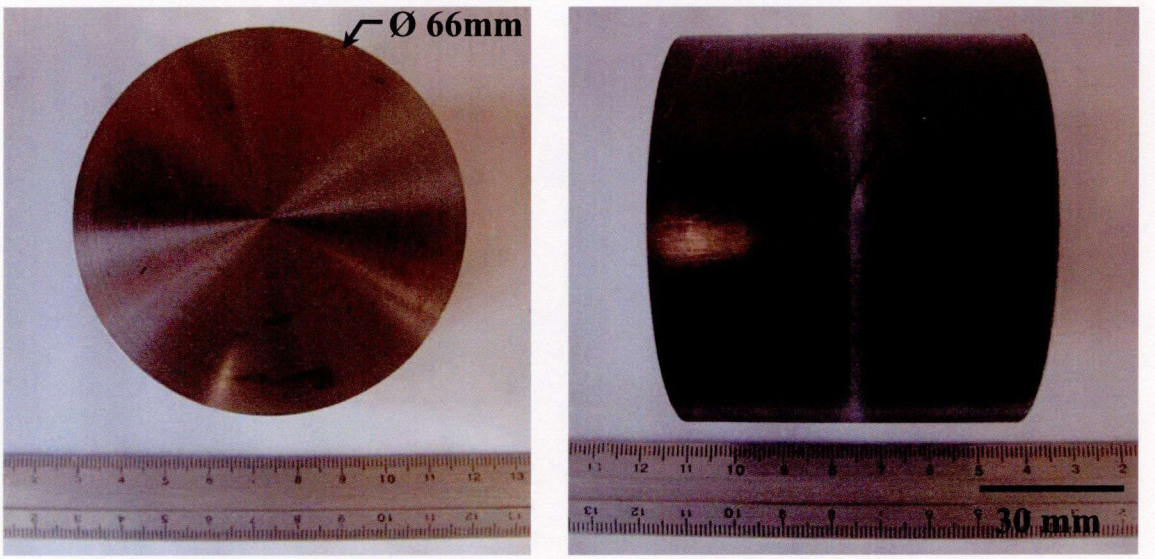

Figure 5.1 Dimension of the SPS consolidated billet of Ti/MWCNTs composite.

Table 5.1 Bulk density of the SPSed fine Ti composite billets

SPS billet	Weight (g)	Volume (cm^3)	Bulk density ($g \cdot cm^{-3}$)	Relative density (%)
1.0 wt.%MWCNT	834.33	189.33	4.41	97.9
2.0 wt.%MWCNT	841.00	191.84	4.38	97.4

Figure 5.2 shows a successful extrusion of the Ti composite billet. The estimation of bulk density of the extruded rods shows a higher value than that theoretical value of pure Ti [1], which can be deduced that full density of the extruded Ti composite can be obtained. This is a reasonable comparison for the pure Ti matrix reinforced with very low amount of second phases. The microstructure and the fatigue strength evaluation results of the extruded Ti composite will further be discussed in the next section. The extruded Ti composite are finally machined into tensile test bars and fatigue test specimens.

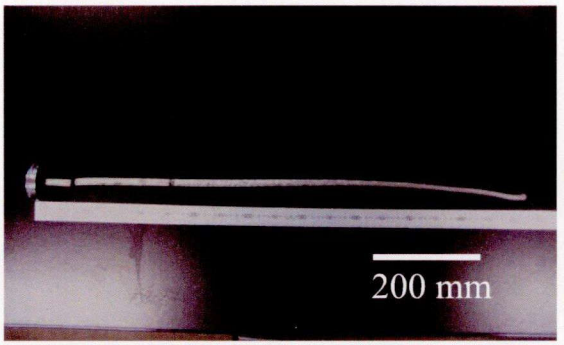

Figure 5.2 Successful extruded billet of fine Ti coated with 2.0wt.% MWCNTs/zwitterionic solution.

5.2 Fatigue strength analysis

The microstructure of the extruded fine Ti composites in the section 5.1 is primarily observed to compare the results between laboratory and industrial scale. After that, the extruded Ti composite rods are machined into tensile specimen bars and fatigue test specimen, according to ASTM E8M and E466 standards, respectively [2-3]. The optical microstructure observation of the extruded fine Ti composites is shown in Figure 5.3. The microstructures show the same TiC particles and Ti matrix similar to the extruded fine Ti composites in chapter 4. The TiC particles size measurements of all extruded fine Ti composites prepared by the solution-coating technique containing 1.0 and 2.0 wt.% MWCNTs, indicate that TiC particles measure 2.8 and 4.0 μm, respectively, while the Ti grain size measurements average 12.6 and 13.2 μm, respectively.

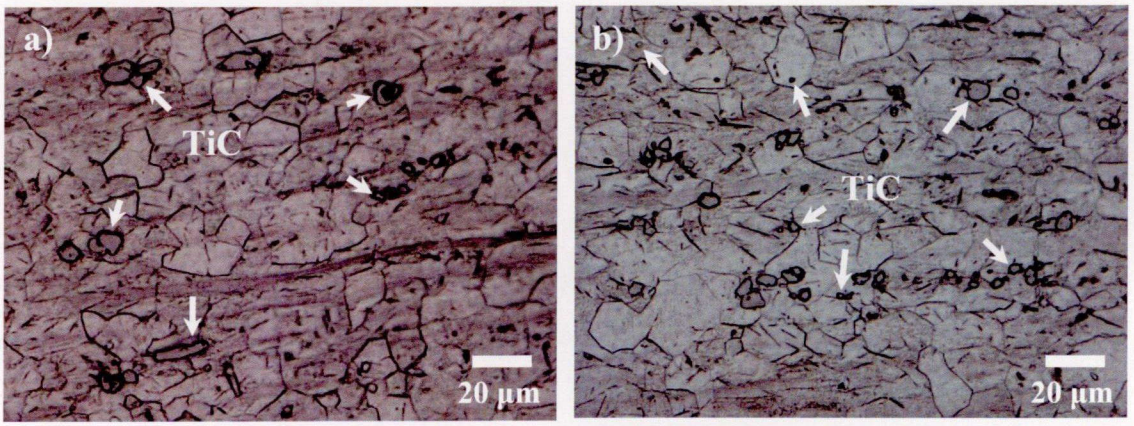

Figure 5.3 Microstructure of the extruded fine Ti composite coated by the solution-coating technique containing a) 1.0 and b) 2.0 wt.% MWCNTs.

The amount of TiC particles is estimated using the comparison with the TiC calibration curve. The estimation results have confirmed that the TiC fraction increases with increasing MWCNTs content, which are 1.042 and 1.775 wt.% for the extruded fine Ti composite prepared by 1.0 and 2.0 wt.% MWCNTs/zwitterionic solution, respectively. It should be noted that the increased Ti grain size is due to the difference of some thermal parameters used, in particular the total preheating time before extrusion, in laboratory and industrial scale. That can be contributed to a slight decrease in the tensile strength.

Table 5.2 Average tensile test results of all test samples, Ti grain size, TiC particle size with their fraction and the carbon content of the extruded fine Ti composites prepared by the solution-coating of 1.0 and 2.0 wt.% MWCNTs.

Extruded fine Ti composites	Scale	YS, MPa	TS, MPa	e_f, %	HV	Grain size, μm	TiC size, μm	TiC fraction, (wt.%)	Carbon content, (wt.%)
1wt.% MWCNTs	Laboratory	750	883	29.3	345	6.5	1.4	0.812	0.250
	Industrial	711	839	35.39	291	13.2	4.0	1.042	0.280
2wt.% MWCNTs	Laboratory	808	918	28.2	370	6.0	1.7	1.267	0.463
	Industrial	741	869	33.79	302	12.6	2.84	1.775	0.380

The average tensile test results of all test samples, Ti grain size, TiC particle size with their fraction and the carbon content analysis results are summarized in Table 5.2, compared to the previous results in laboratory scale. Due to the difference of carbon content in each sample, the tensile properties results should be normalized by dividing by their carbon content. The correction results of the incremental tensile properties per 0.1 wt.% of carbon content are also summarized in Table 5.3. In the case of 1.0 wt.% MWCNTs/zwitterionic solution, it is clarified that the tensile properties of industrial scale production are higher than those of laboratory scale materials. On the other hand, the case of 2.0 wt.% MWCNTs/zwitterionic solution shows results adversely. However, a difference of tensile

properties between laboratory and industrial scale in the corrected data is very small. Therefore, the scale up of the solution-coating technique is possible to be used in the industry.

Table 5.3 Incremental tensile properties per 0.1 wt.% of carbon content of the results in Table 5.2.

Extruded fine Ti composites	Incremental value / 0.1wt.% of carbon content			
	Scale	YS, MPa	TS, MPa	e_l, %
1wt.%MWCNTs	Laboratory	300	353	11.7
	Industrial	254	300	12.6
2wt.%MWCNTs	Laboratory	175	198	6.1
	Industrial	195	229	8.9

To evaluate the performance of the extruded fine Ti composites in dynamic mode, the fatigue test is performed using a servo-hydraulic axial fatigue testing machine. Based on the yield stress results as shown in Table 5.2, a fully reversed cycle of stress below the yield stress is applied to the fatigue specimen for evaluating the fatigue strength in this experiment. Figure 5.4 shows the S-N curves of the extruded Ti composites, compared to those of extruded fine Ti with no reinforcement and the previous work [4]. Table 5.4 shows the summarization of the fatigue limit of each extruded fine Ti composite. The extruded fine Ti composite prepared by 2.0 wt.% MWCNTs/zwitterionic solution shows a considerable fatigue limit of 450 MPa with a number of cycles to failure at 632,718 cycles, compared to those of extruded fine Ti composite prepared by 1.0 wt.% MWCNTs and pure Ti. The increase of fatigue strength can be explained through the effect of strain hardening and dispersion of second phases. The cyclic applied stress generates dislocation and deformation of Ti grain, while the dispersion of TiC particle retards the movement of dislocation and Ti grain sliding.

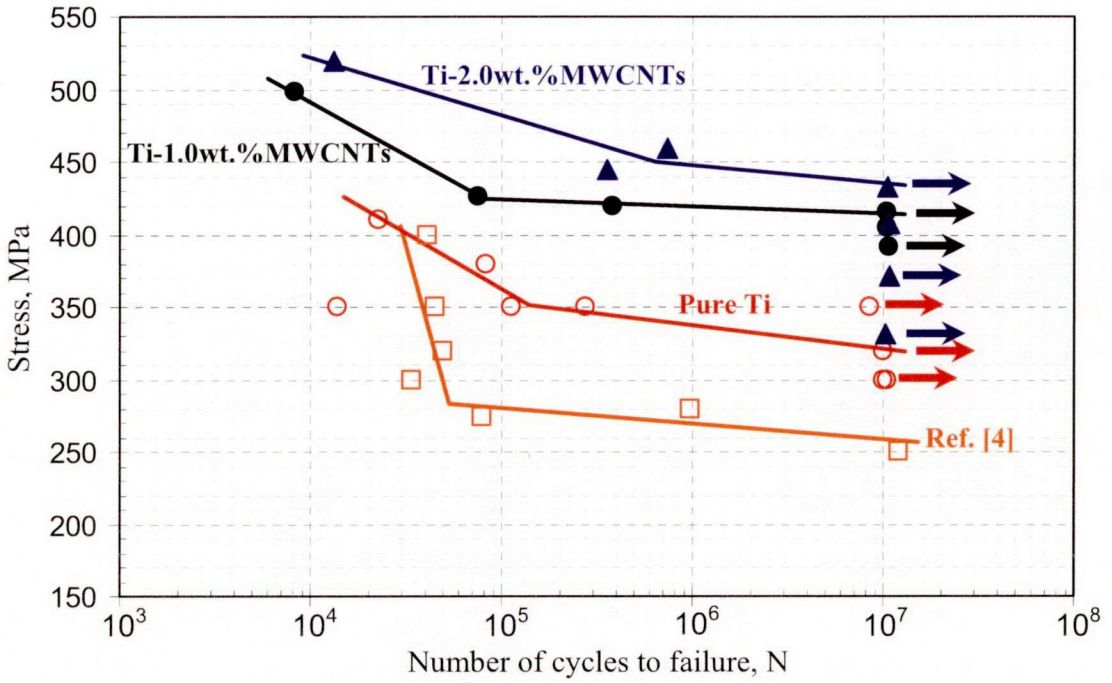

Figure 5.4 S-N curves of the extruded fine Ti composites prepared with 1.0 and 2.0 wt.% MWCNTs and without MWCNTs.

Table 5.4 Fatigue properties of each extruded Ti composite reinforced with MWCNTs.

Extruded Ti composite	Fatigue properties		Tensile properties			Grain size, μm	HV
	Stress, MPa	Cycle, N	YS, MPa	TS, MPa	Elong, %		
Pure Ti	351	139,221	459	625	35.3	10	229
1.0wt.%MWCNTs	424	80,334	710	838	35.3	13.2	291
2.0wt.%MWCNTs	450	632,718	741	869	33.7	12.6	302

The strain hardening of extruded Ti/MWCNTs composites are concerned with the effects of grain size and carbon solid solution in their matrices. The Ti grain size of the extruded fine Ti composites prepared by 1.0 and 2.0 wt.% MWCNTs indicates the value of 13.2 and 12.6 μm, respectively. The estimation of amount of carbon solid solution of those extruded fine Ti composites shows the value of 0.042 and 0.037 wt.% for the samples coated with 1.0 and 2.0 wt.% MWCNTs, respectively. Both of Ti grain size and amount of carbon solid solution in the case of 1.0 and 2.0 wt.% MWCNTs reinforced Ti composites almost

show the same value. Therefore, the strain hardening rates by the effects of grain size and the carbon solid solution in all extruded Ti/MWCNTs composites similarly show in the same level which can imply to the same resistance to the dislocation movement, but the difference in increase of the fatigue strength is the dispersion of the *in-situ* TiC particles in their matrices. Even though the amounts of TiC dispersoids indicate the close value of 1.042 and 1.775 wt.% for 1.0 and 2.0 wt.% MWCNTs samples, but the distribution of TiC dispersoids in the case of 2.0 wt.% is higher than that of 1.0 wt.% MWCNTs, which is more effective to retarding the dislocation movement, deformation and sliding of Ti grain during the fatigue test, resulting in increase of fatigue strength as shown in Figure 5.3. Therefore, the required stress for the motion of dislocation either cutting or bypassing the TiC dispersoids will be increased with increasing the distribution of very small TiC particles in the Ti matrix, resulting in the increase of fatigue strength in the extruded fine Ti composites prepared by 2.0 wt.% MWCNTs higher than that of 1.0 wt.% MWCNTs sample.

5.3 High temperature strength evaluation

Although, the mechanical properties response in the static and dynamic modes of the extruded Ti composites reinforced with MWCNTs show superior performance at room temperature, but some applications need to use or exposure to high temperature such as exhaust system of automotives, airplanes and power plants. Recently, commercially pure (CP) titanium grade 2 has been considered as a replacement material in the whole manufacturing process especially in the exhaust system by Volkswagen [1, 5], which is also used as starting material in this study. Therefore, the evaluation of mechanical properties at the elevated temperatures is required for proving the ability of the produced Ti composites. The fine Ti powders coated with 1.0, 2.0 and 3.0 wt.% MWCNTs/zwitterionic solution and without solution are consolidated at 1073 K, and subsequently extruded at 1273 K. In order to reduce the effect of strain hardening during thermo-mechanical processing, the extruded samples are annealed with low temperature at 473 K for 360 ks.

The effect of annealing on the mechanical properties of extruded pure Ti matrix without reinforcement shows the slight decreases of yield stress and tensile strength at the levels of 531 and 672 MPa, respectively, compared to those yield stress and tensile strength of as-extruded pure Ti matrix at 550 and 702 MPa, respectively. The ductility of the annealed pure Ti matrix is slightly increased at the level of 32.35%, while that of the as-extruded pure Ti matrix is 29.05%. These are due to the recovery process and coarsening of Ti grains occur during long time annealing at low temperature, which are confirmed by the decreasing yield stress and tensile strength and microstructure observation in Figure 5.5.

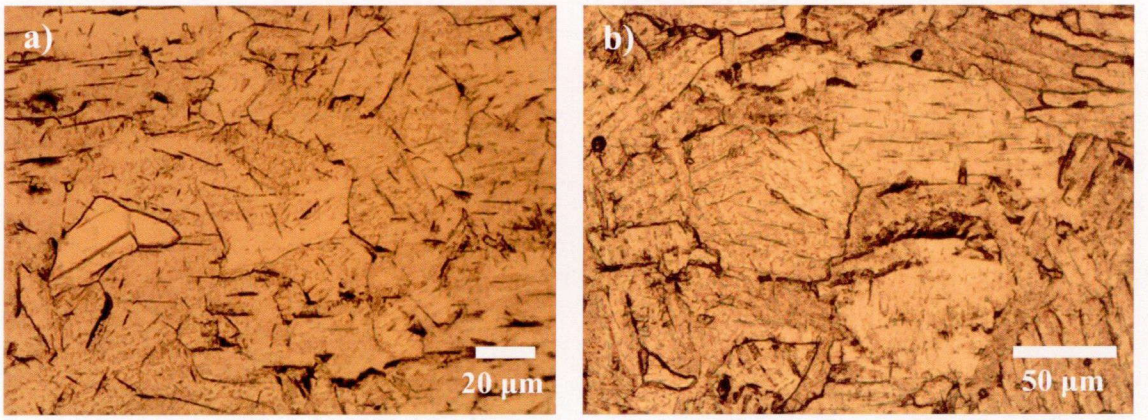

Figure 5.5 Microstructures of the extruded pure Ti matrix a) before annealing and b) after annealing at 473 K for 360 ks.

The grain size measurements of extruded pure Ti matrix before and after annealing process indicate the average value of 11.7 and 44.7 μm, respectively. In addition, the recovery process also occurs in the other extruded Ti reinforced with MWCNTs composites, resulting in annihilation of dislocations and simultaneous decrease in tensile strength slightly. However, the grain size measurement results of all extruded Ti reinforced with MWCNTs composite before and after annealing almost show a small variation in the range of 7 to 10 μm. Table 5.5 summarizes the average value of Ti grain size and TiC particle size before and after annealing process. The average values of Ti grain size and TiC at all tensile tested temperatures of the test samples measured at the area of grip section are also included in Table 5.5. The effects of the elevated temperatures on tensile properties of the test samples are summarized in Table 5.6 and also shown in Figure 5.6.

Table 5.5 Average Ti grain size and Ti particle size before and after annealing at 473 K for 360 ks and after high temperature tensile testing.

Size measurement	Extruded Ti	As-extruded	As-annealed	Tensile test temperature, K		
				473	573	673
Ti grain size, μm	Pure Ti	11.7	44.7	45.2	45.7	52.0
	1.0wt.%MWCNT	8.6	8.4	8.4	8.5	10.3
	2.0wt.%MWCNT	8.6	8.4	8.4	8.2	8.7
	3.0wt.%MWCNT	7.4	7.7	7.4	7.7	7.7
TiC particle size, μm	1.0wt.%MWCNT	2.0	2.1	2.2	2.2	2.1
	2.0wt.%MWCNT	2.0	1.9	2.1	2.0	2.0
	3.0wt.%MWCNT	2.1	2.0	2.1	1.9	2.1

Table 5.6 Tensile properties on elevated temperatures of extruded fine Ti composites prepared by 1.0, 2.0 and 3.0 wt.% MWCNTs/zwitterionic solution.

Tensile properties	Extruded Ti	Test temperature, K			
		298	473	573	673
YS, MPa	pure Ti	531	290	189	156
	1.0wt.%MWCNT	625	327	189	156
	2.0wt.%MWCNT	662	325	207	175
	3.0wt.%MWCNT	853	403	256	219
TS, MPa	Pure	672	339	215	176
	1.0wt.%MWCNT	812	404	314	264
	2.0wt.%MWCNT	820	428	343	281
	3.0wt.%MWCNT	922	496	412	368
Elongation, %	Pure	32.4	35.4	35.7	24.4
	1.0wt.%MWCNT	29.2	34.7	26.3	19.6
	2.0wt.%MWCNT	19.1	32.4	25.9	22.1
	3.0wt.%MWCNT	19.9	27.3	20.8	17.5

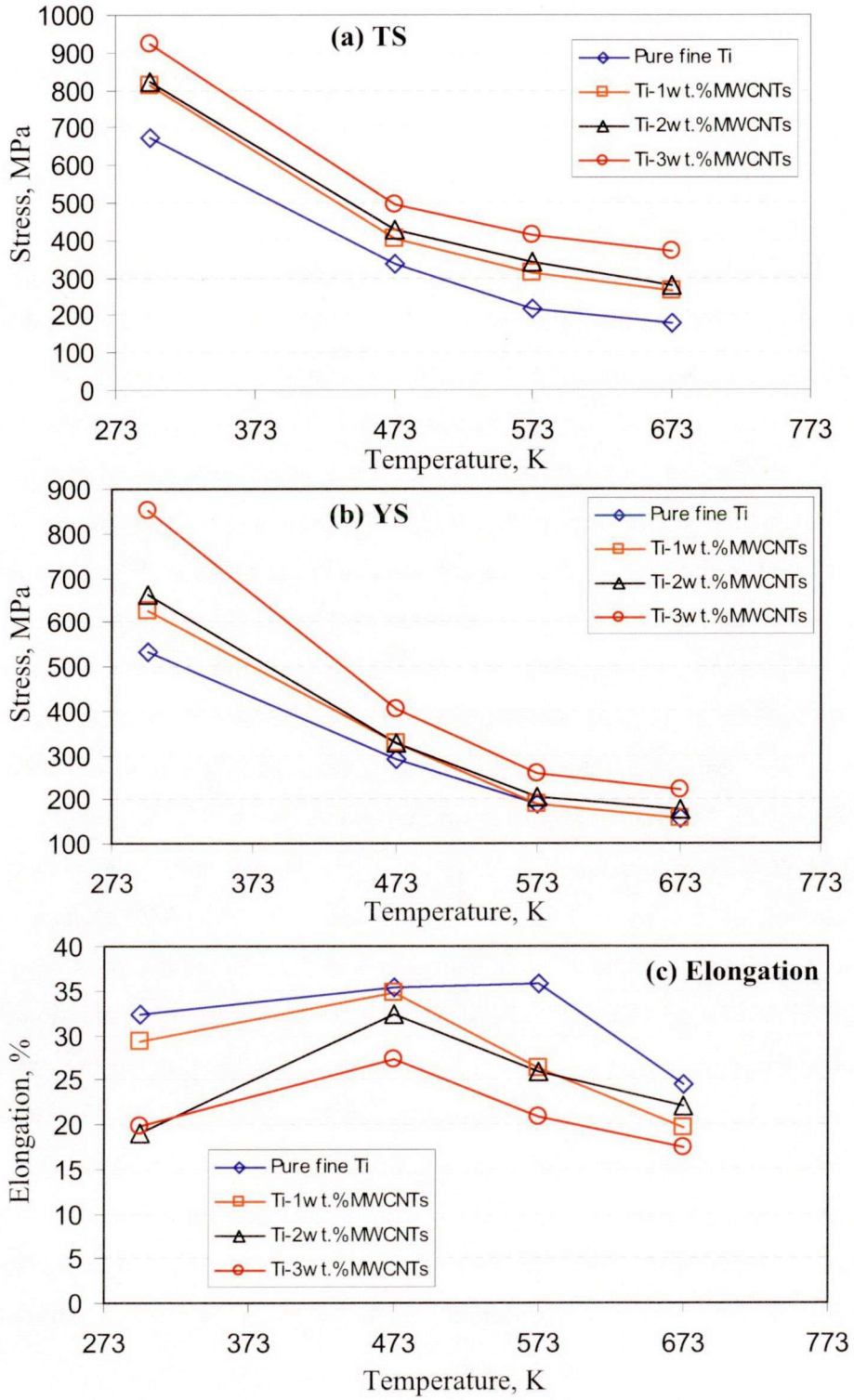

Figure 5.6 Dependence of tensile properties on elevated temperatures of the extruded fine Ti composites prepared by 1.0, 2.0 and 3.0 wt.% MWCNTs/zwitterionic solution.

The higher testing-temperature causes the lower yield stress and tensile strength of the samples. That can be explained by the diffusion-controlled creep behavior [6-8]. At elevated temperature, Ti atoms at grain boundaries which are parallel to the tensile stress axis can be diffused into another side of grain boundaries which are perpendicular to the tensile stress axis, resulting in a plastic elongation of Ti grain along the stress axis. This causes a decrease of cross sectional area of the test specimen during high-temperature tensile test. In the case of extruded Ti composite prepared by 3.0 wt.% MWCNTs, the yield stress and tensile strength are higher than those of extruded Ti composite prepared with 2.0 and 1.0 wt.% MWCNTs and extruded pure Ti matrix at the elevated testing-temperature. This is because the *in-situ* formed TiC dispersoids at the grain boundaries inhibit the motion of Ti grain boundaries which in turn impede the motion of Ti atoms to the another side of the grain boundaries located in the vertical direction of the tensile stress axis. Pinning effect of TiC dispersoids on Ti grain coarsening has confirmed by the growth of Ti grain size, not only during high temperature tensile testing, but also during annealing process as summarized in Table 5.5. The growth of Ti grain is obviously shown in the case of extruded pure Ti matrix in Figure 5.5. The grain size after hot extrusion averages at 11.7 μm, and then after the annealing process at 473 K for 360 s, grain size increases to 44.7 μm, while that of the extruded Ti/MWCNTs composites both after hot extrusion and annealing process indicates the same value of 8.4, 8.4 and 7.7 μm for 1.0, 2.0 and 3.0wt.% MWCNTs, respectively. In addition, the Ti grain coarsening is obviously found in the case of extruded pure Ti matrix and extruded Ti reinforced with 1.0 wt.% MWCNTs during the tensile evaluation at 573 and 673 K. Their microstructures are shown in Figure 5.7. It should be noted that the long time annealing causes the growth of lamellar structure in the extruded pure Ti matrix. This is presumed that the massive martensite structure, as shown in Figure 5.5 (a), which contains packets of small α plates or laths precursor with a thickness of about 0.5-1 μm [5], is thermally activated and grew along the same direction of the primary structure, resulting in coarse lamellar or laths structure inside grain of the annealed sample of extruded pure Ti matrix.

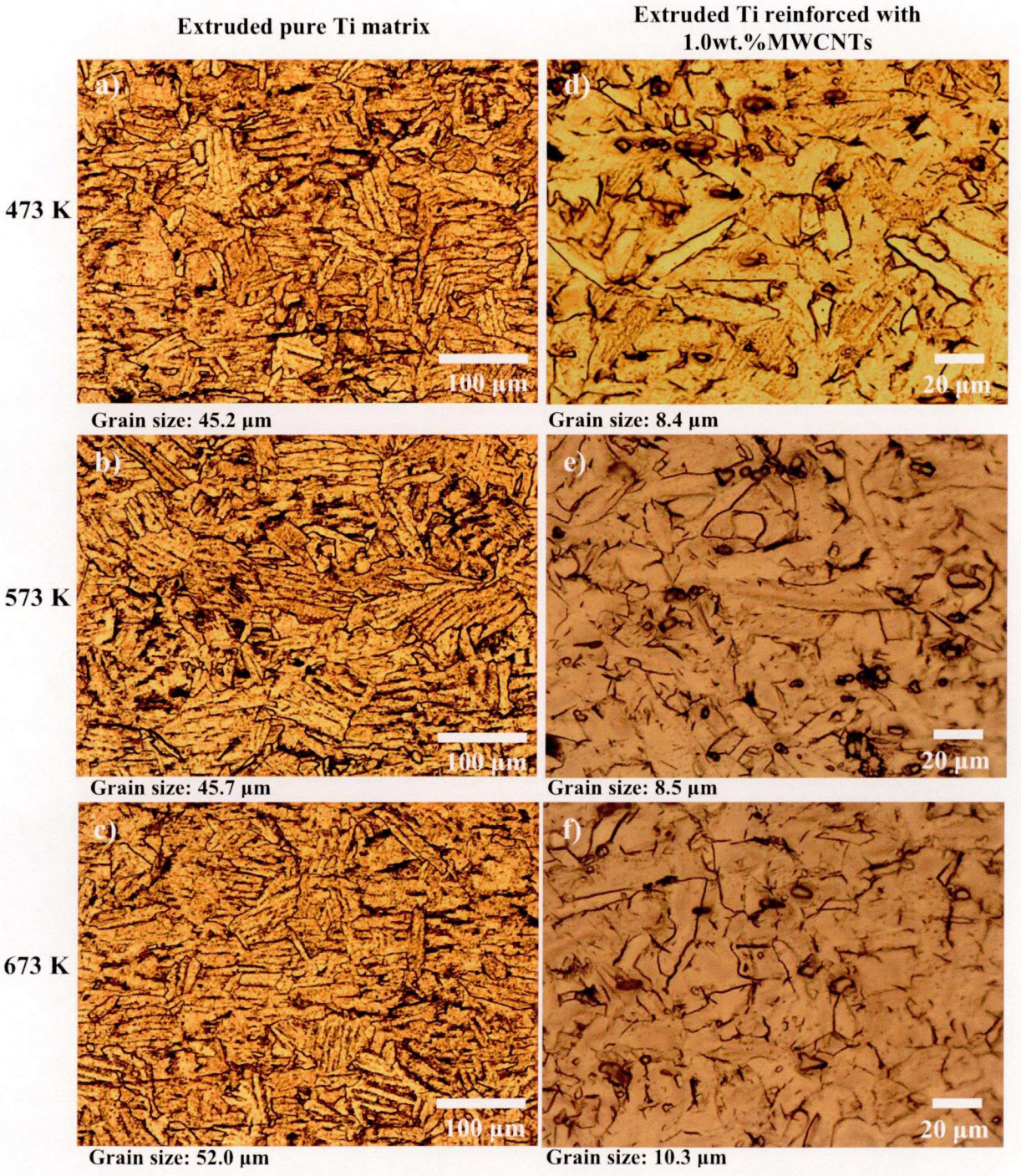

Figure 5.7 Microstructures of high temperature tensile tested samples of a)-c) extruded pure Ti matrix and d)-f) extruded Ti reinforced with 1.0wt.% MWCNTs.

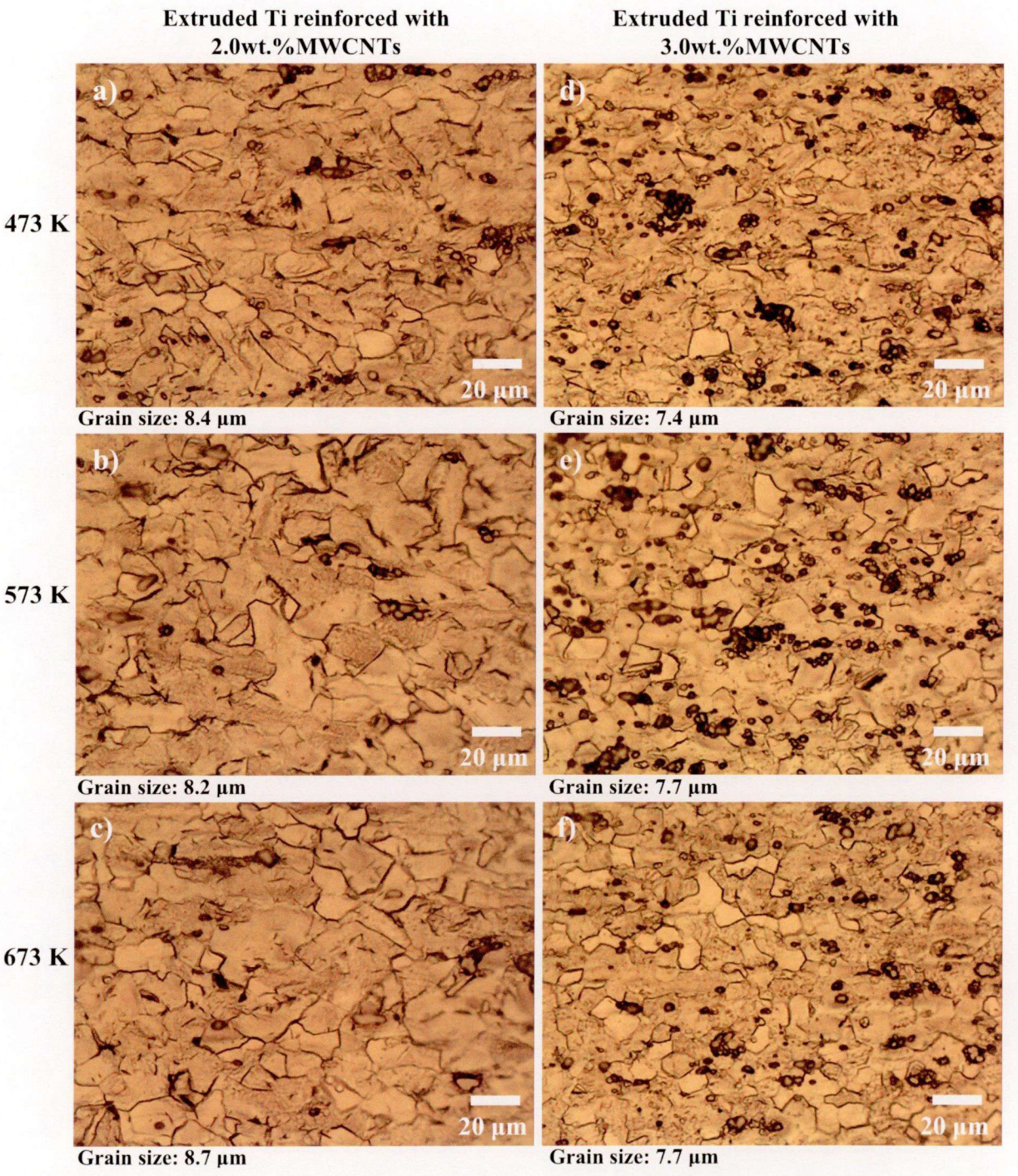

Figure 5.8 Microstructures of high temperature tensile tested samples of extruded Ti reinforced with a)-c) 2.0 wt.% and d)-f) 3.0 wt.% MWCNTs.

In contrast, that phenomenon never occurs with the extruded Ti reinforced with MWCNTs, as shown in Figure 5.7 (d)-(f) and Figure 5.8. This is because the driving force by the thermal activation during annealing may not be high enough to drive the formation of lamellar structure, which is related to the pinning effect of high distribution of TiC dispersoids retarding the motion of Ti atoms at grain boundaries. Moreover, the same mechanism can be used to explain the unchanged Ti grain size of extruded Ti/MWCNTs composites during tensile testing at the elevated temperatures in this study. Except for the extruded Ti composite coated with 1.0 wt.% MWCNTs tested at 673 K, the Ti grain size is slightly increased, compared to the other contents of MWCNTs used in extruded Ti composites. This is possibly due to the effects of thermal activated diffusion of Ti atoms associated with the induced strain energy from tensile loading are higher than the effect of TiC dispersoid pinning at the grain boundaries, which contribute to the diffusion of the Ti atoms along grain boundaries quickly, resulting in the growth of Ti grain size. Therefore, the increase of TiC dispersoid amount in the extruded Ti/MWCNTs composites can effectively improve the retardation of Ti grain coarsening during high temperature tensile testing, which in turn increases the stability of strength of the extruded Ti/MWCNTs composites. Moreover, the increase of TiC dispersoids is also effective to improve the retardation of Ti grain sliding. The microstructure observation at the necking area confirms the retardation of grain boundary sliding by TiC particle as shown in Figure 5.9.

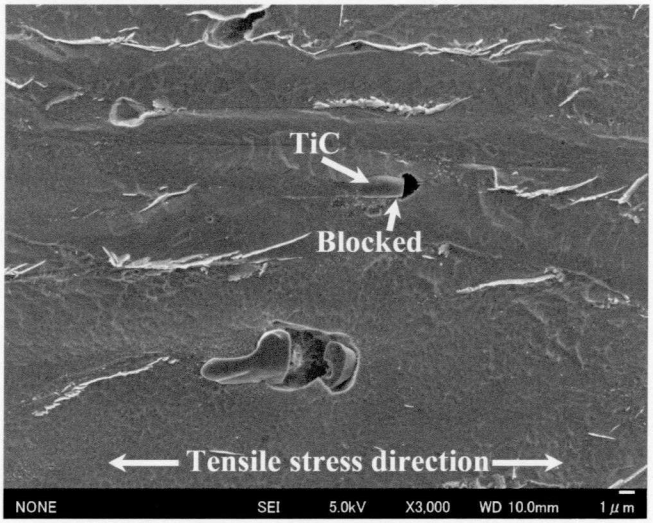

Figure 5.9 Microstructure of high temperature tensile tested sample at necking area revealed retardation of grain boundary sliding by TiC particle.

The effect of the elevated temperatures on hardness of the test samples is also shown in Figure 5.10. The results show the same decreasing tendency upon exposure at high temperature. The explanation is based on the softening mechanism [9] of materials. At elevated temperatures below 0.5 of the melting temperature, the dislocation and other defects are annihilated by the recovery process, resulting in decrease of the hardness of material. The rate of recovery is strongly dependent on temperature. Therefore, the micro hardness measurements of all samples at 573 K yield the lowest value, compared to the other temperatures. The increase of TiC particles in the Ti matrix also helps to increase the resistance to the applied pressure from the diamond indenter. Consequently, the extruded Ti composite coated by 3.0 wt.% MWCNTs can maintain the higher value of hardness at high temperatures than those of 1.0 and 2.0 wt.% MWCNTs samples.

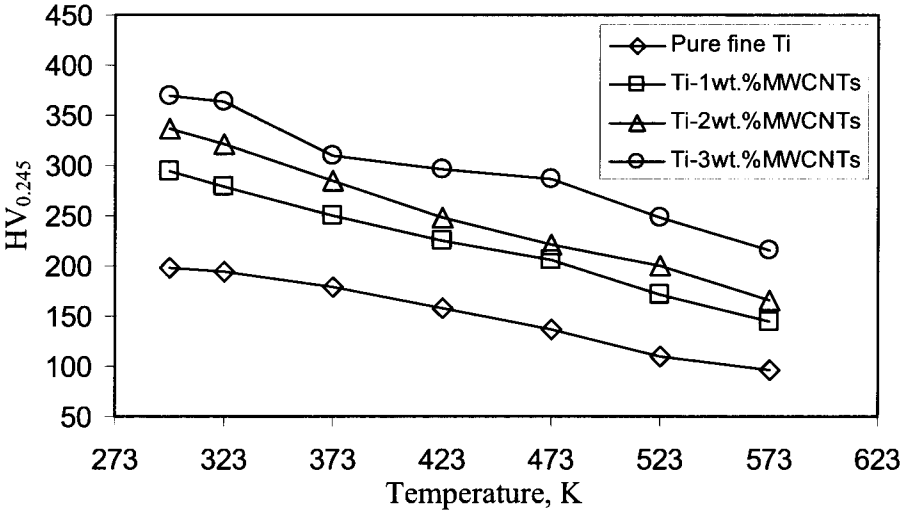

Figure 5.10 Dependence of hardness on elevated temperatures of the extruded fine Ti composites coated with 1.0, 2.0 and 3.0 wt.% MWCNTs/zwitterionic solution.

In addition to the effect of TiC dispersoids on the stability of strength at elevated temperatures, the effect of carbon solid solution is also considered as the minor factor to improve the strength of extruded Ti/MWCNTs composites at elevated temperatures lower than 775 K. In the previous study, H. Conrad [10] reported that the temperature where the first occurring migration at a significant rate of carbon interstitial solute was 775 K, which based on the mean atomic jump time at one second for the interstitial solutes in commercially

pure titanium. According to that report, the carbon solid solution atoms in the extruded Ti/MWCNTs composites are expected as the stationary interstitial solute atoms, which hardly diffused to other sites in the Ti lattice even though they are activated by thermal fluctuations during testing in the temperature range of 473-673 K. Therefore, the carbon solid solution can behave as obstacles to dislocation motion, similar to the TiC dispersoids, resulting in maintain the strength of extruded Ti/MWCNTs at elevated temperatures in this study.

5.4 Estimation of incremental stress by TiC dispersoids

The above results show good improvements of stability strength of the extruded Ti/MWCNTs composite at elevated temperature. Similar to the estimation of incremental yield stress in chapter 4, the estimations of the incremental yield stress due to effects of the grain refinement and dispersed TiC second phase particles are performed because those two effects strongly govern the stability of strength of the extruded Ti/MWCNTs composites at elevated temperatures. The smaller Ti grain size increases the diffusion-controlled creep rate, resulting in decrease of mechanical properties, while the TiC dispersoids resist the diffusion of Ti atoms along grain boundaries, dislocation movement and grain sliding, resulting in maintaining strength of the extruded Ti/MWCNTs composites at elevated temperature. Therefore, the quantitative estimation of those two effects in the extruded Ti/MWCNTs composites can give a better understanding of their stabilities during elevated temperatures tensile testing. In the estimation procedure, the increased yield stress by strain hardening, in particular effect of Ti grain size, is firstly calculated and the increased yield stress by the Ti dispersoids will be obtained by subtracting the calculated results of Ti grain size effect from the experimental yield stress.

The calculation of incremental yield stress by effect of Ti grain size is carried out using Hall-Petch relationship. It should be noted that the effect of strain hardening for the most metals are much reduced by the recovery process as the temperature increases [11, 12], resulting in invalidity of the Hall-Petch relationship at high temperature [13]. However, the strain hardening effect in the terms of Hall-Petch relationship, in the case of titanium, has been validated until 800 K in accordance with the previous reports [14]. In addition, the k constant value in the Hall-Petch relationship may be decreased with increasing temperature,

according to a previous report [15]. Therefore, the k constant value for each testing temperature, i.e., 473, 573 and 673 K, should be employed in the estimation. Unfortunately, due to the lack of information of k constant values, the calculation will begin by the estimation of k constant for each temperature.

The yield stress results of extruded pure Ti matrix in this study are compared to those results of commercially pure Ti grade 2 bars with the average grain size of 72 μm in the previous study [16] at the same temperature, as shown in Figure 5.11. It is appeared in Figure 5.11 that both of the yield stress values between previous study and this experiment are close together for each temperature used, thus the estimation of k constant is assumed that those materials exhibit the same strain hardening behavior during heating, which is allowed to calculate the k and σ_0 constant values by fixing one of the constant values in the Hall-Petch relationship and solving for the rest constant.

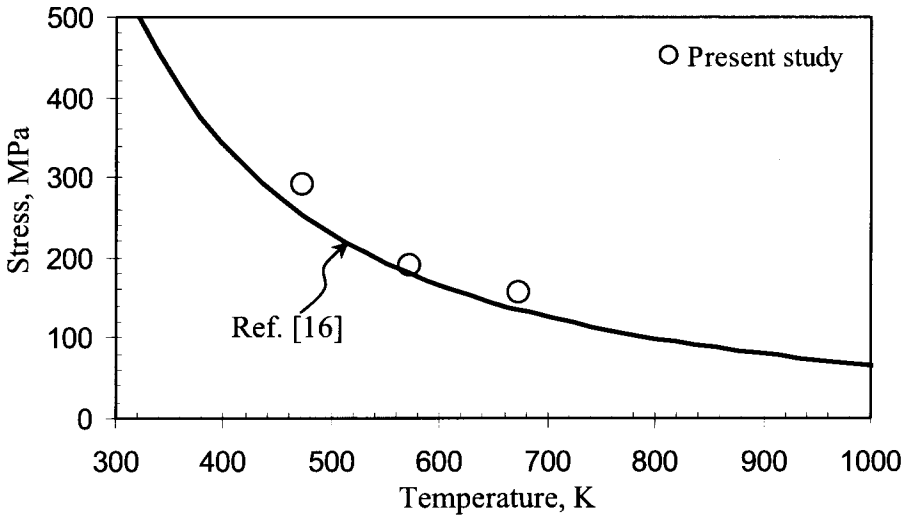

Figure 5.11 Dependence of yield stress on temperature for estimation of k constant.

The calculation result of k constant is 17.5, 8.4 and 9.3 MPa $\sqrt{mm}$, while the σ_0 constant is 1.9, 2.7 and 2.0 MPa for the extruded pure Ti matrix at 473, 573 and 673 K, respectively. It should be noted that the k constant of 17.5 MPa $\sqrt{mm}$ at 473 is close to 18 MPa $\sqrt{mm}$ [17] at room temperature. This can be implied that the strain hardening effect due to grain size is strongly dominated the yield stress of extruded pure Ti during tensile testing until 473 K. After 473 K, the k constant is obviously decreased because of the increasing effect of recovery process in accordance with the previous reports [15].

Therefore, the estimation of the incremental yield stress due to Ti grain size effect in the extruded Ti/MWCNTs composites has further estimated, which based on the same k constant value at each temperature estimated in the case of extruded pure Ti matrix and the grain size in Table 5.5. The estimation results, including the incremental yield stress due to TiC dispersoids, are listed in Table 5.7. The incremental yield stress due to grain size and TiC dispersoids effects of all extruded Ti/MWCNTs composites is shown in Figure 5.12.

Table 5.7 Estimation of yield stress increment due to Ti grain size and TiC dispersoids of extruded Ti/MWCNTs composites at different tensile testing temperature.

Extruded fine Ti composites	Tensile tested temperature, K	Experimental yield stress, MPa	Incremental yield stress, MPa		Incremental yield stress, %	
			Grain size	TiC dispersoid	Grain size	TiC dispersoid
1wt.% MWCNTs	473	327	136	191	42	58
	573	189	98	91	52	48
	673	156	64	92	41	59
2wt.% MWCNTs	473	325	134	191	41	59
	573	207	114	93	55	45
	673	175	75	100	43	57
3wt.% MWCNTs	473	403	199	204	49	51
	573	256	160	96	63	38
	673	219	112	107	51	49

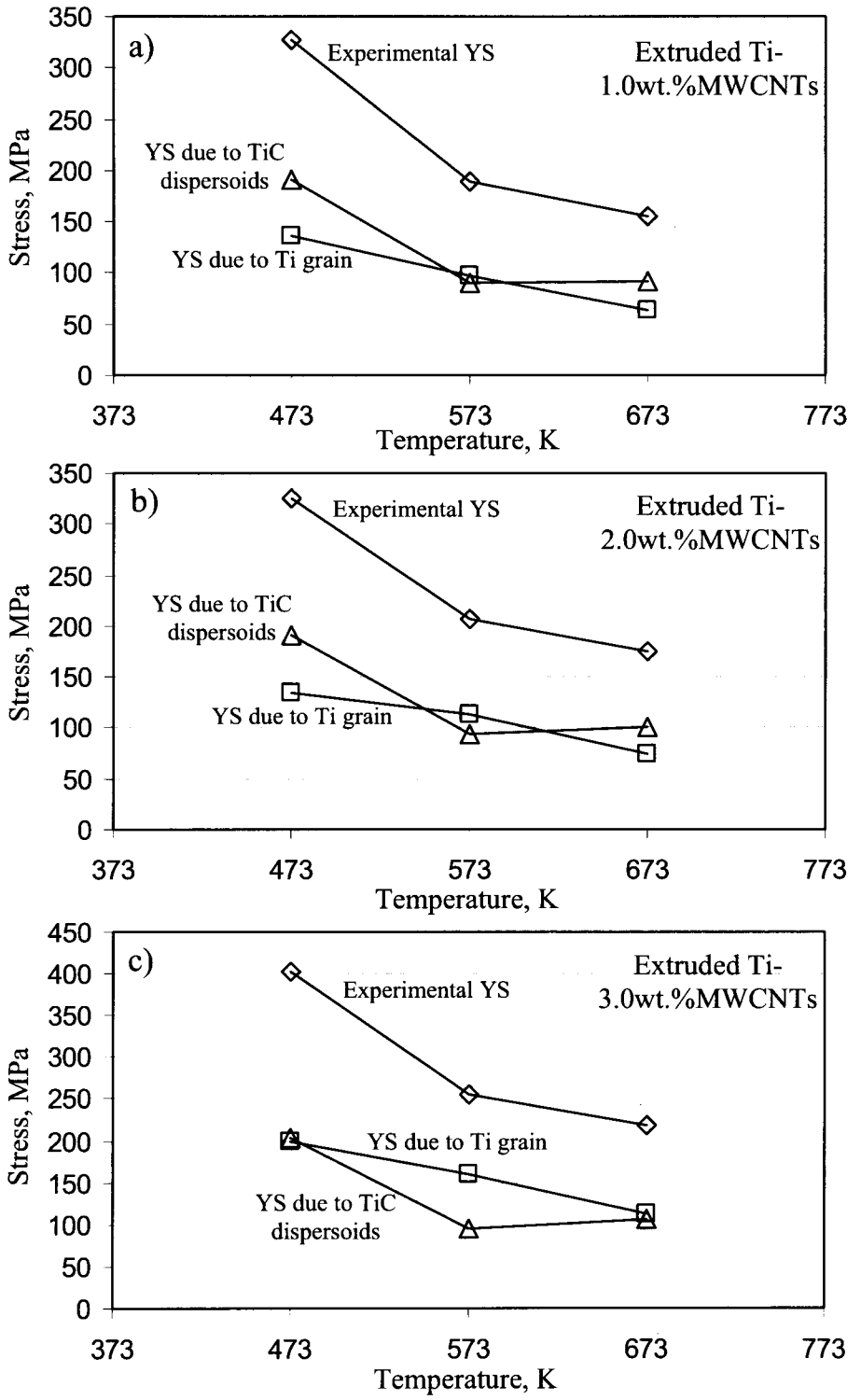

Figure 5.12 Estimation of yield stress increment due to Ti grain size and TiC dispersoids of extruded Ti composites coated by a) 1.0 wt.%, b) 2.0 wt.% and c) 3.0 wt.%MWCNTs.

The effect of Ti grain size has shown decreasing tendency with increasing tensile tested temperature. This can be attributed that the strain hardening effect in the terms of Ti grain size of the extruded Ti/MWCNTs composites is reduced by the recovery process during heating, resulting in the decrease of yield stress. However, the recovery process rate at elevated temperatures can be retarded by the TiC dispersoids in which resist the Ti grain coarsening by pinning effect. The dependent yield stress as function of Ti grain size at the same tensile tested temperature of all extruded Ti/MWCNTs composites is plotted in Figure 5.13. Figure 5.13 suggests that the strain hardening rate at each temperature during elevated temperature tensile testing can be increased with controlling Ti grain sizes as small as possible by the assistance of TiC dispersoids.

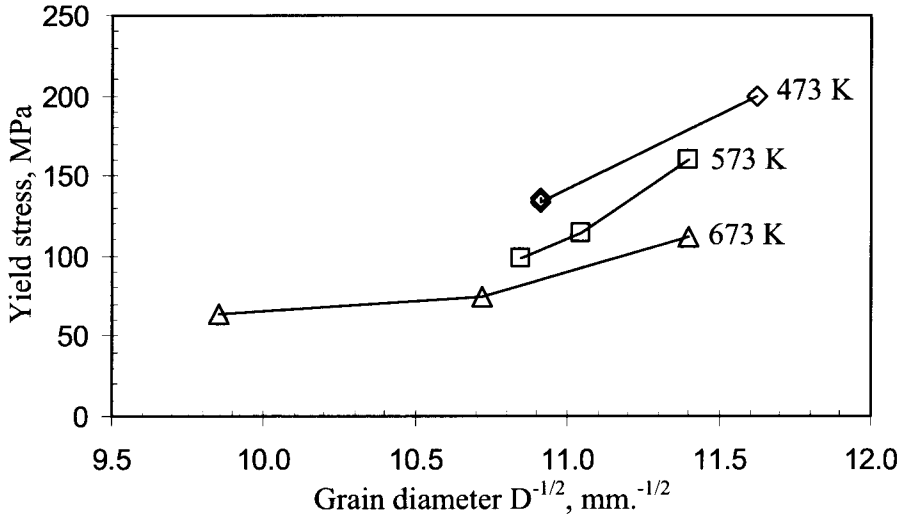

Figure 5.13 Dependence of yield stress as function of Ti grain size at different tensile tested temperatures of extruded Ti/MWCNTs composites in this study.

Moreover, the incremental yield stress percentage due to the Ti grain size and TiC dispersoids effect as shown in Tables 5.7 suggests that both effects are close together. This can be attributed that the resistance to the applied stress of the extruded Ti/MWCNTs composites during heating is caused by the strain hardening effect, in the terms of grain sizes, associated with pinning effect of TiC dispersoids. The pinning effect of TiC dispersoids is also interrelated to the strain hardening process, which helps to retard Ti grain coarsening during heating of all extruded Ti/MWCNTs composites.

5.5 Annealing of Ti/TiC extruded materials

In order to investigate the microstructural stability of extruded Ti/MWCNTs composites at elevated temperatures, the extruded Ti/MWCNTs composites are annealed at the temperatures of 573 and 673 K for 36 ks. The annealing process at 673 K for 360 ks is also carried out to investigate effect of annealing time on the microstructural changes of extruded Ti/MWCNTs composites. The microstructure changes of all annealed Ti composites are shown in Figure 5.14. The grain size measurements of all annealed samples are also summarized in Table 5.8.

Table 5.8 Average Ti grain size of extruded Ti composites after annealing at 573 and 673 K for 360 ks

Extruded fine Ti composites	Average Ti grain size, μm			
	As-extruded	Annealing time: 36 ks		Annealing time: 360 ks
		573 K	673 K	673 K
Extruded pure Ti	11.7	28.5	46.2	10.6
1wt.%MWCNTs	8.6	8.9	10.4	10.9
2wt.%MWCNTs	8.6	8.4	9.5	9.6
3wt.%MWCNTs	7.4	7.5	7.7	7.6

By observing the grain size of the extruded Ti/MWCNTs composites after annealing process, the microstructure of the extruded pure Ti matrix shows the increase of grain size when the annealing temperature is increased from 573 to 673 K, as shown in Figure 5.14 (a) and (b). On the other hand, the grain size measurement results of the extruded Ti/MWCNTs composites show very small increase of Ti grain size as shown in successive Figure 5.14 (d)-(l). The small increase of Ti grain size of the extruded Ti/MWCNTs composites can confirm the pinning effect of TiC dispersoids which help to suppress Ti grain growth during the annealing process. The annealing at 673 K for 360 ks also shows very small changes in Ti grain size in the case of extruded Ti/MWCNTs composites. In contrast, the extruded pure Ti matrix shows the decrease in grain size as shown in Figure 5.14 (c). This may be due to the recrystallization process occurs during long time annealing process.

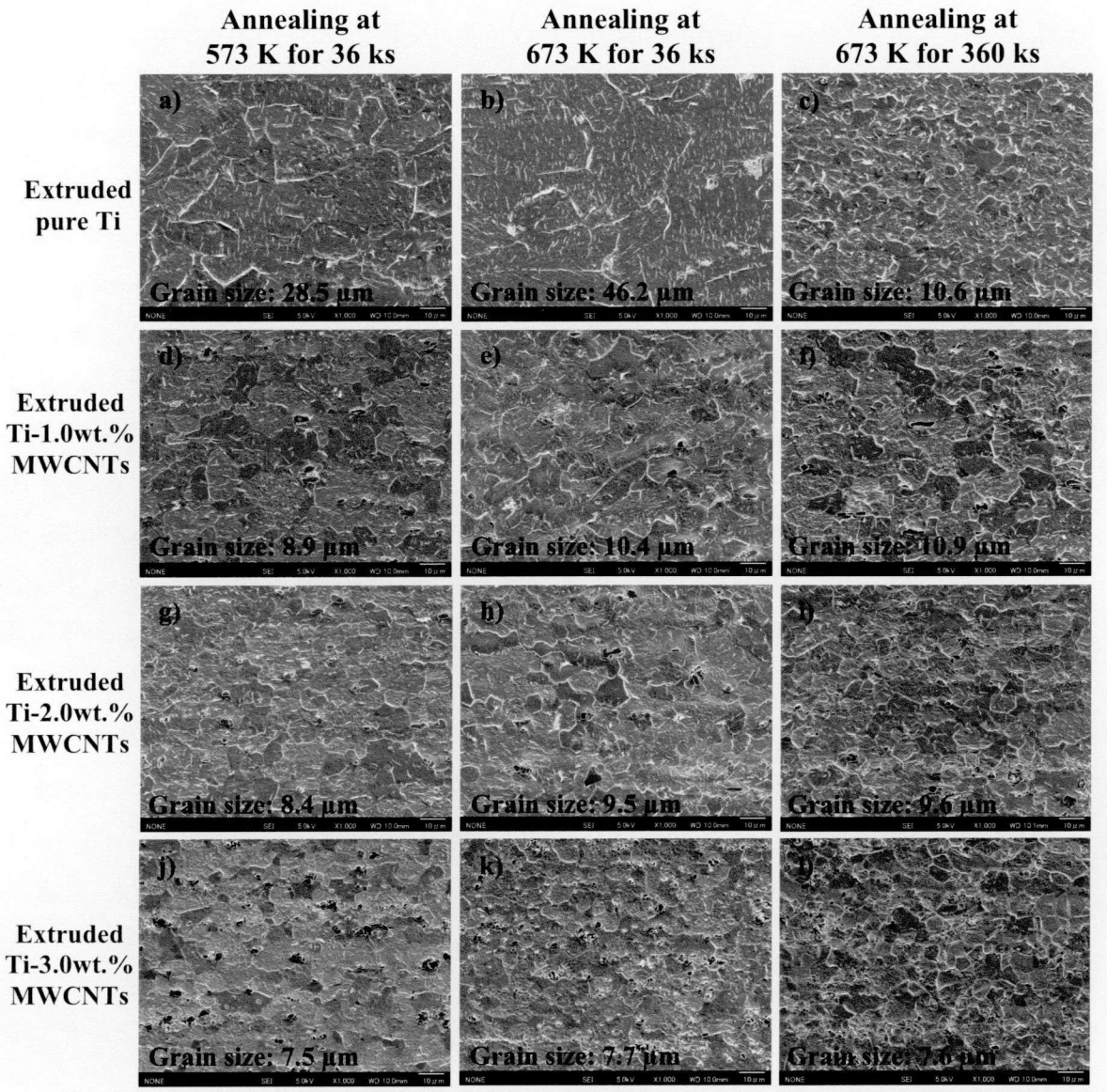

Figure 5.14 Microstructure of extruded Ti composites after annealing at 573 and 673 K for 36 ks and 673 K for 360 ks.

The microstructure observation results in Figure 5.14 (a)-(c) and grain size measurement results in Table 5.8 suggest the presence of grain growth (Figure 5.14(a)-(b)) and recrystallized Ti grain (Figure 5.14 (c)). The grain growth easily occurs as the annealing temperature increases because the higher annealing temperature helps to increase the activation energy for the mobility of grain boundary. That causes the increase of Ti grain size when the extruded pure Ti matrix is annealed at 573 and 673 K, respectively. On the other

hand, Figure 5.14 (c) shows the presence of recrystallized Ti grains when annealing at 673 K for 360 ks. This is due to the long time annealing affects the decrease of recrystallization temperature according to the previous reports [12, 18]. However, grain growth and recrystallization of Ti grain can be inhibited by the presence of TiC dispersoids. TiC dispersoids are effective to restrict grain-boundary movement by pinning effect during annealing at 573 and 673 K for 36 ks and 673 K for 360 ks. Moreover, TiC dispersoids also retard the recrystallization of new grains when the long time annealing because the TiC pinning pressure is higher than driving pressure for recrystallization nucleation of new grain. Therefore, the recrystallization may never occurs in the case of extruded Ti/MWCNTs composites which are annealed at 673 for 360 ks as shown in Figure 5.14 (f), (i) and (l), respectively, compared to the extruded pure Ti matrix in Figure 5.14 (c). In addition, the driving force for grain growth is generally lower than that of recrystallization [18]. Hence, the change of grain size in the extruded Ti/MWCNTs composites is concerned with grain growth and TiC pinning effect. In the case of 1.0 wt.% MWCNTs sample, Ti grain size gradually increases from 8.9 μm (Figure 5.14 (d)) to 10.4 μm (Figure 5.14 (e)) as annealing temperature increases from 573 K to 673 K. Under this condition, some Ti subgrains may grow much faster than average, leading to coalescence of Ti subgrains, in which the localized growth of large grains can be found in microstructure [18], as shown in Figure 5.15.

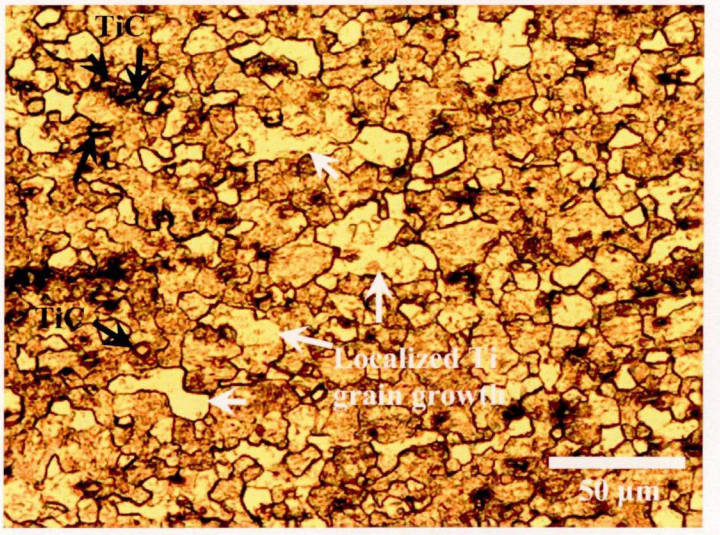

Figure 5.15 Optical microstructure image of extruded Ti-1.0wt.%MWCNTs composite, showing localized Ti grain growth after annealing at 673 K for 36 ks.

Figure 5.15 indicates that the discontinuous subgrain growth tends to occur in the areas where the TiC dispersoids are not encircling the Ti grain. High magnification image confirms that the area without the encirclement of TiC dispersoids shows the larger grain size as shown in the area A of Figure 5.16, compared to Ti gain size which is encircled by TiC dispersoids in the area B.

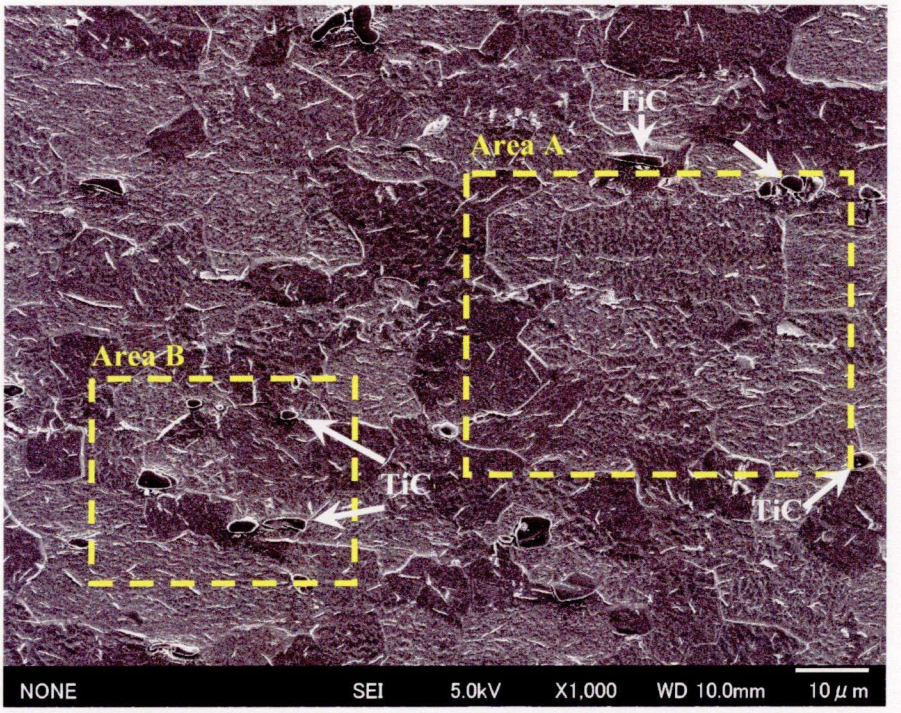

Figure 5.16 SEM image of extruded Ti-1.0wt.%MWCNTs composite, showing the localized Ti grain growth in area A and the unchanged Ti grain size due to TiC pinning effect in area B after annealing at 673 K for 36 ks.

Grain growth in the area B is inhibited by the increasing distribution of TiC dispersoids in the Ti matrix such in the case of Ti-3.0wt.% MWCNTs composite. In the case of Ti-3.0wt.% MWCNTs composite, the TiC pinning pressure is increased higher than driving force for the mobility of grain boundary, resulting in inhibition grain growth as show in Figure 5.14 (j) and (k). Optical microstructure image of extruded Ti-3.0wt.% MWCNTs composite does not reveal any localized subgrain growth evidence significantly as shown in Figure 5.17.

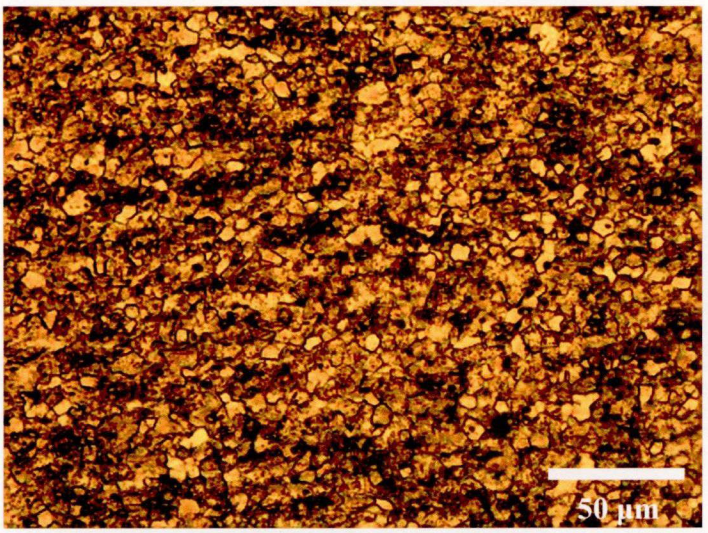

Figure 5.17 Optical microstructure image of extruded Ti-3.0wt.%MWCNTs composite after annealing at 673 K for 36 ks.

High magnification images have also confirmed the unchanged Ti grain size of extruded Ti-3.0wt.% MWCNTs composite after annealing at 563 and 673 K for 36 ks, as shown in Figure 5.18 (a) and (b) respectively.

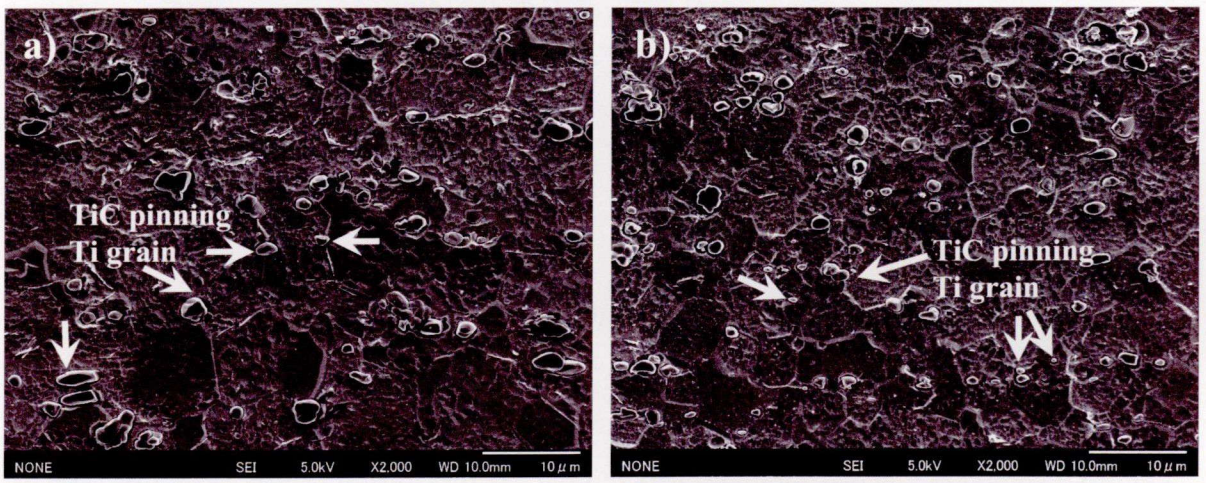

Grain size: 7.5 μm **Grain size: 7.7 μm**

Figure 5.18 SEM image of extruded Ti-3.0wt.%MWCNTs composite, showing the unchanged Ti grain size due to TiC pinning effect after annealing at a) 573 and b) 673 K for 36 ks.

The distribution and amount of TiC dispersoids are also important to suppress grain growth. The annealing of the lower distribution of TiC dispersoids such in the case of Ti-1.0wt.% MWCNTs sample, lead to localized discontinuous grain growth, but the annealing of the higher distribution of TiC dispersoids such in the case of Ti-3.0wt.% MWCNTs (Figure 5.18) never shows the discontinuous grain growth because the pinning pressure due to TiC dispersoids is increased with increasing amount of TiC dispersoids in Ti matrix. In addition, the long time annealing of extruded Ti/MWCNTs composites at 673 K for 360 ks does not significantly affect the increase of Ti grain size. High magnification images have also confirmed the unchanged Ti grain size of extruded Ti/MWCNTs composites after annealing at 673 K for 360 ks as shown in Figure 5.19.

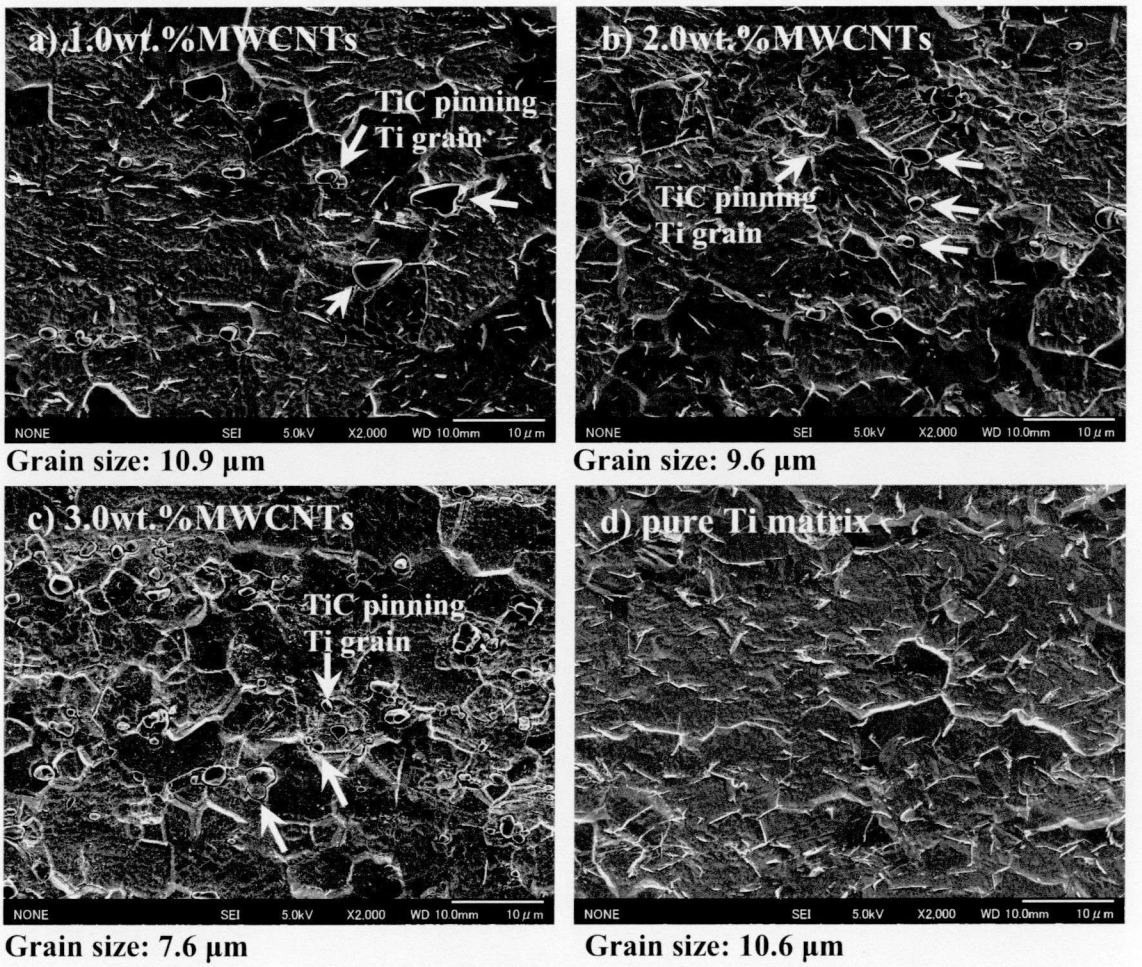

Figure 5.19 SEM images of extruded Ti-a) 1.0wt.%, b) 2.0wt.% and c) 3.0 wt.% MWCNTs composites show the unchanged Ti grain size due to TiC pinning effect, compared to d) recrystallized grain of extruded pure Ti matrix after annealing at 673 K for 360 ks.

The results of grain size of the extruded Ti/MWCNTs composites after annealing at 673 K for 36 and 360 ks indicate the same value. It means that the pinning pressure due to TiC dispersoids is higher than the thermal activation energy for the movement of grain boundary at 673 K, even though the extruded Ti/MWCNTs composites are annealed for long time, resulting in the unchanged Ti grain size. The microstructural stability of the extruded Ti/MWCNTs after annealing at different temperatures and times can be used to confirm the pinning effect due to TiC dispersoids which help to maintain the Ti grain size invariably during tensile testing at elevated temperatures in the section 5.3 and 5.4.

5.6 Conclusions

The extruded fine Ti composites reproduced for the industrial approach showed promising mechanical properties approximate to the same mechanical properties results in laboratory scale. The fatigue strength and the stability strength of the extruded Ti composites at elevated temperatures also showed the promising properties similar to the static mechanical properties evaluation at room temperature. The conclusions of this chapter are as follows.

(1) High strength Ti composite reinforced with MWCNTs using the solution-coating technique could be mass produced for the P/M industry.

(2) The resistances to the dislocation movement during fatigue test caused by the grain size and carbon solid solution of the extruded Ti composites coated with 1.0 and 2.0 wt.% MWCNTs suggested the same amount because those composites almost showed the same value of grain size and amount of carbon solid solution in their matrices.

(3) The increase of fatigue limit of the extruded Ti composite reinforced with MWCNTs was mainly due to the dispersion strengthening effect of the TiC dispersoids in which they retarded the dislocation movement, deformation and sliding of Ti grain during the fatigue test.

(4) The annealing process at 473 K for 360 ks significantly affected to the change of microstructure of extruded pure Ti matrix from the normal grain to coarse lamellar structure, while microstructures of extruded Ti/MWCNTs composites never affected because they contained TiC dispersoids which impeded the diffusion of Ti atoms and stabilized the primary Ti grain size.

(5) The mechanical properties at the elevated temperatures of the extruded Ti/MWCNTs composites indicated the decreasing tendency of tensile strength, yield strength and hardness because the recovery process and diffusion of Ti atoms along grain boundary easily occurred in Ti matrix by the thermal activation, which resulted the matrix could not resist the higher applied stress when the testing temperature was increased.

(6) The increased Ti dispersoids in the Ti matrix of extruded Ti/MWCNTs composites were effective to increase the resistance to the diffusion of Ti atoms along grain boundaries, dislocation movement and grain sliding, resulting in improvement the stability strength of the extruded Ti/MWCNTs composites during the elevated temperatures tensile test.

(7) The stain hardening due to the decreasing Ti grain size could increase stability strength of extruded Ti/MWCNTs composites, which needed the assistance of TiC dispersoids in which resisted the Ti grain coarsening by pinning effect during heating in the temperature range of 473-673 K

References

1. C. Leyens and M. Peters, *Titanium and Titanium alloys*, Wiley-VCH, Germany (2003).
2. ASTM E8M: Standard Test Methods for Tension Testing of Metallic Materials [Metric], ASTM international, West Conshohocken, PA, USA (2001).
3. ASTM E466: Standard Practice for Conducting Force Controlled Constant Amplitude Axial Fatigue Test of Metallic Materials, ASTM international, West Conshohocken, PA, USA (1996).
4. P. E. Markovsky and S. L. Semiatin, "Microstructure and Mechanical Properties of Commercial-Purity Titanium after Rapid (Induction) Heat Treatment", *Journal of Materials Processing Technology*, 210 (2010) 518-528.
5. G. Lütjering and J.C. Williams, *Titanium*, 2nd ed., Springer-Verlag, Germany (2007).
6. W. F. Hosford, *Mechanical Behavior of Materials*, Cambridge University Press, UK (2005).
7. Y. Estrin, G. Gottstein, L. S. Shviddlerman, "Diffusion Controlled Creep in Nanocrystalline Materials under Grain Growth", *Scripta Materialia*, 50 (2004) 993-997.
8. M. J. R. Barboza, E. A. C. Perez, M. M. Medeiros, D. A. P. Reis, M. C. A. Nono, F. Piorino Neto and C. R. M. Silva, "Creep Behavior of Ti-6Al-4V and A Comparison with Titanium Matrix Composites", *Materials Science and Engineering A*, 428 (2006) 319-326.
9. B. Verlinde, J. Driver, I. Samajdar and R. D. Doherty, *Thermo-Mechanical Processing of Metallic Materials*, 1st ed., Pergamon, Netherlands (2007).
10. H. Conrad, "Effect of Interstitial Solutes on The Strength and Ductility of Titanium", *Progress in Materials Science*, 26 (1981) 123-403.
11. O. D. Sherby and P. M. Burke, "Mechanical Behavior of Crystalline Solids at Elevated Temperature", *Progress in Materials Science*, 13 (1968) 323-390.
12. G. E. Dieter, *Mechanical Metallurgy*, SI Metric ed., McGraw-Hill (1988).
13. N. K. Sinha, "Microcrack-Enhanced Creep in Polycrystalline Materials at Elevated Temperature", *Acta Metallurgica*, vol. 37, 11 (1989) 3107-3118.

14. R. C. Picu and A. Majorell, "Mechanical Behavior of Ti-6Al-4V at High and Moderate Temperatrues-Part II: Constitutive Modeling", *Materials Science and Engineering A*, 326 (2002) 306-316.
15. M. E. Kassner and X. Li, "The Effect of Grain Size on The Elevated Temperature Yield Strength of Polycrystalline Aluminum", *Scripta Metallurgica et Materialia*, 25 (1991) 2833-2838.
16. M. A Meyers, G. Subhash, B. K. Kad and L. Prasad, "Evolution of Microstructure and Shear-Band Formation in α-hcp Titanium", *Mechanics of Materials*, 17 (1994) 175-193.
17. Y. Kobayashi, Y. Tanaka, K. Matsuoka, K. Kinoshita, Y. Miyamoto and H. Murata, "Effect of Forging Ratio and Grain Size on Tensile and Fatigue Strength of Pure Titanium Forgings", *Journal of the Society of Materials Science*, Japan, vol. 54, 1 (2005) 66-72 (In Japanese).
18. F. J. Humphreys and M. Hatherly, *Recrystallization and Related Annealing Phenomena*, 2nd ed., Elsevier Ltd., Netherlands (2004)

Chapter 6
Application of Solution-Coating Technique on Various Nano Carbon Sources

Superior mechanical properties of Ti composites reinforced MWCNTs can be obtained by a combination of solution-coating technique and powder metallurgy process. A small amount of added MWCNTs tremendously increases the yield stress and tensile strength with considerable ductility of the extruded Ti powder composites. Moreover, the solution-coating technique has also shown to the potential to scale up. In this chapter, the applicability of this technique is examined again by changing the dispersive substances in zwitterionic solution. Commercially cheap carbon substances, carbon black and acetylene black [1], are used replacing MWCNTs in this study. The abilities of solution-coating technique with different kinds of carbon particles will be investigated, including their effects on mechanical responses of extruded Ti composites. In addition, the mechanical properties of Ti reinforced with a special kind of carbon materials, graphene sheets, are also present in the end of chapter.

6.1 Thermal analysis of solid carbon/zwitterionic substances

Due to the change of carbon substances, the debinding temperature of each different coated carbon nanoparticles on Ti powders will be changed. Therefore, thermal-gravitational (TG) analysis is used to determine the debinding temperature again. The zwitterionic solution with and without acetylene black and carbon black are completely dried in the oven at 373 K. The solid thin films of those dried carbon/solid zwitterionic substances are measured the weight loss upon heating using the TG analyzer with heating rate of 10 K/min at room temperature to 873 K under an Ar gas atmosphere. The TG results are shown in Figure 6.1 The TG results indicate that the onset temperatures of weight loss of dried solid zwitterionic substance containing 0.5wt.% acetylene black and carbon black particles are 537 and 488 K. The onset temperatures of those carbon nanoparticles are close to the previous result of MWCNTs at 503 K as shown in Figure 3.1.

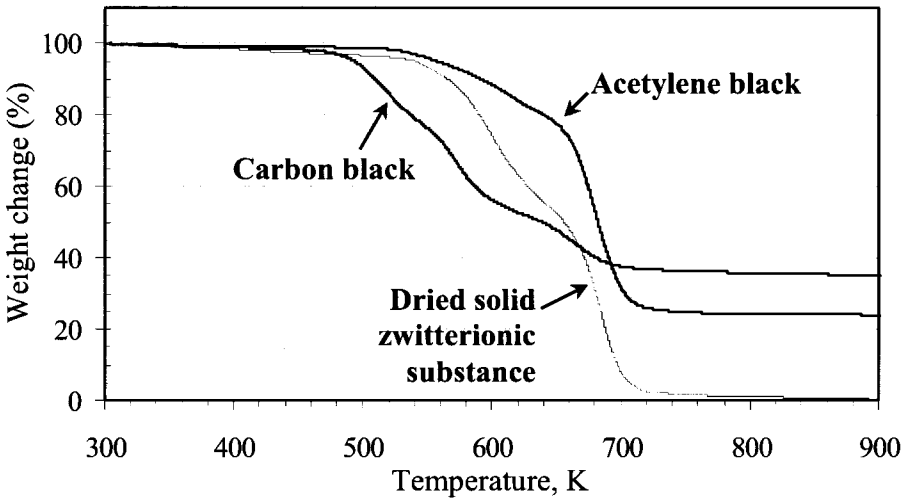

Figure 6.1 Weight change of the solid zwitterionic substance containing with and without acetylene black and carbon black particles.

The weight change of acetylene black and carbon black samples is terminated at 705 and 695 K respectively, while that of dried solid zwitterionic substance is terminated at 704 K. The terminated temperatures of weight change are almost the same value. This suggests that the terminated temperature hardly depends on the type of carbon nanoparticles used, but that essentially depends on the thermal characteristic of zwitterionic substance [2-4]. Therefore, the debinding temperature of acetylene black and carbon black coated Ti powders can be used the same temperature of 873 K as described in the section 3.3.1.

6.2 Morphologies of carbon nanoparticles coated Ti powders

The morphologies of fine Ti powders coated with acetylene black and carbon black after debinding process are shown in Figure 6.2. SEM images reveal Ti powders coated with acetylene black (Figure 6.2 (a)-(b)), carbon black (Figure 6.2 (c)-(d)) particles. The coating via the solution-coating technique has shown a good distribution of carbon nanoparticles on the Ti powder surface. The distribution of both acetylene black and carbon black particles primarily consists of local deposition on the facet of the Ti powder surfaces. The amount of carbon nanoparticles coated on the Ti powder surfaces can be measured by the carbon content analysis of the extruded materials. The carbon content analysis results of the extruded

materials indicate that the acetylene black and carbon black nanoparticles can be deposited on Ti surface at 0.121 and 0.162 wt.%, respectively.

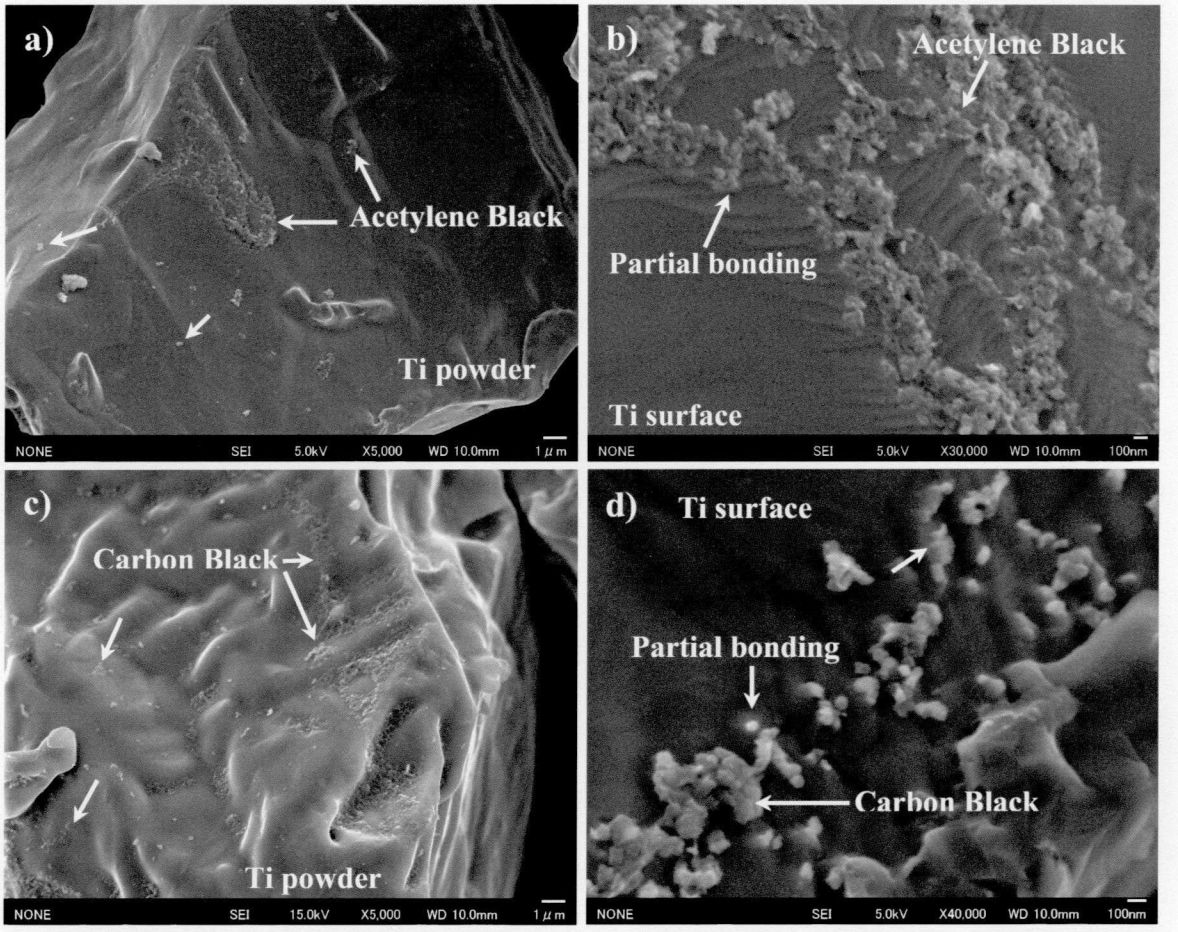

Figure 6.2 Distribution of a) acetylene black particles, b) high magnification image, and c) carbon black particles on Ti surface with d) high magnification showing a partially reacted bonding at the interface.

The results suggest that the amount of carbon deposited on Ti powders strongly depends on size of carbon nanoparticles. In this study, the average size of acetylene black and carbon black particles is 398 and 290 nm. The smaller size of carbon nanoparticles has a higher probability of deposition on Ti powder than that of bigger size. High magnification images in Figure 6.2 (b) and (d) reveal the partially reacted bonding of acetylene black and carbon black particle and Ti surface. This formation of TiC interface maintains the amount of

the coated carbon particles on the Ti powder surfaces until the SPS consolidation process. It means that those carbon nanoparticles are hardly detached from Ti powder surface by partial bonding via *in-situ* formed TiC particles.

6.3 Microstructure and mechanical properties

The debinded fine Ti coated with acetylene black and carbon black are consolidated at 1073 K for 1.8 ks, and subsequently extruded at 1273 K with a preheating time of SPSed billet of 180 s. Figure 6.3 shows the microstructure of extruded Ti reinforced with acetylene black and carbon black. Similar to the use of MWCNT, the presences of TiC particles have two different shapes, i.e., elongated and spherical shapes. The grain size measurement of extruded Ti composites averages 8.1 and 5.8 μm, while the TiC particles average 2.1 and 3.0 μm, for the acetylene black and carbon black reinforced Ti composites, respectively. The fractional amount of TiC particle can also estimate by comparing with the same calibration curve in Figure 4.30. The amount of TiC particle of each extruded Ti composite using acetylene black and carbon black is 0.134 and 0.528 wt.%, respectively.

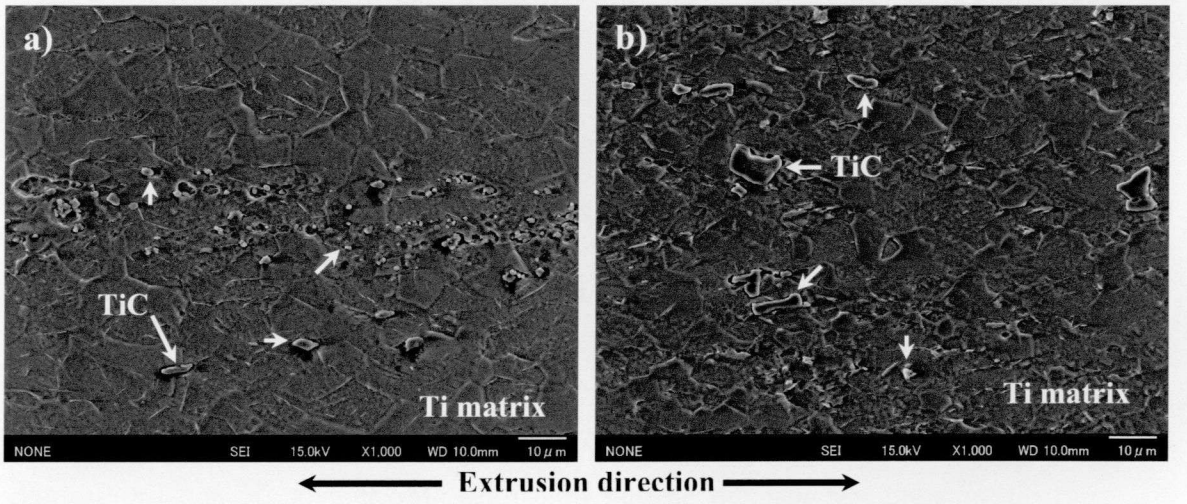

Figure 6.3 Microstructures of extruded Ti reinforced with a) acetylene black and b) carbon black reveal the distribution of *in-situ* formed TiC.

The average mechanical properties results of the extruded Ti/carbon nanoparticles are listed in Table 6.1 and Figure 6.4 shows their stress-strain curves. The yield stress and tensile strength values the extruded Ti/acetylene black are increased by 52.0% and 26.9%, while those of the extruded Ti/carbon black are remarkably increased by 76.7% and 40.5%, compared to the extruded fine Ti matrix.

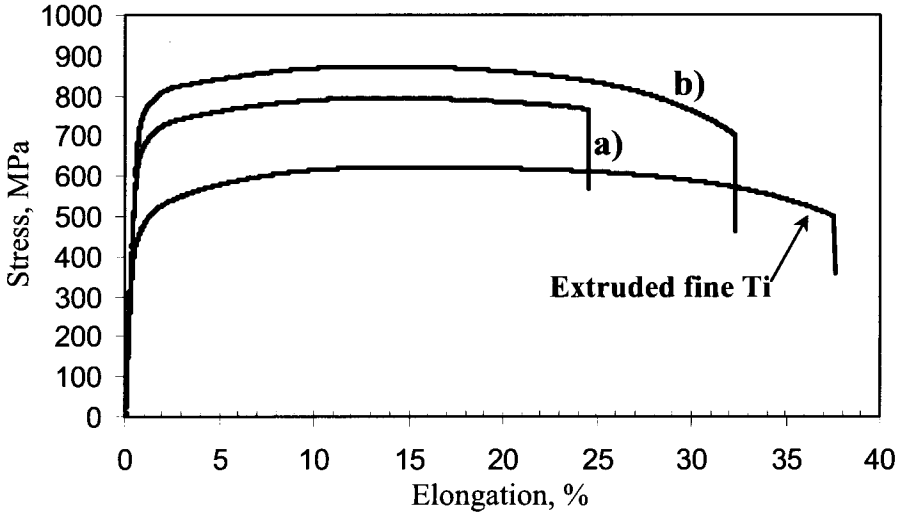

Figure 6.4 Stress-strain curves of the extruded fine Ti composites reinforced with a) acetylene black and b) carbon black nano particles via the solution-coating technique.

Table 6.1 Average value of mechanical properties, average size of Ti and TiC, amount of TiC and carbon content of the extruded Ti/carbon nanoparticles composites.

Extruded fine Ti composites	YS, MPa	TS, MPa	e_f, %	HV	Grain size, μm	TiC size, μm	TiC fraction, (wt.%)	Carbon content, (wt.%)
Ti – Acetylene black	640	793	28.8	286	8.1	2.1	0.134	0.121
Ti – Carbon black	744	878	29.3	340	5.8	3.0	0.528	0.162
Extruded fine Ti	421	625	35.3	261	4.1	-	-	0.012

The effect of Ti grain size is similar to the extruded Ti reinforced MWCNTs. Ti grain size does not significantly affect the increase of tensile properties of those extruded Ti composites. According to Hall-Petch relationship in section 4.3.1, the calculation of the incremental yield stress by the effect of grain size shows the value of 372 and 408 MPa. which are incomparable to the experimental value of 640 and 744 MPa. for the acetylene black and carbon black reinforced Ti matrix, respectively. In addition, the effect of carbon solid solution shows a slight increase of yield stress of 34.2 and 38.1 MPa for the acetylene black and carbon black reinforced Ti matrix. Therefore, the increased yield stress is mainly due to the effect of dispersion TiC particles similar to the extrude Ti reinforced MWCNTs. The summarization of each strengthening mechanism is listed in Table 6.2.

Table 6.2 Summarization of the increased yield stress by each strengthening mechanism.

Extruded fine Ti composites	Experimental yield stress, MPa	Grain size effect, MPa	Incremental yield stress, MPa	
			Carbon solid solution	Second phase (TiC)
Ti – Acetylene black	640	372	34.2	233.8
Ti – Carbon black	744	408	38.1	297.9

6.4 Ti reinforced with graphene sheets

Graphene is a single layer of carbon atoms densely packed in a honeycomb crystal lattice [5-6]. C. Lee, *et al.* measured the intrinsic strength of a defect-free graphene sheet which provided a Young's modulus of 1.0 TPa [7]. This value is close to a Young's modulus of CNT [8-10]. Therefore, the graphene sheets reinforced Ti matrix are expected to show superior mechanical properties responses similar to MWCNTs. 1.0 wt.% graphene sheets are dispersed in the zwitterionic solution, and then coated on the fine Ti powders. The graphene coated fine Ti powders are dried and debinded by the same procedure as mentioned in chapter 2. The Ti powers coated with graphene sheets are consolidated using the SPS process at 1073 K for 1.8 ks. Subsequently, the SPS billet is heated to 1273 K with 180 s holding times. The heated billet is then immediately extruded by the same extrusion machine. The extruded fine Ti powder composite coated with 1.0wt.% MWCNTs will be used as a comparative sample for the extruded Ti/graphene composite. Microstructures of the extruded Ti composite reinforced with graphene sheets are similar to the previous results which consist of TiC and Ti matrix. The average Ti grain size, TiC particle size, amount of TiC particle and mechanical properties of the extruded Ti/graphene composite are listed in Table 6.3, compared to the extruded Ti/MWCNTs composite.

Table 6.3 Average value of mechanical properties, average size of Ti and TiC, amount of TiC and carbon content of the extruded Ti/graphene composite.

Extruded fine Ti composites	YS, MPa	TS, MPa	e_f, %	HV	Grain size, μm	TiC size, μm	TiC fraction, (wt.%)	Carbon content, (wt.%)
Ti – Graphene sheets	657	809	34.0	332	7.0	2.8	0.492	0.170
Ti – MWCNTs	750	883	29.3	345	6.5	1.4	0.812	0.250
Extruded fine Ti	421	625	35.3	261	4.1	-	-	0.012

The summarization of the incremental yield stress by the effect of grain size, carbon solid solution and second phase dispersion of the extruded Ti/graphene composites are also given in Table 6.4. Similar to previous calculation, the increased yield stress by effect of carbon solid solution and second phase dispersion will be normalized to the same level of the carbon content. The increased yield stress per 0.1 wt.% carbon content of extruded Ti/graphene and Ti/MWCNTs are 158.2 and 141.6 MPa, respectively. The normalized value of the extrude Ti/graphene is slightly higher than that of the extruded Ti/MWCNTs just only 16.6 MPa. The results suggest that both graphene sheets and MWCNTs are considered to be very promising reinforcing materials for high strength Ti matrix composite production.

Table 6.4 Incremental yield stress by the effect of grain size, carbon solid solution and second phase dispersion of the extruded Ti/graphene composite.

Extruded fine Ti composites	Experimental yield stress, MPa	Grain size effect, MPa	Incremental yield stress, MPa	
			Carbon solid solution	Second phase
Ti – Graphene sheets	657	388	41.3	227.7
Ti – MWCNTs	750	396	51.8	302.2

The above results clearly demonstrate the powerful application of the solution-coating technique on various kinds of carbon nano substances. Although, the MWCNTs and graphene sheets have considered as the promising reinforcements for the fabrication of high strength pure Ti matrix composite, but their prices are higher than those of acetylene black and carbon black materials significantly. Engineering economic viewpoints may sometime require high strength materials with low cost, acetylene black and carbon black will be the best answers [11], but some applications need high strength and high safety or high strength and value added products, MWCNTs and graphene sheets will become the best solution instead.

6.5 Conclusions

Solution-coating technique could be applied to different kinds of carbon nanoparticles. This technique was identified as a promising method to produce high strength and ductility of Ti matrix composites. The following conclusions can be drawn from the experiment.

(1) The debinding temperature of the carbon nanoparticles coated Ti powders hardly depended on type of carbon nanoparticles, but depending on the thermal characteristic of zwitterionic substance.

(2) Solution-coating technique, using zwitterionic solution, was effective to coat various kinds of nano carbon substances on Ti powder surface, resulting in increase of mechanical properties of the extruded Ti/nano carbon composite materials.

(3) The increased yield stress and tensile strength of the extruded Ti reinforced with carbon nanoparticle composites were mainly due to the dispersion strengthening of the *in-situ* formed TiC particles, while the grain refinement and carbon solid solution strengthening mechanisms did not strongly affect the increased tensile properties of those Ti composites.

(4) High strength and ductility of Ti matrix composites could be obtained by a combination of this advanced solution-coating technique and powder metallurgy process

References

1. K.-H. Köchling, B. McEnaney, S. Müller and E. Fitzer, "International Committee For Characterization and Terminology of Carbon", *Carbon*, vol. 23, 5 (1985) 601-603.
2. K. Kondoh, H. Fukuda, H. Imai and B. Fugetsu, "Microstructures and Mechanical Properties of Magnesium Composite Alloys Dispersed with Carbon Nanotube via Powder Metallurgy Process", *TMS annual meeting and exhibition*, Proc. Int. Conf. on Magnesium Technology, (2008) 289-291, New Orleans, USA.
3. T. Threrujirapapong, K. Kondoh, H. Imai, J. Umeda and B. Fugetsu, "Fabrication of High Strength Pure Ti Matrix Composite Reinforced with Carbon Black Particle via Wet Process", *TMS Annual Meeting & Exhibition*, Supplemental Proceedings, vol. 2, (2010) 181-187, Seattle, USA.
4. T. Threrujirapapong, K. Kondoh, H. Imai, J. Umeda and B. Fugetsu, "Advantages of a Wet Process for the Production of Ti Matrix Composite Reinforced with Carbon Nano Materials by Powder Metallurgy Route", *International Powder Metallurgy Congress & Exhibition*, CD Proceedings World PM2010 (2010) Florence, Italy.
5. K. S. Novoselov, D. Jiang, F. Schedin, T. J. Booth, V. V. Khotkevich, S. V. Morozov and A. K. Geim, " Two-Dimensional Atomic Crystals", *Physics*, vol. 102, 30 (2005) 10451-10453.
6. J. C. Meyer, A. K. Geim, M. I. Katsnelson, K. S. Novoselov, T. J. Booth and S. Roth, "The Structure of Suspended Graphene Sheets", *Nature*, vol. 446 (2007) 60-63
7. C. Lee, X. Wei, J. W. Kysar and J. Hone, "Measurement of The Elastic Properties and Intrinsic Strength of Monolayer Graphene", *Science*, vol. 321 (2008) 385-388.
8. R. S. Ruoff and D. C. Lorents, "Mechanical and Thermal Properties of Carbon Nanotubes", *Carbon*, vol. 33, 7 (1995) 925-930.
9. J.-P. Salvetat, J.-M. Bonard, N.H. Thomson, A. J. Kulik, L. Forró, W. Benoit and L. Zuppiroli, "*Mechanical Properties of Carbon Nanotubes*", *Applied Physics A*, 69 (1999) 255-260.
10. V. N. Popov, "Carbon Nanotubes: Properties and Application", *Materials Science and Engineering R*, 43 (2004) 61-102.

11. T. Threrujirapapong, K. Kondoh, H. Imai, J. Umeda and B. Fugetsu, "Mechanical Properties of A Titanium Matrix Composite Reinforced with Low Cost Carbon Black via Powder Metallurgy Processing", *Materials Transactions*, vol. 50, 12 (2009) 2757-2762.

Chapter 7
Summary

This research focused on the fabrication process of high strength Ti composite reinforced with MWCNTs via a combination of the solution-coating technique and powder metallurgy process. In chapter 1, the zwitterionic surfactant solution was introduced for the uniform dispersion of MWCNTs on the Ti powders, compared to the other methods such as ball milling. This was due to the characteristic of zwitterionic surfactant which contained both hydrophobic and hydrophilic groups in its structure. The electrostatic forces were generated at the hydrophilic groups because of the associated cation and anion, which had larger attractive force than the van der Waals forces between bundled MWCNTs. Therefore, the bundle problems of MWCNTs due to the van der Waals force between carbon atoms at nanotube surfaces could be eliminated by the effective zwitterionic solution.

In chapter 2, the experimental procedure and equipments used in this research, including the coating method of MWCNTs on the Ti powders surface were introduced. The successful coating by the solution-coating technique could be identified by the uniform distribution of the MWCNTs on the Ti powders surface, microstructures and mechanical properties responses of the extruded Ti/MWCNTs composite materials

The processing parameters for the fabrication of Ti reinforced with MWCNTs were determined in chapter 3. The thermal characteristics of the solid zwitterionic substances with and without MWCNTs existing on the Ti powder surface showed the complete decomposition at 773 and 873 K, respectively. Therefore, the debinding temperature was selected at 873 K. In addition, the debinding atmosphere was also determined by the comparison of Ar and H_2-Ar mixed gases. The inert Ar atmosphere used for the debinding process yielded superior ductility for the extruded Ti composites. The formation of TiH_2 brittle compounds by the H_2-Ar mixed gases caused the reduction of ductility of the extruded Ti composite.

The amounts of deposited MWCNTs on fine Ti powders were higher than those of sponge Ti powders because fine Ti powders had a smaller size which exhibited a larger specific surface area, resulting in higher probability of being coated MWCNTs than sponge Ti powders. In addition, the amount of deposited MWCNTs on Ti surface increased with increasing their concentration in zwitterionic surfactant solution, but this solution-coating technique did not succeed to control the deposition of MWCNTs on Ti powders linearly by adjusting their concentration in zwitterionic surfactant solution.

In chapter 4, microstructure of extruded Ti/MWCNTs composites showed the high distribution of the *in-situ* formed TiC particles throughout the α-Ti matrices, which accounted for the high distribution of MWCNTs on the Ti powder surface in the context of solution-coating technique. The static mechanical properties of both extruded sponge and fine Ti composites increased with increasing the MWCNTs content, while the ductility of those extruded Ti composite still maintained high enough for the applications. The main strengthening mechanism of the extruded Ti/MWCNTs composite was the dispersion of second phases, i.e., the *in-situ* formed TiC particles and the remained MWCNTs, while the carbon solid solution slightly affected to strengthen those extruded Ti/MWCNTs composites. On the other hand, the Ti grains never showed their significant effect on the improvement of mechanical properties of both extruded sponge and fine Ti/MWCNTs composites. In addition, the sintering temperature and time of the Ti powder composites directly affected the formation of the *in-situ* TiC dispersoids. The higher SPS temperatures consolidation resulted in the increase of TiC particles size with decreasing in mechanical properties of the composites. In other words, amount of the remained MWCNTs decreased with increasing SPS temperatures, resulting in decrease of mechanical properties. The good balance of SPS temperature and time, which meant the optimum amount of TiC particles and the remained MWCNTs, yielded the highest mechanical properties at 1073 K and 1.8 ks.

In chapter 5, the dynamic properties and stability at elevated temperature of Ti/MWCNTs were evaluated using fatigue test and high temperature tensile test. Moreover, the ability to scale up process from laboratory to industrial scale was investigated simultaneously during fabrication of fatigue test samples. The tensile properties evaluation of

the scaled-up samples showed good results similar to those of laboratory. Therefore, the mass production of high strength Ti/MWCNTs composites prepared by solution-coating technique was possible.

The fatigue test results of the extruded Ti/MWCNTs also showed good results, compared to those of extruded fine Ti matrix and the previous study. The increase of fatigue strength of the extruded Ti/MWCNTs composites was mainly due to the dispersion strengthening mechanism of the TiC particles which retarded the dislocation movement, deformation and sliding of Ti grain during cyclic applied loading. Furthermore, the results of stability of strength of the extruded Ti/MWCNTs composites at elevated temperature still showed good results in the satisfied level, compared to extruded pure Ti matrix. The yield stress, tensile strength and hardness of the extruded Ti/MWCNTs composites showed the decreasing tendency because the recovery process and diffusion of Ti atoms along grain boundary quickly occurred by the assistance of thermal activation during elevated temperature testing, which resulted the Ti matrix could not resist the higher applied stress when the testing temperature increased. The increases of Ti dispersoids could improve the stability strength of the extruded Ti/MWCNTs composites because those Ti dispersoids behaved as obstacles to resist the diffusion of Ti atoms, dislocation movement and grain sliding, known as pinning effect, during the elevated temperature tensile test.

In chapter 6, the solution-coating technique showed the ability to be applied to other nano carbon reinforcing materials, i.e., acetylene black, carbon black particles and graphene sheets. The determination of debinding temperature for the Ti powder coated with acetylene black, carbon black particles suggested that the debinding temperature depended on the thermal characteristic of solid zwitterionic substances. The mechanical properties of the extruded Ti/ nano carbons composites were also highly improved by adding small amount of those nano carbon materials via the solution-coating technique. The main strengthening mechanism of the extruded Ti/nano carbon composite materials was the dispersion of *in-situ* formed TiC particles similar to the strengthening mechanism of the extruded Ti/MWCNTs composites, while the strengthening mechanism by Ti grain size and carbon solid solution did not strongly affect the improvement of mechanical properties.

The above improvements of the mechanical properties in static and dynamic modes including the stability strength at elevated temperature of the extruded Ti reinforced with MWCNTs clearly verified the application of the solution-coating technique in the powder metallurgy process for fabrication of high strength titanium metal matrix composites.

List of Contributions

A. International Journals

1) T. Threrujirapapong, K. Kondoh, H. Imai, J. Umeda and B. Fugetsu, "Mechanical Properties of a Titanium Matrix Composite Reinforced with Low Coat Carbon Black via Powder Metallurgy Processing", *Materials Transactions*, vol. 50, 12 (2009) 2757-2762.
2) T. Threrujirapapong, K. Kondoh, H. Imai, J. Umeda and B. Fugetsu, "Hot Extrusion of Pure Titanium Reinforced with Carbon Nanotubes", *Steel Research International*, vol. 81, 9 (2010) 1320-1323.
3) K. Kondoh, T. Threrujirapapong, H. Imai, J. Umeda and B. Fugetsu, "CNTs/TiC Reinforced Titanium Matrix Nanocomposites via Powder Metallurgy and Its Microstructural and Mechanical properties", *Journal of Nanomaterials*, vol. 2008 (2008) Article ID127538, 4 pages, doi:10.1155/2008/127538
4) K. Kondoh, T. Threrujirapapong, H. Imai, J. Umeda and B. Fugetsu, "Characteristics of Powder Metallurgy Pure Titanium Matrix Composite Reinforced with Multi-Wall Carbon Nanotubes", *Composites Science and Technology*, 69, (2009) 1077-1081.
5) K. Kondoh, T. Threrujirapapong, H. Imai, J. Umeda and B. Fugetsu, "Microstructural and Mechanical Properties of Titanium Matrix Composites Reinforced with Nano Carbon Materials via Powder Metallurgy Process", *Materials Science Forum*, vol. 618-619 (2009) 495-499.
6) T. Yoshimura, T. Threrujirapapong, H. Imai, K. Kondoh, "Cost Effective Pure Titanium with High Mechanical Response by Oxide Dispersion Strengthening", *Materials Transactions*, vol. 50, 12 (2009) 2751-2756.
7) T. Yoshimura, T. Threrujirapapong, H. Imai, K. Kondoh, "Mechanical Properties of Oxide Dispersion Strengthened Pure Titanium Produced by Powder Metallurgy Method", *Materials Science Forum*, vol. 654-656 (2010) 815-818.

B. International Conferences

1) T. Threrujirapapong, K. Kondoh, H. Imai, J. Umeda and B. Fugetsu, "Fabrication of High Strength Pure Ti Matrix Composite Reinforced with Carbon Black Particle via Wet Process", *TMS 2010 139th Annual Meeting & Exhibition*, Supplemental Proceedings, vol. 2, (2010) 181-187, 14-18 February 2010, Seattle, Washington USA.
2) T. Threrujirapapong, K. Kondoh, H. Imai, J. Umeda and B. Fugetsu, "Hot Extrusion of Pure Titanium Reinforced with Carbon Nanotubes", *Metal Forming 2010*, Steel Research International, vol. 81, 9 (2010) 1320-1323, 19-22 September 2010, Toyohashi, Japan.
3) T. Threrujirapapong, K. Kondoh, H. Imai, J. Umeda and B. Fugetsu, "Advantages of a Wet Process for the Production of Ti Matrix Composite Reinforced with Carbon Nano Materials by Powder Metallurgy Route", *International Powder Metallurgy Congress & Exhibition*, CD Proceedings World PM2010 (2010), 10-14 October 2010, Florence, Italy.
4) T. Threrujirapapong, T. Mimoto, K. Kondoh, J. Umeda and B. Fugetsu, "Effects of SPS Parameters on The Mechanical Properties and Microstructures of Titanium Reinforced with Multi-Wall Carbon Nanotubes Produced by Hot Extrusion", *TMS 2011 140th Annual Meeting & Exhibition*, Supplemental Proceedings, vol. 2, (2011) 821-828, 27 February-3 March 2011, San Diego, California USA.

C. Domestic Journals

1) T. Threrujirapapong, K. Kondoh, H. Imai, J. Umeda and B. Fugetsu, "Microstructures and Mechanical Properties of Powder Metallurgy Pure Ti Composite Reinforced with Carbon Nanotubes", *Transactions of JWRI*, vol. 37, 1 (2008) 57-61.
2) T. Threrujirapapong, K. Kondoh, J. Umeda and H. Imai, "Friction and Wear Behavior of Titanium Matrix Composite Reinforced with Carbon Nanotubes Under Dry Conditions", *Transactions of JWRI*, vol. 37, 2 (2008) 51-56.
3) T. Threrujirapapong, K. Kondoh, H. Imai, J. Umeda and B. Fugetsu, "Titanium Matrix Composite Reinforced with In-situ Formed TiC Using Carbon Black Nano Particles via A Wet Process", *Transactions of JWRI*, vol. 38, 1 (2009) 13-17.

D. Domestic Conferences

1) T. Threrujirapapong, K. Kondoh, H. Imai and T. Yoshimura, "Mcrostructure and Mechanical Properties of Pure Ti Reinforced with Multi-Wall Carbon Nanotubes", 第52回　日本学術会議材料工学連合講演会, 22-24 October 2008, Kyoto.
2) T. Threrujirapapong, K. Kondoh, H. Imai and J. Umeda, "Tribology of Pure Ti Reinforced with Multi-Wall Carbon Nanotubes", 第144回日本金属学会春期大会, 28-30 March 2009, Tokyo.
3) T. Threrujirapapong, K. Kondoh, H. Imai and T. Yoshimura, "Fabrication of Ti/CNTs Metal Matrix Composite via Powder Metallurgy and Its Mechanical Properties", 第116回春季大会講演概要, 21-22 May 2009, Hokkaido.
4) T. Threrujirapapong, K. Kondoh, H. Imai and T. Yoshimura, "Friction Behavior of CNT-Reinforced Ti Composite Materials", 粉体粉末冶金協会第103回講演大会, 2-4 June 2009, Kyoto.

Acknowledgments

The author would like to express deepest gratitude to Professor Dr. Katsuyoshi Kondoh for his kind advices, technical support and great valuable discussion on the direction and the many issues of the research. The sincere gratitude is then extended to the thesis committee, Professor Dr. Kohji Minoshima, Professor Dr. Kazuhiro Nakata and Professor Dr. Seiji Katayama for their valuable and constructive comments on this thesis, and also to Professor Dr. Bunshi Fugetsu who kindly provided the chemical solution from Hokkaido University.

The author was given an opportunity to conduct the research as part of the fulfillment for doctorate program at Osaka University. This will not be possible without the assistance and recommendations of Professor Dr. Katsuyoshi Kondoh, Associate Professor Dr. Sawai Danchaivijit, Associate Professor Dr. Tachai Luangvaranunt.

The author highly appreciates to Dr. Hisashi Imai, Dr. Junko Umeda, Ms Hiroko Takeda and Mrs Eri Nishiyama for their kind help and support in every issue, not only related to study, but also to student life in Japan. Special thanks are also sent to all staffs and students in Kondoh Laboratory for their technical help and support in the experimental works, especially Mr. Tomohiro Yoshimura and Mr. Takanori Mimoto. Sincere thanks are given to Dr. Isamu Otsuka, manager of Epson Atmix, for analyzing carbon content, and for Mr. Yoshio Enomoto, the president of Enomoto Machine Co., Ltd, for providing scholarship.

The author acknowledges the Ministry of Education, Culture, Sports, Science and Technology (MEXT), Japan for the financial support and the Faculty of Engineering, Naresuan University, Thailand for the opportunity to study abroad.

Kind words of encouragement have been constantly given by Thai friends both in Japan and Thailand, particularly Ms. Asaya Siriaotharn, Ms Rathaporn Boonlert, Ms Patchamon Thianpattaranun and Mr.Napadon Wantamanee.

The author would like to express the great gratitude and respect to his family and relative in Thailand for the perpetual personal support and encouragement through all the years he has been abroad.

September 2011

Thotsaphon Threrujirapapong